Summer 1998

Approximate Analytical Relationships for Linear Optimal Aeroelastic Flight Control Laws

Ayman Hamdy Kassem
Old Dominion University

APPROXIMATE ANALYTICAL RELATIONSHIPS FOR LINEAR OPTIMAL AEROELASTIC FLIGHT CONTROL LAWS

by

Ayman Hamdy Kassem
B.Sc. August 1990, Cairo University, Egypt
M.Sc. June 1993, Cairo University, Egypt

A Dissertation Submitted to the Faculty of
Old Dominion University in Partial Fulfillment of the
Requirements for the Degree of

DOCTOR OF PHILOSOPHY

AEROSPACE ENGINEERING

OLD DOMINION UNIVERSITY

August 1998

Approved by :

_____
Brett A. Newman (Director)

_____
Colin P. Britcher (Member)

_____
Thomas E. Alberts (Member)

_____
Jen K. Huang (Member)

ABSTRACT

APPROXIMATE ANALYTICAL RELATIONSHIPS FOR LINEAR OPTIMAL AEROELASTIC FLIGHT CONTROL LAWS

Ayman Hamdy Kassem

Old Dominion University, August 1998

Director: Dr. Brett Newman

This dissertation introduces new methods to uncover functional relationships between design parameters of a contemporary control design technique and the resulting closed-loop properties. Three new methods are developed for generating such relationships through analytical expressions: the Direct Eigen-Based Technique, the Order of Magnitude Technique, and the Cost Function Imbedding Technique. Efforts concentrated on the linear-quadratic state-feedback control-design technique applied to an aeroelastic flight control task. For this specific application, simple and accurate analytical expressions for the closed-loop eigenvalues and zeros in terms of basic parameters such as stability and control derivatives, structural vibration damping and natural frequency, and cost function weights are generated. These expressions explicitly indicate how the weights augment the short period and aeroelastic modes, as well as the closed-loop zeros, and by what physical mechanism. The analytical expressions are used to address topics such as damping, nonminimum phase behavior, stability, and performance with robustness considerations, and design modifications. This type of knowledge is invaluable to the flight control designer and would be more difficult to formulate when obtained from numerical-based sensitivity analysis.

This dissertation is dedicated to the memory of

my father, grandfather and uncle Mahmoud.

ACKNOWLEDGEMENTS

I would like to express my sincere thanks to my advisor; Dr. Brett Newman, for his guidance throughout this research project. His vast knowledge and innovative ideas guided the project from inception. I extend many, many thanks to my committee for patience and hours of editing of this manuscript.

I am truly blessed to have a wonderful supportive family. Although miles have often separated us, they have all been a constant source of love and encouragement. I am very thankful to my entire family for their unfailing belief in my ability, My deepest thanks go to my mother, who has inspired me throughout my life, my sister, and my grandmother.

TABLE OF CONTENTS

Chapter Page

Chapter Page

LIST OF TABLES

TABLE Page

LIST OF FIGURES

FIGURE Page

FIGURE Page

CHAPTER I

INTRODUCTION

1.1 Problem Motivation

Increased reliance upon flight control systems to meet mission design requirements, while retaining exceptional flying qualities, has been the trend for several decades.[1] For example, in advanced vehicle concepts, where overall flight characteristics are influenced by various factors such as rigid-body motion, structural vibration, unsteady aerodynamic flow, and propulsion system behavior, multiple feedback loops are designed to actively control key dynamic features in the vehicle system in an integrated fashion. Often these control loops must operate near maximum performance levels, with stability margins approaching minimum required limits, just to retain economic or functional viability of the concept.

The theoretical control community has been concentrating on contemporary design techniques for such applications for over three decades. Powerful methods such as LQR/LQG/LTR, H_2, H_∞, and many others, have been created to close multiple feedback loops simultaneously in a well coordinated manner.[2-8] Recent activity has concentrated on tuning existing methods to provide closed-loop robustness properties. These methods offer significant potential for increased performance, but have been underutilized in practice. Two obstacles limiting the use of these methods in production vehicles are 1) the *lumped nature* of the algorithms which mask detailed information about individual loop characteristics and 2) the *theoretical-mathematical sophistication* which links

---

The journal model for this dissertation is the Journal of Guidance, Control and Dynamics.

relevant closed-loop properties to the design parameters. These obstacles limit available *insight* concerning how the control law stabilizes and/or augments the vehicle dynamics. Further, if design results suggest the need for *modifications*, the flight control designer is often unclear on how to proceed, short of quasi-iterative strategies.

For example, with standard linear quadratic state feedback control, once the input-output suite is specified, the designer must select cost-function weights which provide acceptable trades between stability and performance, in both time, and frequency-domain measures. Detail effects from cost-function weight adjustments on important closed-loop features associated with the poles and zeros, time responses, stability robustness traces, and ultimately the flying qualities, are not readily apparent. Tracing these effects through the numerical solution of Riccati-type equations, in the absence of graphical information, is not easily understood. Further, the role each feedback loop plays in stabilizing and/or augmenting basic vehicle modes like the short period or dutch roll modes is unclear. These weaknesses are emphasized further, when these methods are compared with conventionally based, sequential loop closure design strategies. [9-11]

The need for understanding of the relationships between the design parameters and resulting closed-loop dynamic characteristics is thus apparent. One approach to obtaining this insight, as opposed to costly and burdensome numerical sensitivity studies, is to develop analytical or symbolic expressions linking relevant closed-loop features to basic parameters specified by the designer. These expressions must be of sufficient form to allow useful insight into the design relationships. The objectives of this dissertation are 1) formulation of techniques capable of producing such expressions, 2) generation of candidate expressions for contemporary flight control applications, and 3) utilization of

the expressions to better understand the mechanisms by which a contemporary flight control law augments flight vehicle dynamics.

1.2 Literature Survey and Problem Definition

A broad spectrum of contemporary design techniques exists to generate flight control systems. As an initial step into the analytical expressions research area, this dissertation will consider exclusively the standard linear quadratic (LQ) state feedback strategy for flight control system development.[2] Although better formulations for flight control design exist, the standard LQ approach is a well-known contemporary design technique, and it provides a simple framework for analytical expressions work.

This dissertation will take the perspective that closed-loop transfer function factors, for both the numerator and denominator polynomials in each channel, are fundamental for assessing system stability and performance.[9] If the designer can tailor the numerical values for these factors to desirable levels, then a majority of the design objectives can be met. Therefore, development of techniques which link the control design parameters to the closed-loop factors is of major importance in this work.

A classical factoring technique for open-loop systems, closely related to the topic here, is to first reduce the dynamic order of the open-loop model to two or less and then use the quadratic or linear formulas to factor the polynomials. This technique has found considerable use in aircraft dynamics (i.e., the short period, phogoid, roll, dutch roll, and spiral approximations).[9-11] However, the dissertation topic is distinctly different in that higher order systems, closed-loop systems, and in particular, closed-loop systems

developed from contemporary design strategies, are considered. Analytical factoring of such systems has not been addressed to any significant degree in the literature.

Consider the computational steps associated with generating closed-loop transfer function factors from a LQ design and analysis time-domain perspective. Figure 1.1 illustrates these steps. Given the airframe state space matrices and cost-function weight matrices, the initial task is to construct the Riccati equation (a nonlinear quadratic matrix equation). Once the Riccati solution is established, the feedback gain matrix and closed-loop state space matrices are computed by straightforward matrix operations. The closed-loop transfer function matrix is generated by a transformation to the Laplace domain followed with the construction of the resolvant matrix. Finally, closed-loop transfer function factors are obtained by computing roots of the polynomials within the transfer function matrix. Identifying analytical relationships between the cost-function weights and closed-loop factors as outlined in Figure 1.1 is a challenging task, yet this is precisely the topic of this research effort.

The computational steps outlined in Figure 1.1 are routinely conducted, in a *numerical* sense. Many software packages contain reliable and efficient algorithms for these steps. However, for *analytical* computations, several bottlenecks exist in Figure 1.1. Each of these bottlenecks is discussed below.

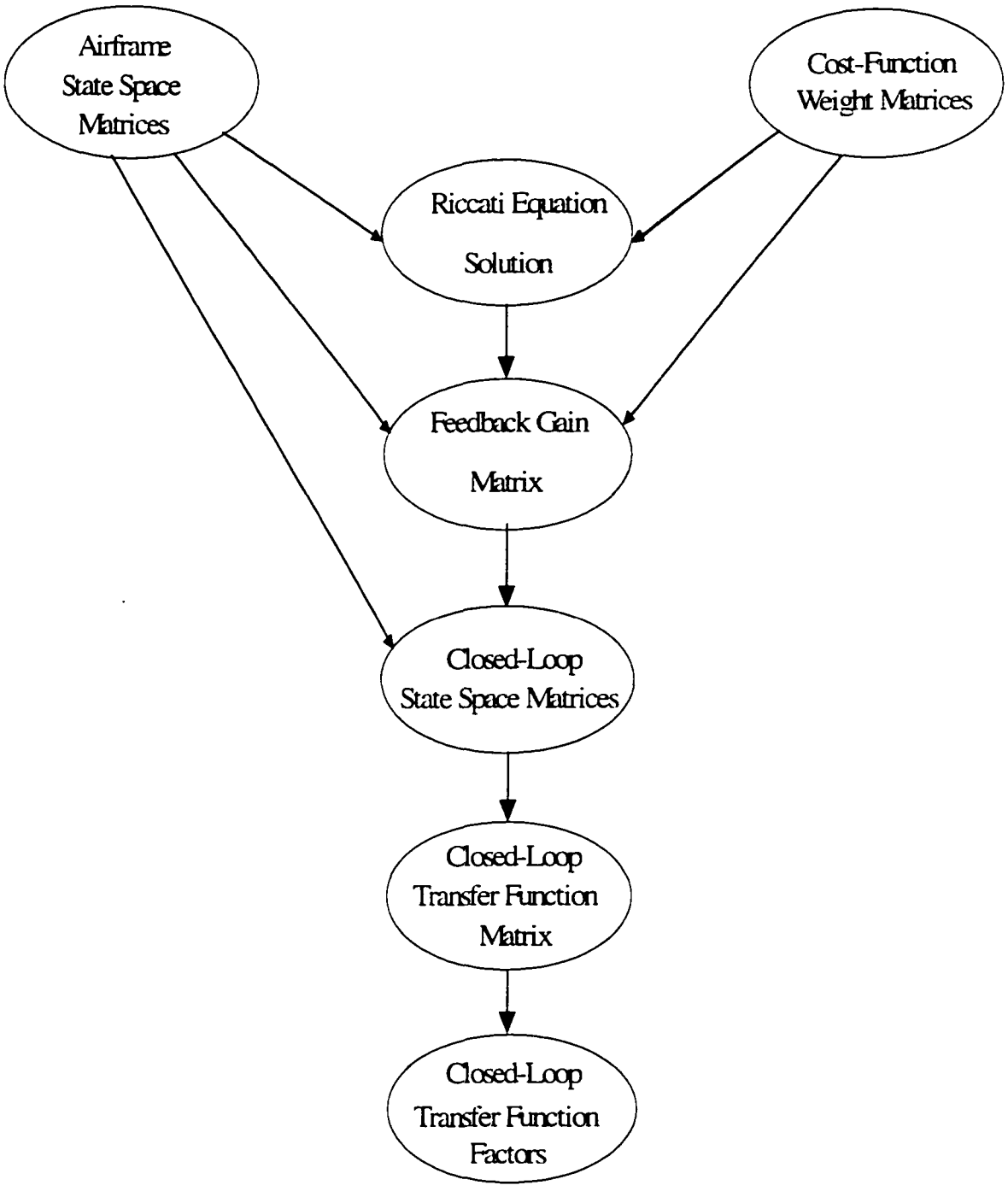

Figure 1.1 Computational Steps in LQ Design and Analysis

As shown in Figure 1.1, to implement the LQ technique with feedback gains, solutions of Riccati-type equations are necessary. This step is a major difficulty. Many numerical methods are available to solve the Algebraic Riccati Equation (ARE), but all methods can be classified into either of the following two categories: 1) Iterative Methods (e.g., Newton, Defect Correction, Sign Function, etc.) and 2) Eigenvalue Methods. Iterative methods start with an initial guess matrix for the solution of the ARE. Using an error function depending on the ARE, or a modified version of the ARE, the schemes calculate a correction matrix and add it to the initial guess. These steps are repeated until the solution converges. These methods typically require constraints on the initial guess to guarantee convergence. Eigenvalue methods depend on constructing the Hamiltonian matrix from the formal optimization process. Eigenvalues and eigenvectors of this matrix are then computed using any eigen solver. The solution of the ARE is then constructed from the eigenvectors. Samples of these numerical methods are given in References 12 through 18.

These two methods are not directly appropriate for analytical computations. For example, with the iterative methods, no guarantee of convergence exists and even if the solution converges, it would have to do so in relatively few steps. One could not expect to carry analytical calculations through many iteration steps. In the eigenvalue methods, a necessary step is calculation of the characteristic polynomial roots. Since there is no exact analytical factoring solution for the roots of polynomials of order higher than four, this method would be limited to low-order systems (even though there are many problems of interest that can be sufficiently modeled by a fourth-order structure). Computing the eigenvectors and formation of the Riccati solution would also involve Gauss elimination

and matrix inversion, non-trivial steps analytically, for systems of higher order. Although these numerical methods are not directly suitable for analytical solutions, they do provide a framework, and suggest strategies for, analytical approaches to solving the Riccati equation. Such modified strategies will be used in the following chapters.

After reviewing the existing literature on symbolic solutions of AREs,[19-26] it is apparent that little progress has been made. In these references, three main issues confront the analytical solution of AREs. The first issue is the difficulty in finding a transformation that converts the quadratic structure of the ARE to a simpler form. The second issue is the difficulty in finding a technique that is not dependent upon the assumption of a symmetric system dynamics matrix. The third issue is the difficulty in symbolically computing the square root of a symmetric matrix. Sometimes more than one of these problems is faced simultaneously. Many assumptions and restrictions are introduced by researchers to allow the possibility for analytical solutions.

In the first issue of transforming the ARE to a simpler form, two assumptions are commonly made. First, the control distribution matrix is assumed to be invertible. Second, the response distribution matrix is assumed to be invertible. In other words, the number of inputs and outputs must equal the number of states. These restrictions can be relaxed to the existence of a solution to a Lyaponov-type equation.[24] The second issue of how to address a nonsymmetric system dynamics matrix is much harder. One option is to exploit the Riccati solution symmetry and reduce the number of unknowns.[25] The third issue concerning matrix square-root computations requires eigenvalue and eigenvector solutions for the symmetric matrix in question.

A second bottleneck indicated in Figure 1.1 is the computation of the closed-loop transfer function matrix. As indicated, this computation utilizes the state space matrices directly. Construction of the resolvant matrix is necessary and is usually handled numerically by the resolvant algorithm.[2] This technique is a recursive algorithm and is inappropriate for analytical computations. Direct closed-form determinate calculations for the resolvant matrix can be used in principle, but working directly with state space matrices is inefficient, as opposed to a more compact formulation like polynomial matrix models.

The final bottleneck for analytical computations illustrated in Figure 1.1 is factoring of the closed-loop transfer function polynomials. It is well known that exact symbolic factoring is only possible for polynomials of degree four or less.[27] The linear and quadratic formulas for first- and second-degree polynomials are well known. However, these formulas can not be applied to many problems of interest which have more than one degree of freedom (or two state variables). Formulas for third and fourth degree- polynomials are cumbersome to use for portraying insight. A factoring technique, possibly approximate in nature and which is not restricted by the polynomial order, is needed. Examples of unique approaches for analytical factoring of low-order polynomials are found in References 28 through 30.

Clearly, there is a need for more efficient and tractable means to conduct these computations symbolically. This dissertation will consider several approaches to circumvent these difficulties. These approaches include: 1) utilization of often overlooked theoretical results, 2) development of alternative techniques for computing relevant

quantities, and 3) relaxation of exact computations (i.e., approximate computations). These alternative strategies are discussed below.

Crucial to the work contained in this dissertation will be the utilization of an existing approximate analytical factoring technique for dynamic systems. This technique has its origins based upon an ad hoc procedure described in References 31 through 33. In these references, calculations were considered well before the advent of modern computers. References 34 through 36 reformulated this procedure with a sound theoretical framework and applied modern computers in the calculations.

This technique has been used successfully to develop analytical relationships for open-loop airframe transfer function poles and zeros in terms of basic parameters such as stability and control derivatives.[35] In this technique, the first two terms of a Taylor series are used to capture the polynomial coefficient dependencies upon the polynomial factors. By analytically inverting the first-order sensitivity matrix, corrections to preliminary factors can be generated. In principle, the technique is applicable to higher order systems (i.e., fifth order and above). Relatively simple and accurate analytical expressions, conducive to obtaining insight into the vehicle physics, have been obtained by this technique. The technique also makes use of polynomial matrix formulations for the dynamic system. Rather than describing the system with state variables, this formulation works with degrees of freedom, allowing a more compact framework for computing determinants. This technique is exploited in later chapters of this work. References 37 and 38 describe additional applications of this factoring technique.

If the aim of the designer is to determine system stability and stability robustness from the closed-loop denominator factors, an efficient tool to bypass the Riccati equation

solution is LQ root locus theory.[2,39-43] With this theoretical framework, the closed-loop characteristic polynomial can be written as a determinate function explicitly involving the cost-function weighting matrices and the airframe transfer-function matrix. The Riccati equation solution and the feedback gain matrix are absent from this expression. Tremendous analytical computation savings can be gained with this result, and is exploited latter in this work.

If the closed-loop numerator factors are of interest, the existing literature does not offer a theoretical result that directly relates the closed-loop transfer function numerator polynomials to the cost function weight matrices. In the archived results, numerator polynomials are typically expressed in terms of the feedback gain matrix, which in turn is expressed as a function of the Riccati equation solution, which ultimately depends upon the cost-weight matrices. These relationships are indirect, involving the intermediate variables. In theory, the "closed-form" eigen method solution for the Riccati equation could be utilized. Even with approximations, the analytical computations necessary with this approach appear to be intractable, and are not considered in this dissertation.

As an alternative to this eigen-based strategy for both numerator and denominator factors, a technique which is based on the indirect relationships is also explored. To circumvent the difficulties associated with the exact analytical solution to the Riccati equation, an approximate technique is used for the solution. Based on neglecting small numerical terms in each element of the matrix Riccati equation, approximate closed-form solutions can be developed. These results provide the analytical relationships between the feedback gain matrix and the cost weighting values, which in turn can be exploited to determine the numerator and denominator factors.

A final approach, unrelated to any of the discussions thus far, will also be considered. Recall that the cost function is the basic relationship where the weighting matrices and time-domain vehicle dynamics meet. By imbedding the closed-loop time-domain responses into the cost function, the closed-loop gains can be introduced into the fundamental relationship. Since the cost is an optimal cost, first-order variations with respect to the closed-loop gains provide a direct link between the feedback gains and the system parameters without the complexity of the Riccati equation and associated solution. However, the resulting equations are nonlinear and are difficult to solve. At this stage, other methods can be utilized to relate the closed-loop factors to the feedback gains.

The strategy here is to explore utilization of these concepts to generate analytical expressions, albeit approximate, between the cost-function weights and closed-loop numerator and denominator factors, for a LQ-based aeroelastic flight control law. Through these expressions, the goal of the research is to foster improved understanding of the cost weighting selection process, and to provide practical, relevant design information to the flight control engineer.[44-46] If successful, the results may contribute to increased application and implementation of contemporary design techniques to advanced vehicle concepts requiring multiple, coordinated feedback loops.

In principle, the techniques presented in this dissertation are not limited by system dynamic order, or input-output dimensions. No theoretical restrictions exist for applying the steps to higher-order dynamical systems with many inputs and outputs. However, in practice, the analytical computations and manipulations can become excessive and intractable for high order systems with a large number of inputs and outputs. Therefore, the work reported on in this dissertation considers vehicle dynamic models of order four

with two input and two output channels. The techniques presented here could be reasonably applied to fifth order systems with significant but tractable increments in computational burdens. Beyond sixth order systems, the calculations are projected to be excessive. This limitation should not be viewed as a major restriction. For example, many flight control problems can be "boiled down" to two channel, fourth-order systems, such as basic stability augmentation systems for the longitudinal and lateral-directional axes.

As discussed previously, many of the analytical relationships that are sought are theoretically unattainable in exact closed-form. Where appropriate, approximate closed-form solution techniques are considered in this research. This limitation should not be considered as a major compromise. Recall the objective is not to compute the closed-loop characteristics with high numerical accuracy since this can already be accomplished by other means. The goal here is to provide more valuable information to the designer by generating analytical expressions that will assist the flight-control engineer in developing the underlying relationships between the design parameters and resulting closed-loop properties. Such expressions will allow the designer to address questions like how do the individual weights affect particular modes, how do the control weights and airframe parameters combine to yield key closed-loop dynamic features, how does the sensor location enter into the characteristics, etc. With the intended application described here, approximate analytical expressions are quite suitable.

As a final comment, all calculations in this dissertation concerning the development of approximate analytical expressions were conducted with symbolic manipulation software. Utilization of these software tools increases computational turn around time, and provides a measure against manually induced errors. However, it is felt

that the techniques can never be fully automated since there is a considerable amount of human judgment involved. Software packages specifically utilized here are Mathematica[47] and Theorist[48]. Theorist is particularly useful in that it allows the calculations to be directed one step at a time and provides the capability to evaluate individual terms numerically for comparison purposes.

1.3 Contributions of the Research

New methods to uncover functional relationships between design parameters of a contemporary control design technique and the resulting closed-loop properties have been proposed. Efforts concentrated on the LQ state feedback technique applied to an aeroelastic flight control task. For this specific application, simple approximate analytical expressions for the closed-loop eigenvalues and zeros in terms of basic parameters such as stability and control derivatives, structural vibration damping and natural frequency, and cost function weights were generated. These expressions explicitly indicate how and by what mechanism the weights augment the short period and aeroelastic modes, as well as the closed-loop zeros. The analytical expressions are used to address topics such as damping, nonminimum phase behavior, stability, and performance, with robustness considerations and design modifications. The additional knowledge afforded by these analytical expressions would be difficult to attain by other means.

1.4 Dissertation Outline

Chapter II is a preliminary chapter that contains development of the airframe dynamic model and flight control design activities. The main body of the dissertation

revolves around Chapters III, IV, and V each dedicated to a specific strategy for developing the desired analytical relationships. Chapter III presents the Direct Eigen-Based Technique, which is built around a key result from LQ root locus theory. Denominator factors are considered exclusively here, numerator factors are not considered. Solution of the Riccati equation is avoided in this approach. Polynomial factoring is accomplished by the existing approximate analytical factoring technique for open-loop systems. Chapter IV presents the Order of Magnitude Technique. Approximate solutions to the Riccati equation are considered in this approach. These solutions are generated by a magnitude analysis technique. Factoring of closed-loop polynomials is also based on an order of magnitude analysis. Both numerator and denominator factors are considered here. Chapter V presents the Cost Function Imbedding Technique. This method is a novel approach that avoids solution of the Riccati equation and polynomial factoring. However, nonlinear algebraic equations, or linearized approximations thereof must be solved. Chapter VI highlights several examples from the analytical expressions generated in Chapters III, IV, and V to demonstrate the practical/useful design information they contain. Chapter VII draws conclusions and gives recommendations.

CHAPTER II

AEROELASTIC MODELING AND CONTROL DESIGN EXAMPLE

2.1 Overview

In this chapter, the vehicle dynamic model and control system development is given. The airframe dynamics are represented by a linear, longitudinal, aeroelastic model that describes the dominant rigid-body pitch mode, the lowest frequency structural mode, and their coupling. Emphasis is given to the analytical model, and numerical data is also provided. Unacceptable dynamic characteristics are noted and motivate the need for feedback augmentation. The LQ state feedback control design technique is reviewed with emphasis given to the algorithm steps and a key result from LQ root locus theory. This technique is used to design a numerical flight control system for the vehicle.

2.2 Aeroelastic Vehicle Model

Within the commercial flight industry there exists considerable interest for the development of a long-range, high-speed, high-capacity vehicle which can serve global transportation markets while remaining a viable concept both economically and environmentally.[49-50] The top-end speeds of this vehicle, coupled with the use of composite materials for the primary structure, will lead to significant interaction between rigid-body and structural dynamics. Lowest frequency structural modes are expected to be well within one frequency decade (rad/s) of the short-period dynamics. This type of vehicle is a prime candidate for, and may necessarily require, a multivariable flight

control system.[51] Therefore, an aeroelastic flight control application is chosen for the analytical expressions work in this dissertation.

To capture the multidisciplinary aspects of rigid-body and vibrational motion, modeling efforts must return to the fundamental governing principles, such as in References 52 through 57. The nonlinear dynamic model generated by such processes can be linearized[11] and reduced in order,[58-66] resulting in a linear model appropriate for flight control design activities. References 67-68 contain a nonlinear model of this flavor for a large, high-speed, elastic vehicle depicted in Figure 2.1. Configuration geometry consists of a low-aspect ratio swept wing, conventional aft tail, and a small canard. Obtaining an accurate linear reduced-order model in the region of crossover for stability augmentation system development was the subject of Reference 35. Reference 35 contains the aeroelastic vehicle model that will be used throughout this research.

A fifth-order polynomial matrix realization of this model is given in Equation (2.1).

$$\begin{bmatrix} s-\frac{Z_\alpha}{V_T} & -(1+\frac{Z_q}{V_T})s & -\frac{Z_\eta}{V_T}s-\frac{Z_\eta}{V_T} & 0 & 0 \\ -M_\alpha & s^2-M_q s & -M_\eta s-M_\eta & 0 & 0 \\ -F_\alpha & -F_q s & s^2+(2\varsigma\omega-F_\eta)s+(\omega^2-F_\eta) & 0 & 0 \\ 0 & -s & 0 & 1 & 0 \\ 0 & -s & \phi's & 0 & 1 \end{bmatrix} \begin{bmatrix} \alpha(s) \\ \theta(s) \\ \eta(s) \\ q(s) \\ q'(s) \end{bmatrix}$$

$$= \begin{bmatrix} \frac{Z_{\delta_E}}{V_T} & \frac{Z_{\delta_C}}{V_T} \\ M_{\delta_E} & M_{\delta_C} \\ F_{\delta_E} & F_{\delta_C} \\ 0 & 0 \\ 0 & 0 \end{bmatrix} \begin{bmatrix} \delta_E(s) \\ \delta_C(s) \end{bmatrix} \qquad (2.1)$$

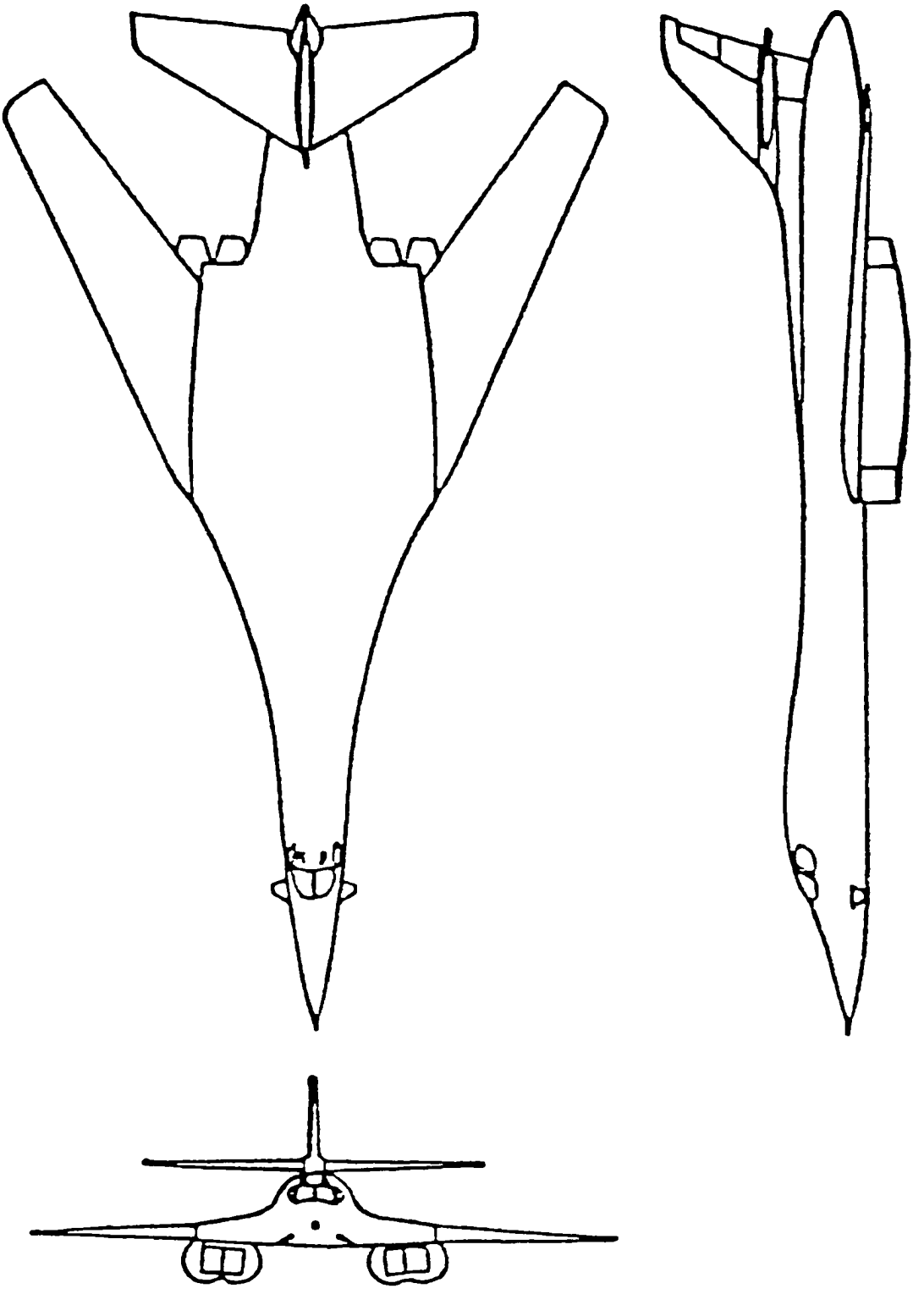

Figure 2.1 Aircraft Configuration Geometry

This model describes the coupled small perturbation longitudinal dynamics of the closely spaced short period and first aeroelastic modes. Degrees of freedom in Equation (2.1) include rigid-body angle of attack and pitch angle denoted as α and θ, while η corresponds to the generalized aeroelasic mode coordinate. Rigid pitch rate q and pitch rate sensed at the cockpit q' are the responses of interest. Control inputs consists of the elevator and canard deflections δ_E and δ_C. The reference flight condition is level, rectilinear, symmetric flight. Other parameters of interest appearing in Equation (2.1) are rigid and aeroelastic stability and control derivatives Z_i, M_i, F_i with i = α, q, η, $\dot{\eta}$, δ_E, δ_C, total flight velocity V_T, structural vibration frequency ω, damping factor ζ, and mode slope at the cockpit ϕ'. These parameters determine the basic dynamic characteristics of the airframe. For example, derivative M_α describes how much pitch acceleration is generated per unit angle of attack. Similarly, F_{δ_c} describes how much generalized force enters into the aeroelastic mode for each unit of canard deflection. Numerical values for the parameters in Equation (2.1) are listed in Table 2.1 corresponding to a flight condition at Mach 0.6 and altitude 5,000 ft. Although the numerical values in Table 2.1 originate from the B-1 aircraft (Figure 2.1) database, the data has been modified to exhibit higher levels of flexibility which are representative of advanced high-speed transport concepts under study today.

Table 2.1 Vehicle Numerical Model Definition

$\frac{Z_\alpha}{V_T} = -0.4158\ s^{-1}$	$(1+\frac{Z_q}{V_T}) = 1.025$

$\frac{Z_\eta}{V_T} = -0.002666\ s^{-1}$	$\frac{Z_{\dot{\eta}}}{V_T} = -0.0001106$
$M_\alpha = -3.330\ s^{-2}$	$M_q = -0.8302\ s^{-1}$
$M_\eta = -0.06549\ s^{-2}$	$M_{\dot{\eta}} = -0.003900\ s^{-1}$
$F_\alpha = -1040\ s^{-2}$	$F_q = -78.35\ s^{-1}$
$(2\zeta\omega - F_\eta) = 0.6214\ s^{-1}$	$(\omega^2 - F_\eta) = 34.83\ s^{-2}$
$\frac{Z_{\delta_E}}{V_T} = -0.08021\ s^{-1}$	$\frac{Z_{\delta_C}}{V_T} = -0.01644\ s^{-1}$
$M_{\delta_E} = -5.115\ s^{-2}$	$M_{\delta_C} = 0.8086\ s^{-2}$
$F_{\delta_E} = -865.6\ s^{-2}$	$F_{\delta_C} = -631.1\ s^{-2}$
$\phi' = 0.02100$ ft/ft	

Denoting y(s) as the output vector and u(s) as the input vector, the transfer function relationships can be expressed as

$$y(s) = G(s)u(s)$$

$$G(s) = \frac{1}{d(s)}\begin{bmatrix} n_{11}(s) & n_{12}(s) \\ n_{21}(s) & n_{22}(s) \end{bmatrix} \tag{2.2}$$

$$y(s) = [q(s) \quad q'(s)]^T$$
$$u(s) = [\delta_E(s) \quad \delta_C(s)]^T$$

In Equation (2.2), G(s) represents the transfer matrix while $n_{ij}(s)$ and d(s) are the numerator and denominator polynomials of the individual transfer functions within G(s). The polynomial d(s) is commonly referred to as the characteristic polynomial for the vehicle. Table 2.2 lists the vehicle transfer function factors corresponding to the numerical model given in Table 2.1. Further, Figures 2.2-2.5 show the q/δ_E, q/δ_C, q'/δ_E and q'/δ_C frequency responses, respectively. For the elevator driven channels, Figures 2.6 and 2.7 indicate the time responses due to a nose up 0.01 rad. elevator step command.

Table 2.2 Vehicle Transfer Function Factors

$$n_{11} = -5.1s(s+0.33)(s^2 - 0.0062s + 24)$$
$$n_{12} = 0.81s(s+0.31)(s^2 + 3.8s + 86)$$
$$n_{21} = 13s(s+0.23)(s-3.4)(s+4.0)$$
$$n_{22} = 14s(s+0.16)(s^2 + 1.3s + 9.4)$$
$$d = s(s^2 + 0.88s + 1.6)(s^2 + 1.0s + 36)$$
$$\psi = -82s^2(s+0.35)$$

From the information given in Table 2.2 and Figures 2.2 through 2.7, important open-loop dynamic deficiencies include the level of damping of both the short-period and aeroelastic modes, as well as aeroelastic contributions to the dynamic responses. Noting the quadratic factors for d(s) in Table 2.2, the short period damping is ζ_{sp}= 0.35 and the aeroelastic mode damping is ζ_{ae}= 0.08. The value for ζ_{sp} is below the necessary value for level 1 flying qualities[69], while the value for ζ_{ae} can be expected to have significant and detrimental effects on flying quality ratings.[70-76]

The presence of the aeroelastic mode peaks near 6 rad/s in Figures 2.2-2.5 indicates high levels of mode interaction are present. This information is also present in Table 2.2 by observing that the factors (s^2-0.0062s+24), (s^2+3.8s+86), (s-3.4)(s+4), and (s^2+1.3s+9.4) in the $n_{ij}(s)$ polynomials do not sufficiently "cover" the aeroelastic factor (s^2+1.0s+36) in d(s). Due to the extreme levels of flexibility in the vehicle structure, and the location of the crew station, the cockpit pitch rate response in Figure 2.7 exhibits high frequency transient motions and response reversal. This nonminimum phase characteristic can be traced directly to the factor (s-3.4) in $n_{21}(s)$ (see Table 2.2). In summary, the airframe dynamics are unacceptable for manual control by the pilot, or for passenger ride comfort, and flight control augmentation is necessary.

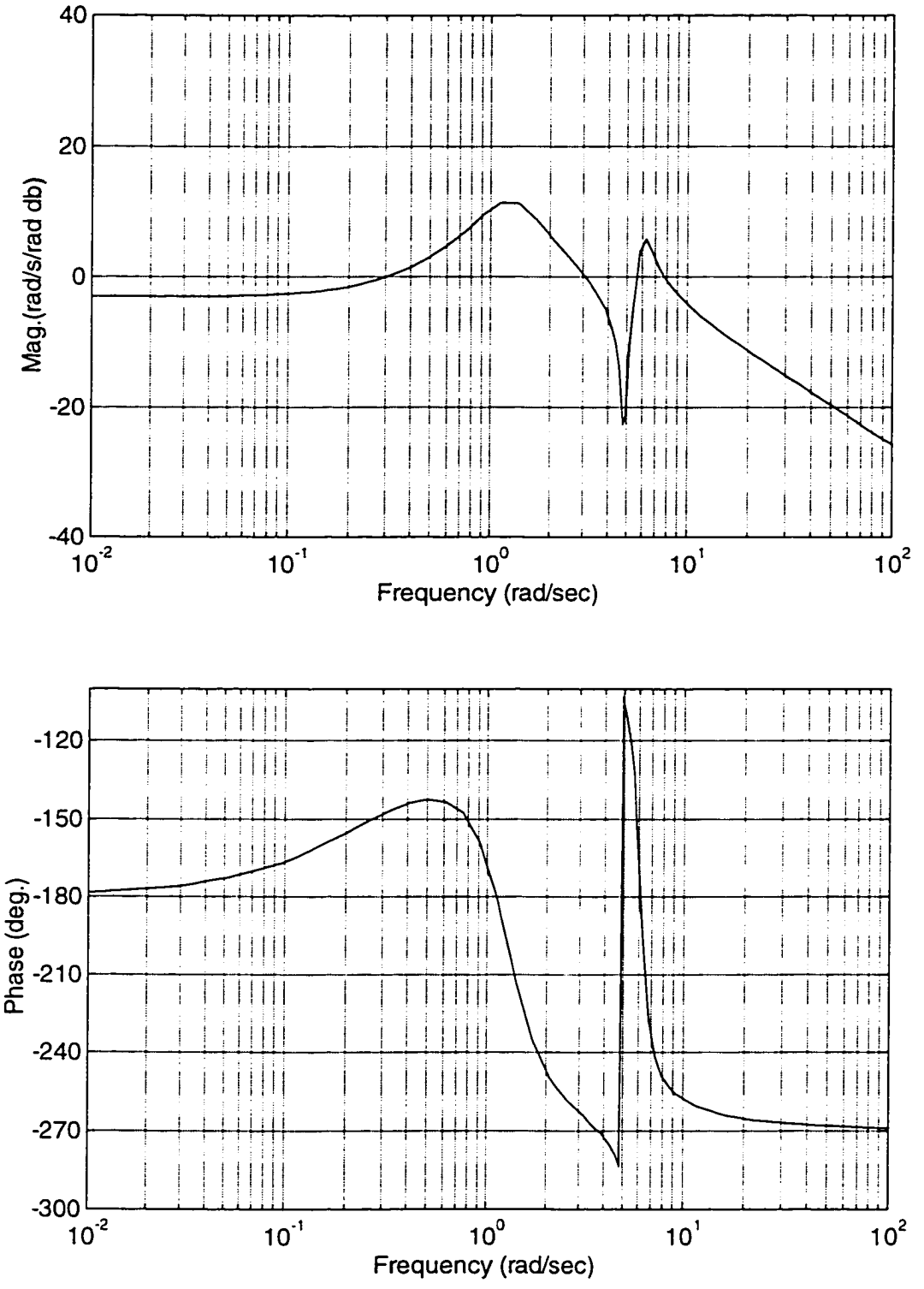

Figure 2.2 Rigid Pitch Rate to Elevator Command Frequency Response

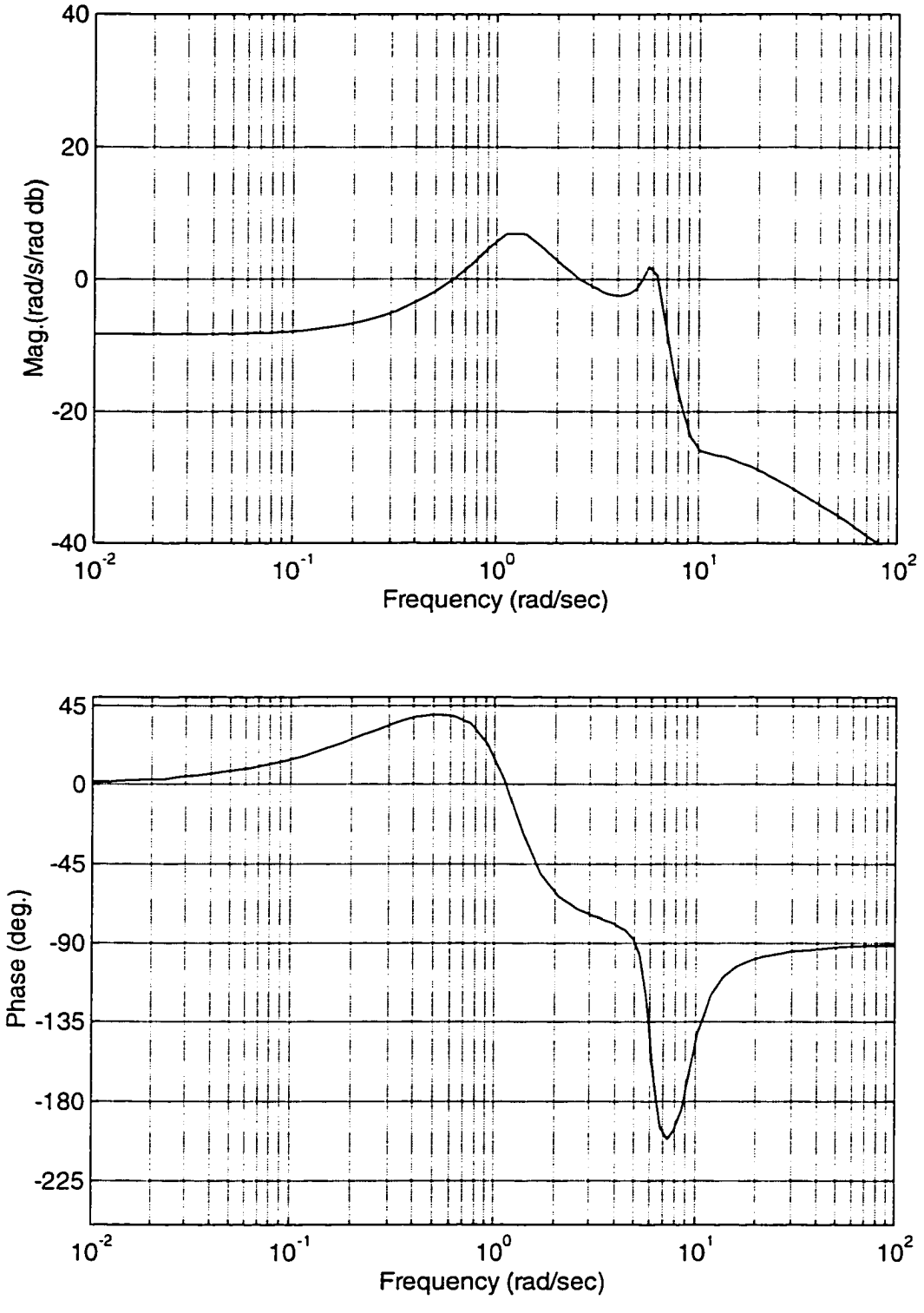

Figure 2.3 Rigid Pitch Rate to Canard Command Frequency Response

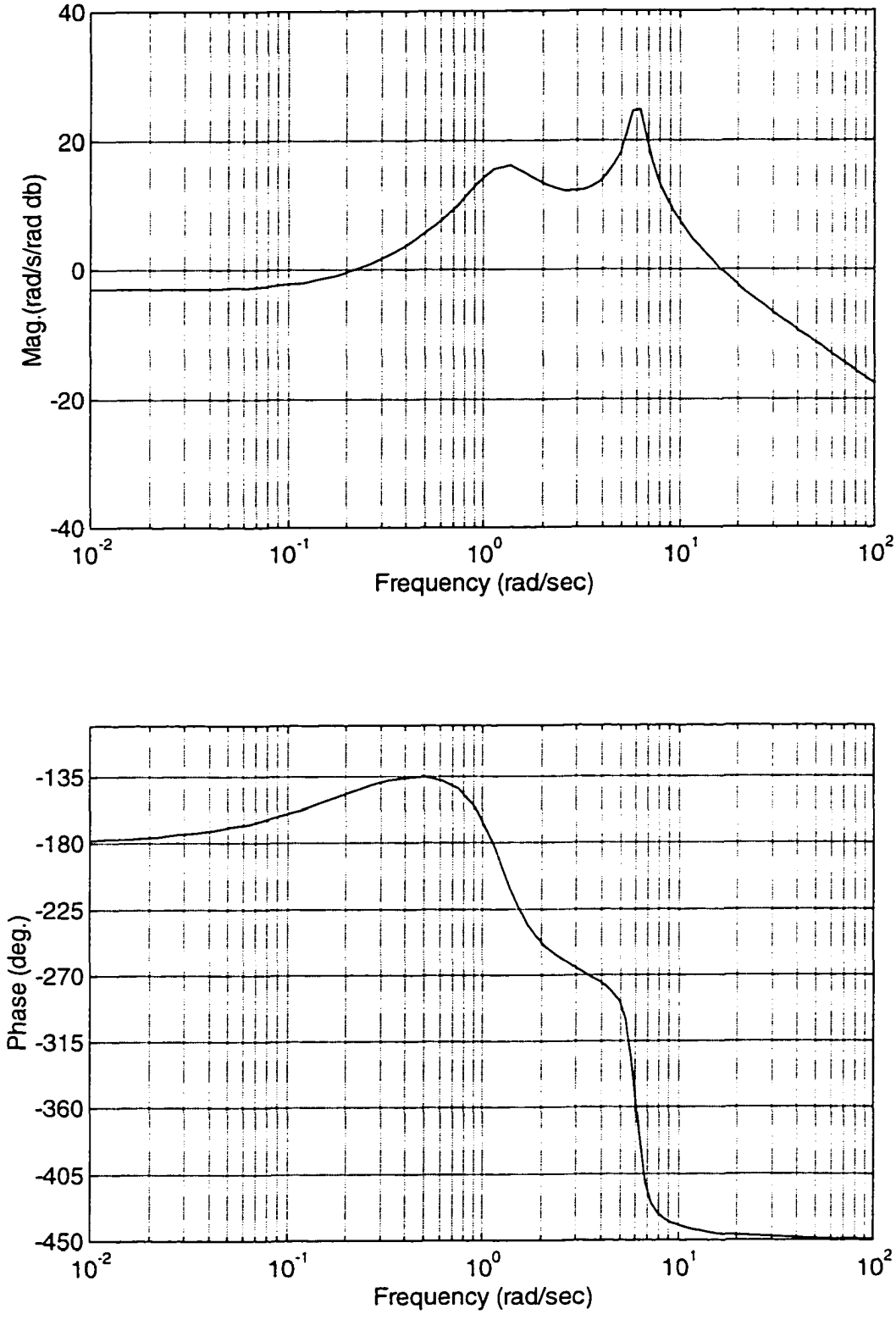

Figure 2.4 Cockpit Pitch Rate to Elevator Command Frequency Response

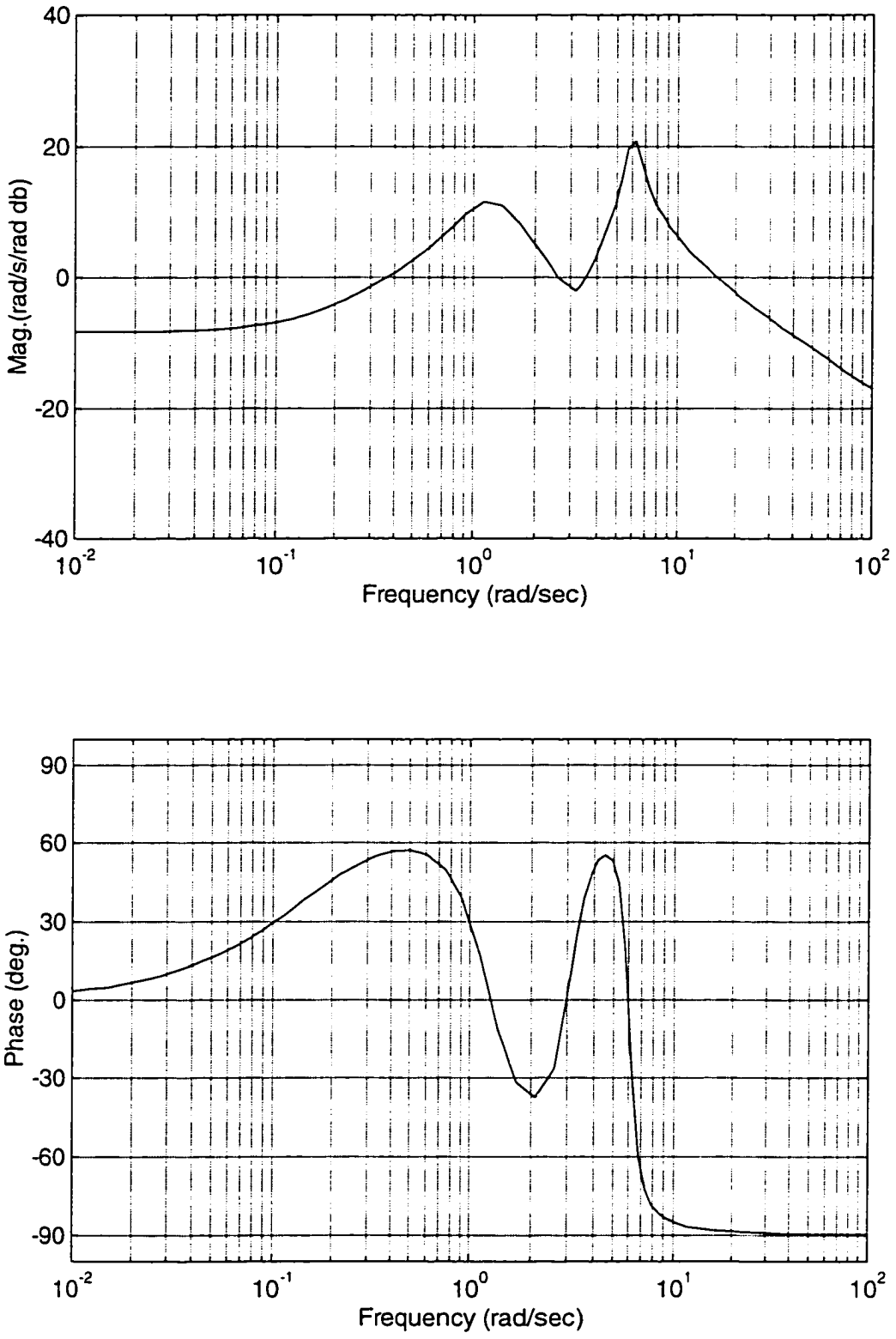

Figure 2.5 Cockpit Pitch Rate to Canard Command Frequency Response

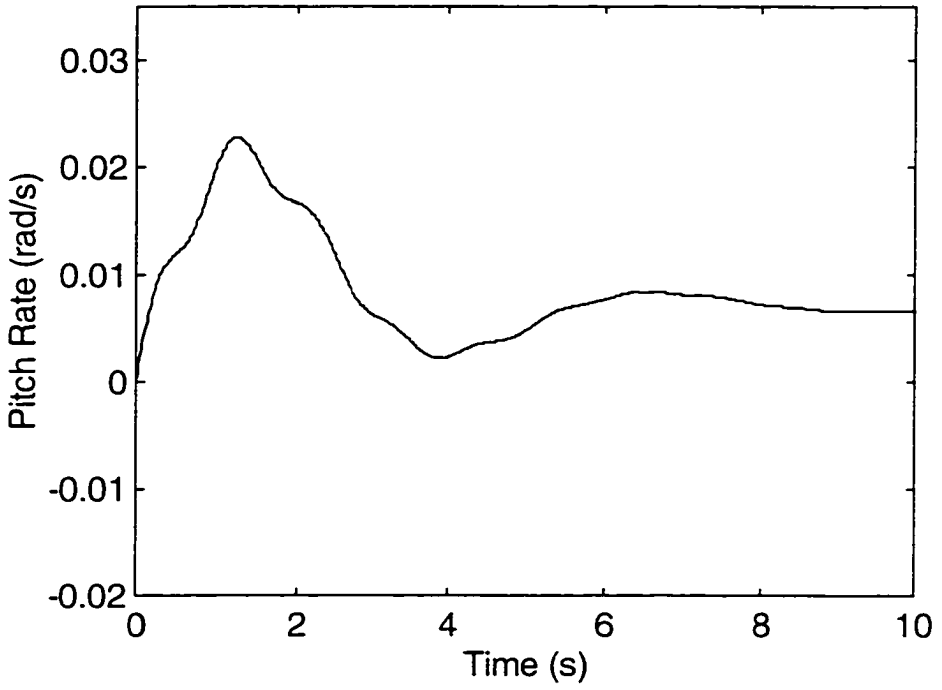

Figure 2.6 Rigid Pitch Rate Time Response for Elevator Command Step

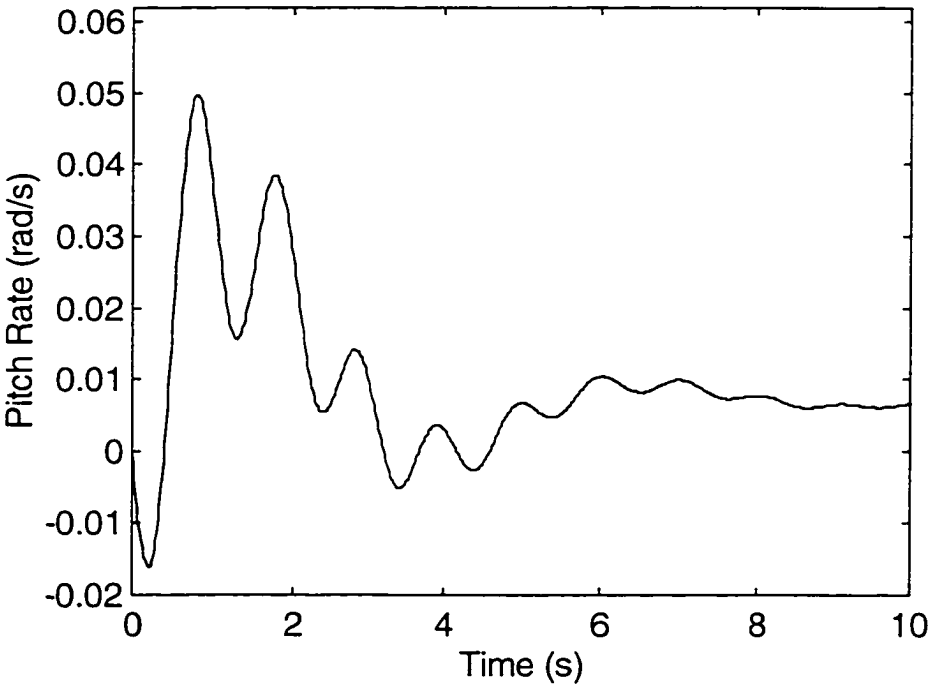

Figure 2.7 Cockpit Pitch Rate Time Response for Elevator Command Step

2.3 Analytical Expressions for Airframe Factors

Before attention is turned to development of the flight control system, consider the origins of the dynamic characteristics discussed above. Key features appearing in Figures 2.2-2.7 have been traced back to the numerical transfer function factors listed in Table 2.2. If these factors could be linked to the basic system parameters appearing in Equation (2.1), the flight dynamics specialist would possess valuable design relationships which could be utilized in configuration layout studies to influence the dynamic characteristics. With such relationships, one can address questions such as how will the modal dampings change if the tail surface is resized or relocated, how will the modal frequencies change if the vehicle structure is stiffened or destiffened, how does the cockpit response behavior change with crew station location along the fuselage, how do characteristics change with flight condition, etc.

Multiple computer runs with adjusted parameters could give answers to these questions, but the results would not indicate how and why these trends occur. To obtain this type of information, analytical relationships between the factors in Table 2.2 and the system parameters in Table 2.1 are necessary. The importance of analytical factoring of transfer function polynomials is thus underscored.

Analytical factoring of the polynomials in Table 2.2 was the subject of Reference 35, and results from this reference will be briefly summarized. Analytical expressions for the transfer function polynomials in Equation (2.2), in a quasi-factored form, can be generated by applying Cramers's rule.[77] Exploiting the resulting structure, preliminary expressions for the factors can be isolated. By expressing the functional dependence of the polynomial coefficients upon the polynomial factors, analytical corrections can also

be generated. Combining the results yields the approximate analytical expressions for the transfer function factors. The details of this process will be deferred until factoring of closed-loop polynomials is considered in Chapter III. Table 2.3 lists the approximate analytical expressions obtained by the above steps for the q/δ_E, q/δ_C, q'/δ_E, and q'/δ_C transfer function factors in Table 2.2.

Before ever using the approximate analytical expressions in Table 2.3, first consider their accuracy. Table 2.4 lists the exact numerical values for the factors (see Table 2.2) along with the numerical values computed from the approximate expressions in Table 2.3. Further, Figures 2.8-2.11 contrast the exact numerical frequency responses with those computed from the expressions in Table 2.3. The comparison in Table 2.4 and Figures 2.8-2.11 indicates the approximate expressions are sufficiently accurate and can be used with confidence to explore the relationship between overall dynamic characteristics and the basic system parameters. To simplify the notation associated with the analytical expression results in Table 2.3, the following substitutions have been used

$$\tilde{Z}_\alpha = \frac{Z_\alpha}{V_T}, \quad \tilde{Z}_q = 1 + \frac{Z_q}{V_T}, \quad \tilde{Z}_\eta = \frac{Z_\eta}{V_T}, \quad \tilde{Z}_\eta = \frac{Z_\eta}{V_T}, \quad \tilde{Z}_{\delta_E} = \frac{Z_{\delta_E}}{V_T}$$

$$\tilde{Z}_{\delta_c} = \frac{Z_{\delta_c}}{V_T}, \quad \tilde{F}_\eta = 2\varsigma\omega - F_\eta, \quad \tilde{F}_\eta = \omega^2 - F_\eta$$

Table 2.3 Approximate Symbolic Expressions for the Factored Transfer Functions

$$n_{11}(s) = K_q^{\delta_E} s[s + {}_{sp}(\frac{1}{\tau})_q^{\delta_E}][s^2 + {}_{ae}(2\varsigma\omega)_q^{\delta_E} s + {}_{ae}(\omega^2)_q^{\delta_E}]$$

$$n_{12}(s) = K_q^{\delta_C} s[s + {}_{sp}(\frac{1}{\tau})_q^{\delta_C}][s^2 + {}_{ae}(2\varsigma\omega)_q^{\delta_C} s + {}_{ae}(\omega^2)_q^{\delta_C}]$$

$$n_{21}(s) = K_{q'}^{\delta_E} s[s + {}_{sp}(\frac{1}{\tau})_{q'}^{\delta_E}][s + {}_{ae}(\frac{1}{\tau_1})_{q'}^{\delta_E}][s + {}_{ae}(\frac{1}{\tau_2})_{q'}^{\delta_E}]$$

$$n_{22}(s) = K_q^{\delta_C} s[s + {}_{sp}(\frac{1}{\tau})_q^{\delta_C}][s^2 + {}_{ae}(2\zeta\omega)_q^{\delta_C} s + {}_{ae}(\omega^2)_q^{\delta_C}]$$

$$d(s) = s[s^2 + (2\zeta\omega)_{sp} s + (\omega^2)_{sp}][s^2 + (2\zeta\omega)_{ae} s + (\omega^2)_{ae}]$$

$$(\omega^2)_{sp} \approx \tilde{Z}_\alpha M_q - \tilde{Z}_q M_\alpha - \frac{\tilde{Z}_q M_\eta F_\alpha}{\tilde{F}_\eta}$$

$$(2\zeta\omega)_{sp} \approx -\tilde{Z}_\alpha - M_q - \frac{(\tilde{Z}_\eta + \tilde{Z}_q M_\eta)F_\alpha + M_\eta F_q}{\tilde{F}_\eta}$$

$$(\omega^2)_{ae} \approx \tilde{F}_\eta + \frac{\tilde{Z}_q M_\eta F_\alpha}{\tilde{F}_\eta}$$

$$(2\zeta\omega)_{ae} \approx \tilde{F}_\eta + \frac{(\tilde{Z}_\eta + \tilde{Z}_q M_\eta)F_\alpha + M_\eta F_q}{\tilde{F}_\eta}$$

$$K_q^{\delta_E} \approx M_{\delta_E}$$

$${}_{sp}(\frac{1}{\tau})_q^{\delta_E} \approx \frac{-\tilde{Z}_\alpha \tilde{F}_\eta M_{\delta_E} - F_\alpha \tilde{Z}_\eta M_{\delta_E} + M_\alpha \tilde{Z}_\eta F_{\delta_E} - \tilde{Z}_\alpha M_\eta F_{\delta_E}}{\tilde{F}_\eta M_{\delta_E} + M_\eta F_{\delta_E}}$$

$${}_{ae}(\omega^2)_q^{\delta_E} \approx \frac{\tilde{F}_\eta M_{\delta_E} + M_\eta F_{\delta_E}}{M_{\delta_E}}$$

$${}_{ae}(2\zeta\omega)_q^{\delta_E} \approx \frac{1}{2}\frac{-M_{\delta_E}^2 \tilde{F}_\eta \tilde{F}_\eta - M_\eta F_{\delta_E} \tilde{F}_\eta M_{\delta_E} - M_\alpha \tilde{Z}_{\delta_E} M_\eta F_{\delta_E}}{M_{\delta_E}(-\tilde{F}_\eta M_{\delta_E} - M_\eta F_{\delta_E})}$$

$$K_q^{\delta_C} \approx M_{\delta_C}$$

$${}_{sp}(\frac{1}{\tau})_q^{\delta_C} \approx \tilde{Z}_\alpha - \frac{F_{\delta_C} M_\alpha \tilde{Z}_\eta}{F_{\delta_C} M_\eta + M_{\delta_C} \tilde{F}_\eta}$$

$${}_{ae}(2\zeta\omega)_q^{\delta_C} \approx \frac{F_{\delta_C} M_\eta}{M_{\delta_C}} + \tilde{F}_\eta$$

$${}_{ae}(\omega^2)_q^{\delta_C} \approx \frac{F_{\delta_C} M_\eta}{M_{\delta_C}} + \tilde{F}_\eta$$

$$K_q^{\delta_E} \approx -\phi' F_{\delta_E} + M_{\delta_E}$$

$$_{sp}(\frac{1}{\tau})_q^{\delta_E} \approx -\tilde{Z}_\alpha - \frac{M_{\delta_E} F_\alpha \tilde{Z}_\eta + F_{\delta_E} \tilde{Z}_\alpha M_\eta}{M_{\delta_E} \tilde{F}_\eta}$$

$$_{ae}(\frac{1}{\tau_1})_q^{\delta_E} \approx \frac{b - [b^2 - 4c]^{\frac{1}{2}}}{2} + \frac{F_q M_{\delta_E}}{2F_{\delta_E}}$$

$$_{ae}(\frac{1}{\tau_2})_q^{\delta_E} \approx \frac{b + [b^2 - 4c]^{\frac{1}{2}}}{2} + \frac{F_q M_{\delta_E}}{2F_{\delta_E}}$$

$$c = \frac{M_{\delta_E} \tilde{F}_\eta}{-\phi' F_{\delta_E} + M_{\delta_E}} \qquad b = \frac{M_{\delta_E} \tilde{F}_\eta + \phi' F_{\delta_E} M_q}{-\phi' F_{\delta_E} + M_{\delta_E}}$$

$$K_q^{\delta_C} \approx M_{\delta_C} - \phi' F_{\delta_C}$$

$$_{sp}(\frac{1}{\tau})_q^{\delta_C} \approx -\tilde{Z}_\alpha + \frac{[\tilde{Z}_\eta M_\alpha + \phi' \tilde{Z}_\alpha \tilde{Z}_q M_\alpha - \tilde{Z}_\alpha M_\eta] F_{\delta_C}}{\tilde{F}_\eta M_{\delta_C}}$$

$$_{ae}(\omega^2)_q^{\delta_C} \approx \frac{\tilde{F}_\eta M_{\delta_C}}{M_{\delta_C} - \phi' F_{\delta_C}} - \frac{M_\eta + \phi' \tilde{Z}_q M_\alpha}{\phi'}$$

$$_{ae}(2\zeta\omega)_q^{\delta_C} \approx \frac{\tilde{F}_\eta M_{\delta_C} + \phi' M_q F_{\delta_C}}{M_{\delta_C} - \phi' F_{\delta_C}} - \frac{\phi' \tilde{Z}_\alpha \tilde{Z}_q M_\alpha F_{\delta_C}}{\tilde{F}_\eta M_{\delta_C}}$$

Table 2.4 Accuracy of Approximate Symbolic Expressions for $n_{ij}(s)$, $d(s)$

Factor	Exact	Approximate Symbolic
$(\omega^2)_{sp}$ $1/s^2$	1.6	1.8
$(\omega^2)_{ae}$ $1/s^2$	36	37

$(2\zeta\omega)_{sp}$ 1/s	0.88	0.90
$(2\zeta\omega)_{ae}$ 1/s	1.0	0.97
$K_q^{\delta_E}$ rad/s/rad	-5.1	-5.1
$_{sp}(\frac{1}{\tau})_q^{\delta_E}$ 1/s	0.33	0.36
$_{ae}(2\zeta\omega)_q^{\delta_E}$ 1/s	-0.0062	-0.016
$_{ae}(\omega^2)_q^{\delta_E}$ 1/s^2	24	24
$K_q^{\delta_C}$ rad/s/rad	0.81	0.81
$_{sp}(\frac{1}{\tau})_q^{\delta_C}$ 1/s	0.31	0.34
$_{ae}(2\zeta\omega)_q^{\delta_C}$ 1/s	3.8	3.7
$_{ae}(\omega^2)_q^{\delta_C}$ 1/s^2	86	86
$K_q^{\delta_E}$ rad/s/rad	13	13
$_{sp}(\frac{1}{\tau})_q^{\delta_E}$ 1/s	0.23	0.20
$_{ae}(\frac{1}{\tau_1})_q^{\delta_E}$ 1/s	-3.4	-3.5
$_{ae}(\frac{1}{\tau_2})_q^{\delta_E}$ 1/s	4.0	3.9
$K_q^{\delta_C}$ rad/s/rad	14	14
$_{sp}(\frac{1}{\tau})_q^{\delta_C}$ 1/s	0.16	0.16

$_{ae}(2\varsigma\omega)^{\delta_c}_{q^*}$ 1/s	1.3	1.5
$_{ae}(\omega^2)^{\delta_c}_{q^*}$ 1/s^2	9.4	8.5

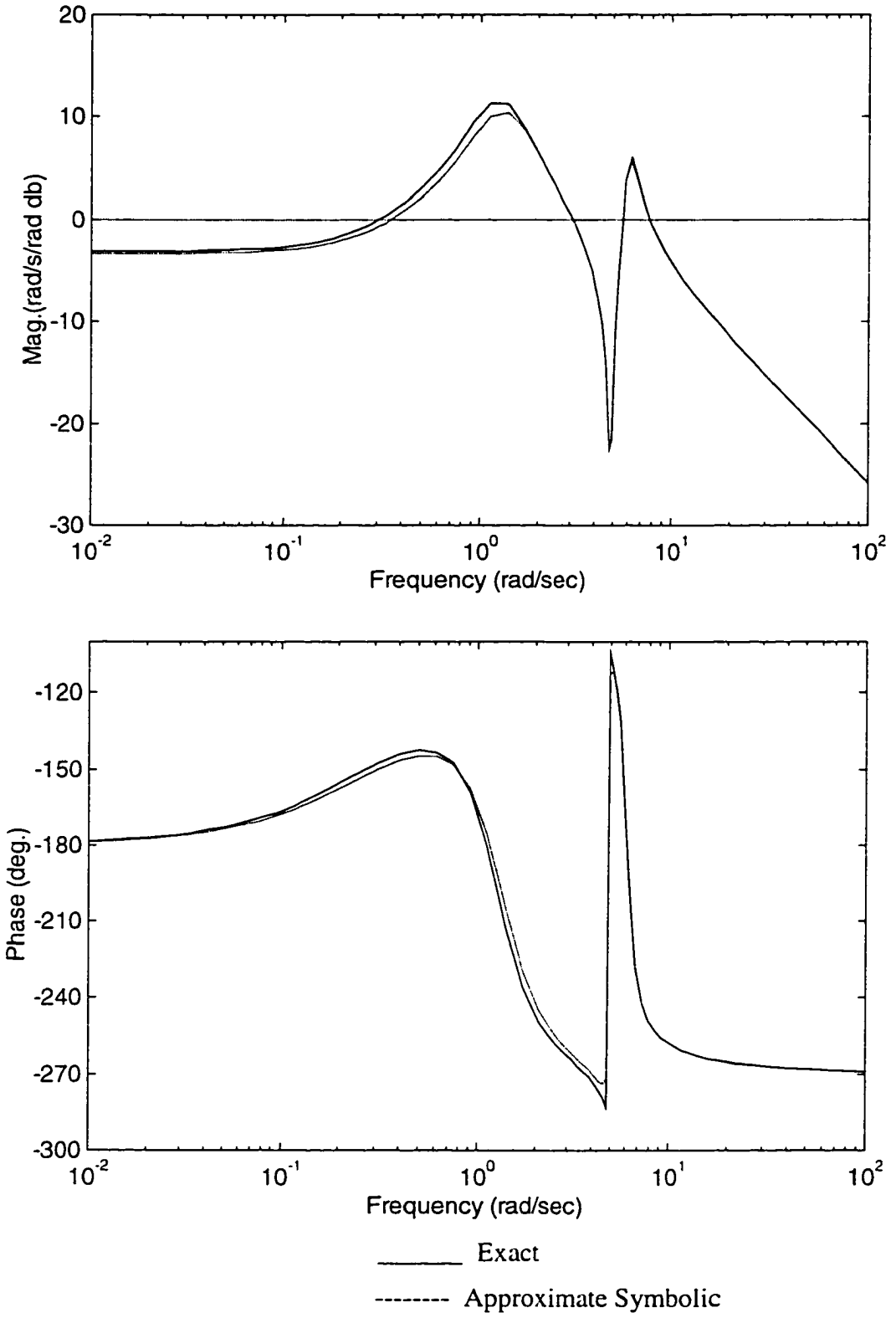

Figure 2.8 Comparison of q/δ_E Frequency Responses Using the Approximate Symbolic Calculations

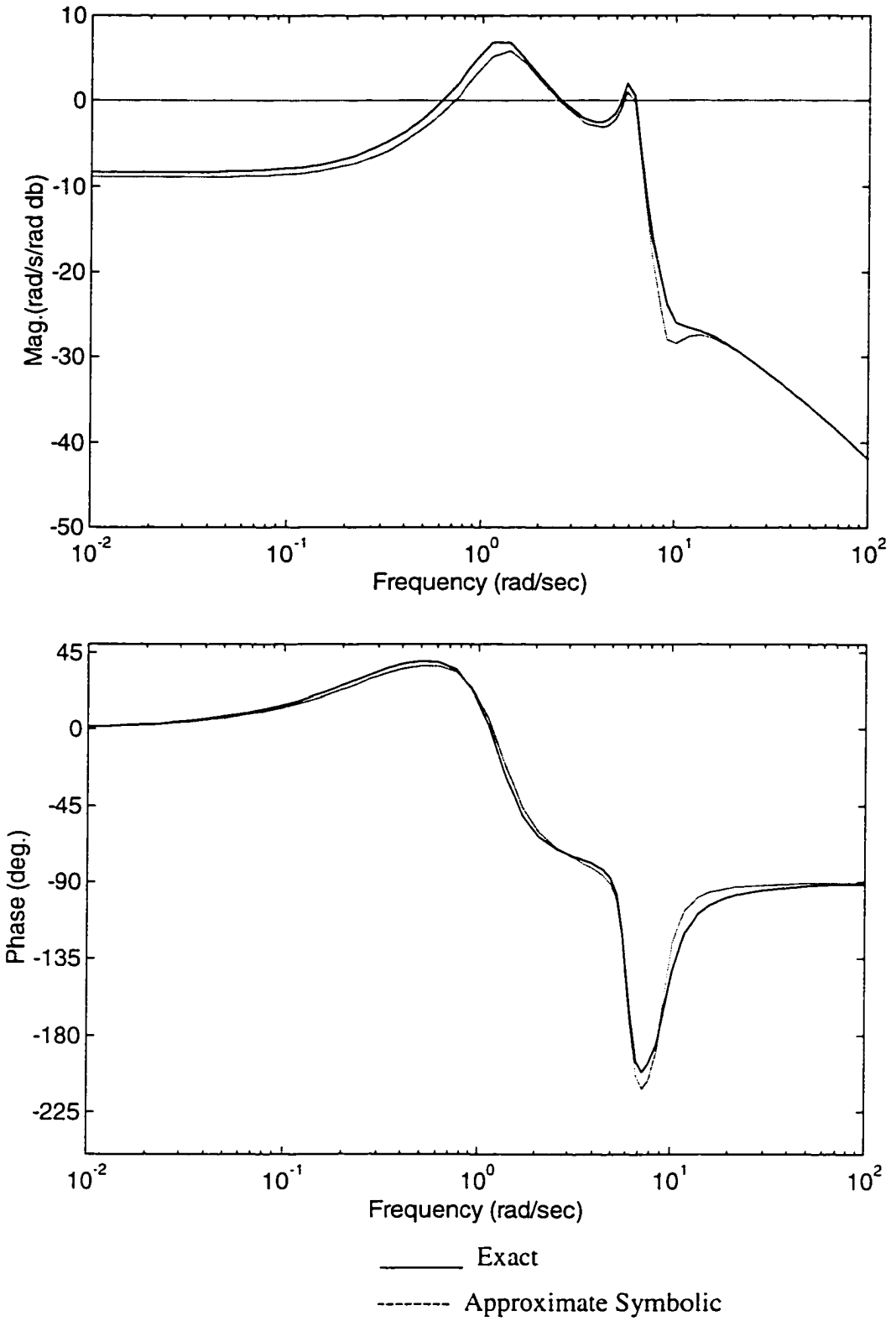

Figure 2.9 Comparison of q/δ_C Frequency Responses Using the Approximate Symbolic Calculations

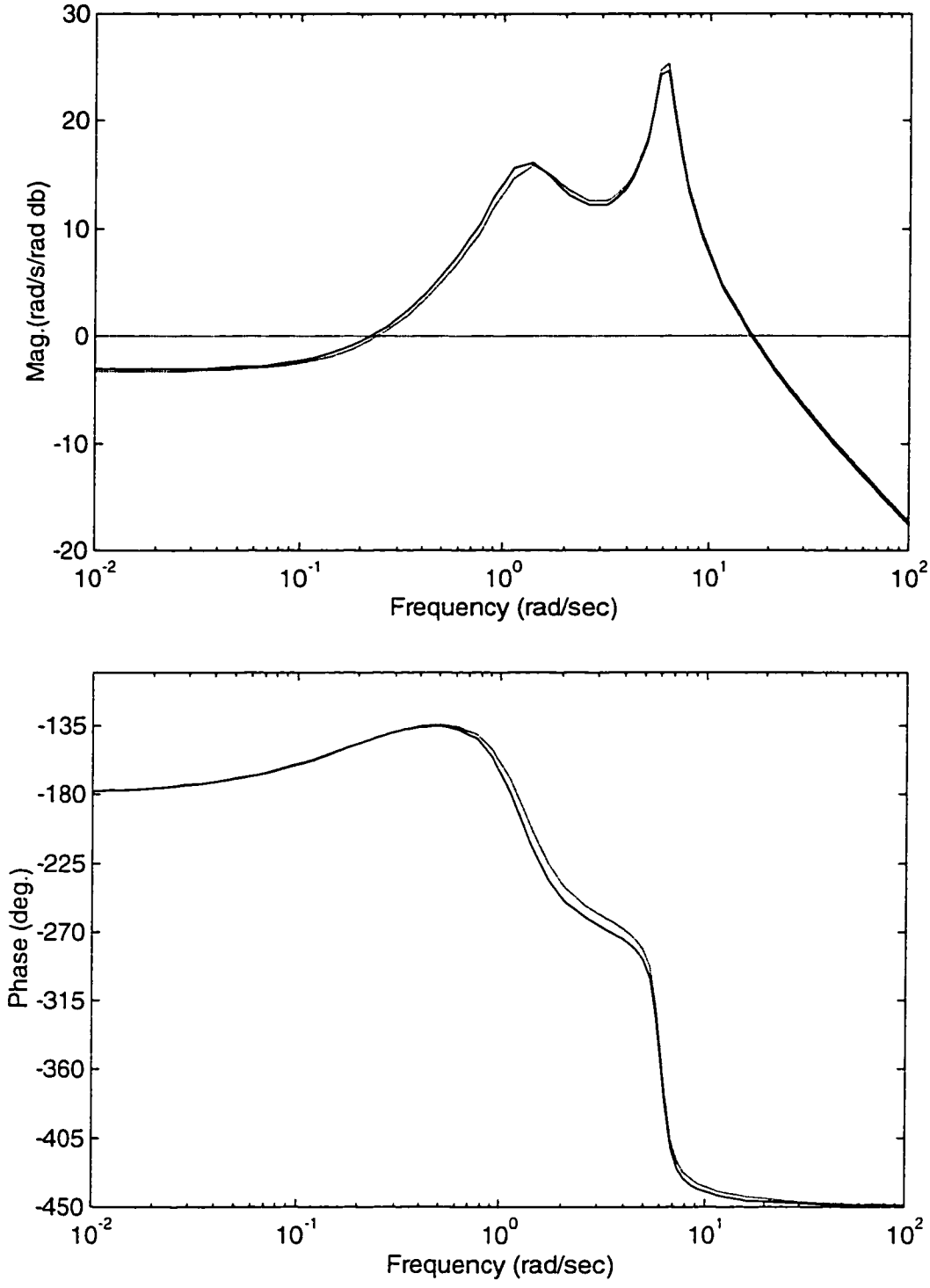

Figure 2.10 Comparison of q'/δ_E Frequency Responses Using the Approximate Symbolic Calculations

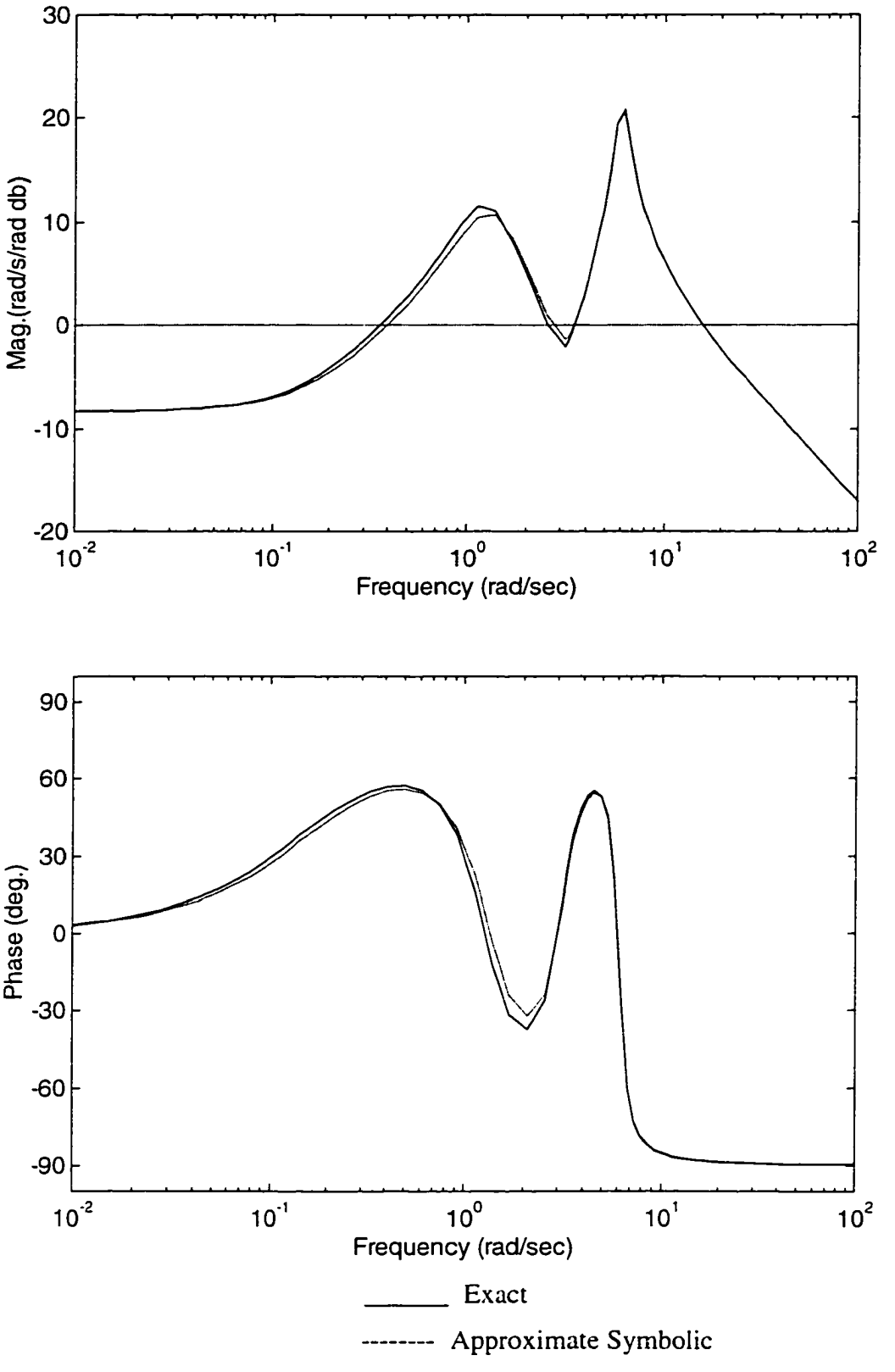

Figure 2.11 Comparison of q'/δ_C Frequency Responses Using the Approximate Symbolic Calculations

Now consider the analytical expressions and the insight they can provide into the dynamic characteristics. First consider the lightly damped complex poles in the airframe characteristic polynomial d(s). Recall the damping of these poles are responsible for the large modal peaks in Figures 2.2-2.5, the high frequency transient motions in Figures 2.6-2.7, and ultimately poor flying qualities. The expression for the damping term $(2\varsigma\omega)_{ae}$ appearing in Table (2.3) is

$$(2\varsigma\omega)_{ae} \approx \tilde{F}_\eta + \frac{(\tilde{Z}_\eta + \tilde{Z}_q M_\eta)F_\alpha + M_\eta F_q}{\tilde{F}_\eta} \qquad (2.3)$$
$$= 0.62 + 0.35$$

As seen from Equation (2.3), the low damping value is primarily due to the inherently low structural damping and aerodynamic damping $\tilde{F}_\eta = (2\varsigma\omega - F_\eta)$.

However, note that approximately one-third of the total damping originates from other sources, such as aerodynamic coupling between the rigid and elastic degrees of freedom, i.e., $M_\eta F_q$, $\tilde{Z}_\eta F_\alpha$, and $\tilde{Z}_q M_\eta F_\alpha$ For example, an initial disturbance in the structural deflection coordinate η generates a pitch moment and pitch rate due to the stability derivative M_η. In turn, with the stability derivative F_q, pitch rate motions will result in a generalized force and structural deflection η that opposes the initial disturbance. This coupling produces a damping effect on the aeroelastic mode. With this insight, adjustments to the vehicle geometry could be tailored to enhance these coupling effects to increase aeroelastic mode damping without increasing structural damping.

Now focus attention on exposing the parameters which strongly affect the nonminimum phase zero in the $n_{21}(s)$ numerator polynomial. Recall this right half plane

zero is responsible for the initial response reversal in the q'/δ_E channel in Figure 2.7. Consider the expression for the numerator term $_{ze}(\frac{1}{\tau_1})^{\delta_E}_{q'}$ from Table 2.3

$$
\begin{aligned}
{}_{ze}(\frac{1}{\tau_1})^{\delta_E}_{q'} &\approx \frac{b-[b^2-4c]^{\frac{1}{2}}}{2}+\frac{F_q M_{\delta_E}}{2F_{\delta_E}} \\
&= -3.3+(-0.23)
\end{aligned}
\tag{2.4}
$$

As seen in Equation (2.4), the zero location is primarily a function of the first term which, in turn, is primarily a function of the parameter c as given in Table 2.3, or

$$
\begin{aligned}
c &= \frac{\tilde{F}_\eta M_{\delta_E}}{M_{\delta_E}-\phi' F_{\delta_E}} \\
&= \frac{-180}{-5.1-(-18)}
\end{aligned}
\tag{2.5}
$$

From the denominator in Equation (2.5), it is apparent that relative control power affecting the rigid and elastic pitch motions (i.e., M_{δ_E} vs. F_{δ_E}) is a key influence on the nonminimum phase characteristics. Note that an up elevation pulse induces rigid-body pitch up and elastic pitch down motions. For this highly flexible vehicle, the elastic pitch control power term determines the sign of c, and ultimately the numerator root location. Further, it can be seen how the pitch-rate sensor location, through ϕ', affects the nonminimum phase characteristic. These results provide valuable insights concerning the tradeoffs existing between tail placement, internal structural layout, and crew station placement, when attempting to reduce the nonminimum phase behavior. The valuable insight obtained by the open-loop analytical expressions discussed here strongly motivates the objectives of this dissertation: to apply these strategies to closed-loop systems developed with contemporary design techniques.

2.4 Linear Quadratic State Feedback Review

In this section, a review of the LQ state feedback control design technique is given.[7,78] Only topics necessary to meet the research objectives are addressed. These topics include steps to exercise the algorithm, and lesser-known, often overlooked closed-loop characteristic polynomial (LQ root locus) results.

Suppose the state space description for the vehicle model in Equation (2.1) is

$$\begin{aligned} \dot{x}(t) &= Ax(t) + Bu(t) \\ y(t) &= Cx(t) \end{aligned} \tag{2.6}$$

The mathematical objective in the LQ state feedback strategy is to minimize a quadratic cost function involving the system response and input subject to Equation (2.6), or

$$J = \frac{1}{2}\int_{t_i}^{t_f} [y^T Q y + u^T R u] d\tau + \frac{1}{2} x^T(t_f) P(t_f) x(t_f) \tag{2.7}$$

The Hamiltonian is given by

$$H(t) = \frac{1}{2}(x^T C^T Q C x + u^T R u) + \lambda^T (Ax + Bu) \tag{2.8}$$

and necessary conditions for optimality are

$$\begin{aligned} \left(\frac{\partial H}{\partial \lambda}\right)^T &= \dot{x} = Ax + Bu \\ \left(\frac{\partial H}{\partial x}\right)^T &= -\dot{\lambda} = C^T Q C x + A^T \lambda \\ \left(\frac{\partial H}{\partial u}\right)^T &= 0 = Ru + B^T \lambda \end{aligned} \tag{2.9}$$

These equations must be solved with boundary conditions at $x(t_i)$ and $\lambda(t_f) = P(t_f)\, x(t_f)$ to find the optimal input u.

Using $\left(\frac{\partial H}{\partial u}\right)^T$ in Equation (2.9), the optimal control input can be expressed in terms of the co-state.

$$u(t) = -R^{-1}B^T\lambda(t) \tag{2.10}$$

Substitute u from Equation (2.10) into $\left(\frac{\partial H}{\partial \lambda}\right)^T$ in Equation (2.9) leads to the homogeneous *Hamiltonian system* for the state and co-state variables, or

$$\dot{z} = Hz$$
$$z = \begin{bmatrix} x \\ \lambda \end{bmatrix} \quad , \quad H = \begin{bmatrix} A & -BR^{-1}B^T \\ -C^TQC & -A^T \end{bmatrix} \tag{2.11}$$

Denote the state transition matrix for Equation (2.11) as $\Phi(t,t_i)$ (i.e., $z(t) = \Phi(t,t_i)z(t_i)$), and partition $\Phi(t,t_i)$ in accordance with Equation (2.11),

$$\Phi(t,t_1) = \begin{bmatrix} \Phi_{11}(t,t_1) & \Phi_{12}(t,t_1) \\ \Phi_{21}(t,t_1) & \Phi_{22}(t,t_1) \end{bmatrix} \tag{2.12}$$

With this notation, the state and co-state at time t can be expressed in terms of final time condition.

$$\begin{aligned} x(t) &= \Phi_{11}(t,t_f)x(t_f) + \Phi_{12}(t,t_f)\lambda(t_f) \\ \lambda(t) &= \Phi_{21}(t,t_f)x(t_f) + \Phi_{22}(t,t_f)\lambda(t_f) \end{aligned} \tag{2.13}$$

By replacing $\lambda(t_f)$ with $P(t_f)x(t_f)$ and in turn eliminating $x(t_f)$, Equation (2.13) becomes

$$\lambda^T(t) = [\Phi_{21}(t,t_f) + \Phi_{22}(t,t_f)P(t_f)][\Phi_{11}(t,t_f) + \Phi_{12}(t,t_f)P(t_f)]^{-1}x(t) \tag{2.14}$$

With the final time representing an infinite horizon ($t_f = \infty$), λ becomes time-invariant proportional to x

$$\lambda(t) = Px(t) \tag{2.15}$$

and the optimal input can now be expressed as a function of the state variable, or

$$\begin{aligned} u &= -K_R x \\ K_R &= R^{-1}B^T P \end{aligned} \tag{2.16}$$

where K_R is the regulator feedback gain. If the closed-loop system is excited by external commands, then

$$u = u_c - K_R x \tag{2.17}$$

where u_c denotes the command signal. The closed-loop state space system becomes

$$\begin{aligned} \dot{x} &= (A - BK_R)x + Bu_c \\ y &= Cx \end{aligned} \tag{2.18}$$

and Figure 2.12 illustrates the closed-loop block diagram.

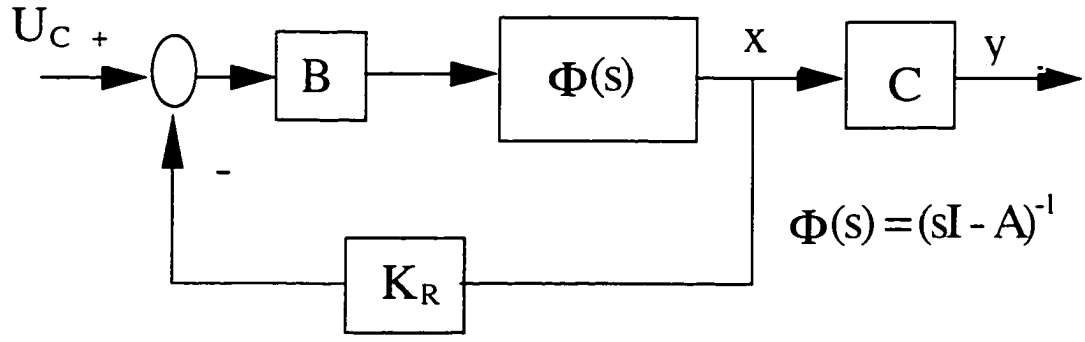

Figure 2.12 The Closed-Loop Block Diagram

To determine the unknown value for P, consider differentiating Equation (2.15) with respect to time.

$$\dot{\lambda} = P\dot{x} \tag{2.19}$$

Substituting for $\dot{\lambda}$ and $\dot{x}$ from Equation (2.11) and eliminating λ with Equation (2.15) yields the algebraic Riccati equation.

$$PA + A^T P - PBR^{-1}B^T P + C^T QC = 0 \tag{2.20}$$

In summary, to exercise the LQ state feedback design technique in the framework just presented, the following steps are necessary:

1. Specify cost weights Q, R.
2. Compute Riccati solution P.
3. Compute the feedback gain K_R.
4. Compute the closed-loop system A-BK_R, B, C.

The result is a closed-loop system with minimal value for J. In practice, these steps are revisited in a design cycle with modified Q and R weights to satisfy engineering requirements associated with closed-loop stability and performance.

A key result, which forms the basis of LQ root locus theory, is highlighted from Reference 2. Reconsider the homogeneous Hamiltonian system in Equation (2.11). Utilizing determinate identities from Reference 77, the function $\det[sI - H]$ can be manipulated as follows.

$$\begin{aligned} \det[sI - H] &= \det\begin{bmatrix} sI - A & BR^{-1}B^T \\ C^T QC & sI + A^T \end{bmatrix} \\ &= \det[sI - A]\det[(sI + A^T) - C^T QC(sI - A)^{-1}BR^{-1}B^T] \end{aligned} \tag{2.21}$$

Further, the function $\det[-sI - H]$ can also be manipulated.

$$\begin{aligned}\det[-sI-H] &= \det\begin{bmatrix} -sI-A & BR^{-1}B^T \\ C^TQC & -sI+A^T \end{bmatrix} \\ &= \det[-sI+A^T]\det[(-sI-A)-BR^{-1}B^T(-sI+A^T)^{-1}C^TQC] \\ &= \det[-sI+A^T]\det[(-sI-A)-BR^{-1}B^T(-sI+A^T)^{-1}C^TQC] \\ &= \det[sI-A]\det[(sI+A^T)-C^TQC(sI-A)^{-1}BR^{-1}B^T]\end{aligned} \tag{2.22}$$

The functions in Equations (2.21) and (2.22) are equivalent. This result implies that if s is an eigenvalue of H, $-s$ is also an eigenvalue. The eigenvalues form a mirror image about the imaginary axis, and the characteristic polynomial for this system is a polynomial in s^2.

The characteristic equation for the closed-loop system is

$$\det[sI-H]=0 \tag{2.23}$$

Manipulation of the left-hand side of Equation (2.23) yields

$$\begin{aligned}\det[sI-H] &= \det\begin{bmatrix} sI-A & BR^{-1}B^T \\ C^TQC & sI+A^T \end{bmatrix} \\ &= \det[sI-A]\det[(sI+A^T)-C^TQC(sI-A)^{-1}BR^{-1}B^T] \\ &= \det[sI-A]\det[sI+A^T]\det[I-C^TQC(sI-A)^{-1}BR^{-1}B^T(sI+A^T)^{-1}] \\ &= (-1)^n\det[sI-A]\det[-sI-A]\det[I+R^{-1}B^T(-sI-A^T)^{-1}C^TQC(sI-A)^{-1}B]\end{aligned} \tag{2.24}$$

where n is the number of state variables. By introducing the vehicle transfer matrix and denominator polynomial notation

$$G(s)=C(sI-A)^{-1}B, \qquad d(s)=\det[sI-A] \tag{2.25}$$

Followed with the same manipulation, the closed-loop characteristic equation in Equation (2.23) becomes

$$d(s)d(-s)\det[R+G(-s)^TQG(s)]=0 \tag{2.26}$$

Note the Riccati equation solution P, and the feedback gain matrix K_R, do not appear in Equation (2.26). This result provides an explicit relationship between the closed-loop denominator factors and the cost weights Q and R. Chapter III exploits this relationship.

2.5 Numerical Design Example

The objectives of the flight control system are to correct the characteristics noted in Section 2.2, as well as provide satisfactory levels of robustness to modeling errors with feedback architecture as simple as possible. As an initial step into the closed-loop analytical expressions work, consider the standard LQ state feedback strategy discussed in Section 2.4 for flight control system development. Although better formulations for flight control design exist,[6.11] the standard LQ approach is the most well-known contemporary design technique, and it provides a simple framework for illustrating the analytical expressions work.

Specification of the control input and response output set is a key step in developing a successful flight control system. The input and output variables considered in Equations (2.1)-(2.2) are utilized here. Selection of q' and δ_C in this set provides a close proximity actuator-sensor pair near the nose of the fuselage. This feedback channel should provide ample opportunity to suppress the harsh vibrational environment predicted at the cockpit. Also included in this set is q and δ_E. Historically, this pair of signals has proven to be effective in basic stability augmentation systems for the pitch axis.[9]

At this stage, the only freedom left unspecified are the weights Q and R. For the 2x2 aircraft system given in Equation (2.1), the cost weighting matrices are

$$Q = q\begin{bmatrix} q_{11} & q_{12} \\ q_{12} & q_{22} \end{bmatrix} \qquad R = r\begin{bmatrix} r_{11} & r_{12} \\ r_{12} & r_{22} \end{bmatrix} \tag{2.27}$$

where q and r represent overall weighing parameters. As seen from Figures 2.4 and 2.7, the aeroelastic contamination at the cockpit is severe. Therefore, the response cost $q_{22}q'^2$ will be scaled 2 to 1 with the $q_{11}q^2$ cost. Accordingly, to utilize the canard for the aeroelastic suppression role, the control cost $r_{22}\delta_C^2$ will be scaled 1 to 2 with the $r_{11}\delta_E^2$ cost. Diagonal Q and R will be enforced with q=1 and r used as an overall control parameter to perform trades.

Figure 2.13 shows the closed-loop pole migration as the overall control weighting value for R is varied with

$$Q = 1\begin{bmatrix} 1 & 0 \\ 0 & 2 \end{bmatrix} \quad s^2/rad^2 \qquad R = r\begin{bmatrix} 2 & 0 \\ 0 & 1 \end{bmatrix} \quad 1/rad^2 \tag{2.28}$$

Both short period and aeroelastic mode damping can be augmented with decreasing values of r. Figure (2.14) shows the resulting closed-loop bandwidth (q/δ_E magnitude crossover with dc value scaled to zero db) generated by a range of values for r. Recall high bandwidth is synonymous with low stability robustness due to amplification of high frequency modeling errors, such as neglected aeroelastic modes.[79] High bandwidth also leads to increased actuator saturation with resulting time delay increments and increased probability for pilot induced oscillations.[80,81] LQ state feedback guaranteed gain and phase margins are also in effect here, and if the design is carried to observer reconstruction of the state, loop transfer recovery concepts can be used to preserve these margins.[79]

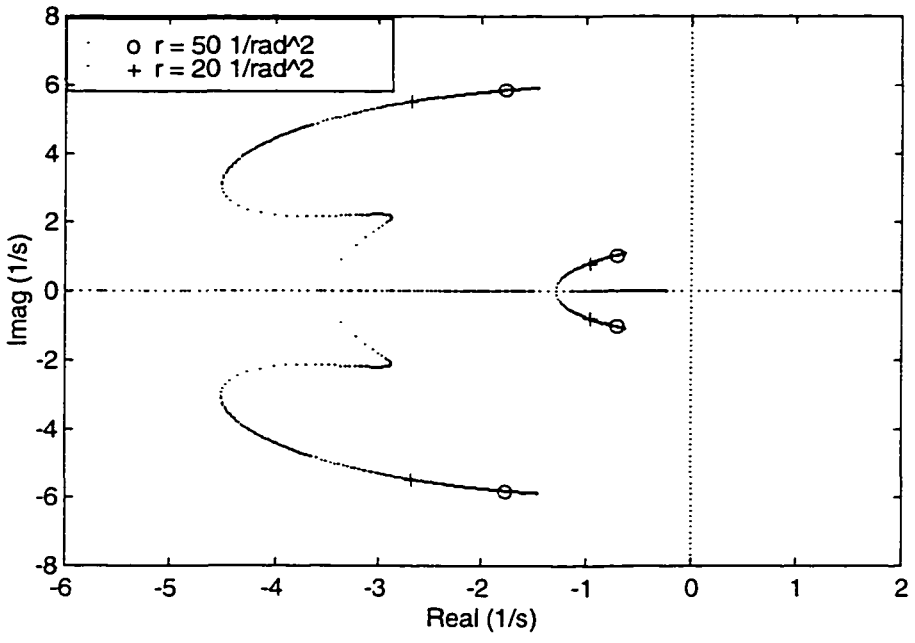

Figure 2.13 Closed-Loop Pole Migration Dependency upon Overall Control Weight

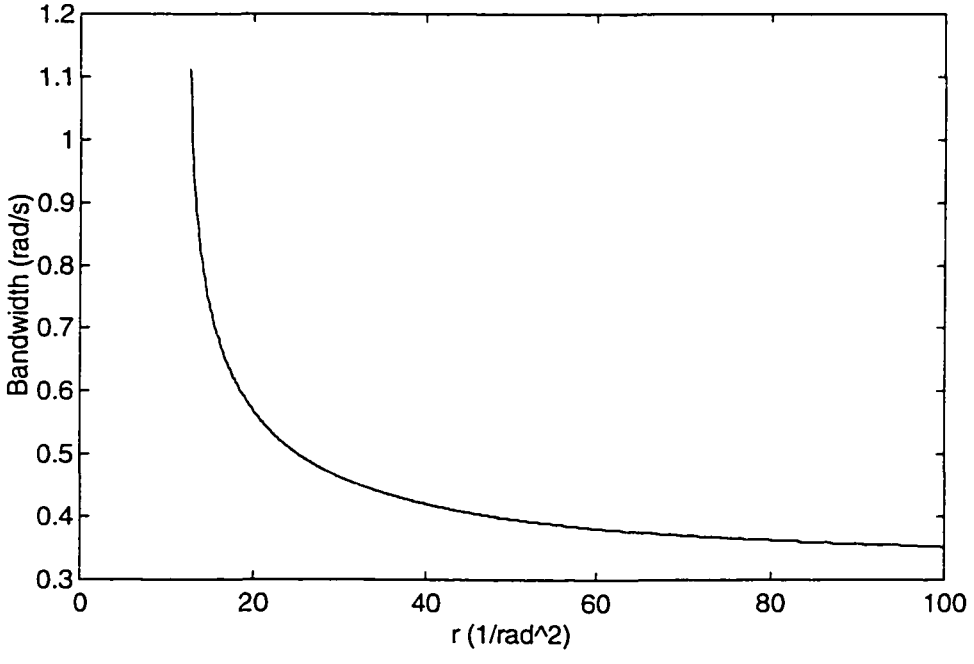

Figure 2.14 Bandwidth Dependency upon Overall Control Weight

A value of r = 50 $1/rad^2$ provides an acceptable trade between damping augmentation and bandwidth limitations. The resulting closed-loop transfer functions are

listed in Table 2.5 where $G_{cl}(s)$ denotes the closed-loop transfer matrix corresponding to Equation (2.18) and

$$G_{cl} = \frac{1}{\delta(s)} \underbrace{\begin{bmatrix} \eta_{11}(s) & \eta_{12}(s) \\ \eta_{21}(s) & \eta_{22}(s) \end{bmatrix}}_{N_{cl}(s)} \tag{2.29}$$

Figures 2.15-2.20 show the closed-loop frequency and time responses corresponding to similar input conditions as in Figures 2.2-2.7. Significant improvements are seen, but it is noted the augmented characteristics may need further improvement for satisfactory handling qualities. However for the research work here, the numerical design will be frozen.

Table 2.5 Closed-Loop Vehicle Transfer Function Factors

$\eta_{11}(s) = -5.1(s+0.33)(s^2+1.6s+21)$
$\eta_{12}(s) = 0.81(s+0.32)(s^2+10s+98)$
$\eta_{21}(s) = 13(s+0.24)(s-3.2)(s+3.7)$
$\eta_{22}(s) = 14(s+0.17)(s^2+2.3s+11)$
$\delta(s) = (s^2+1.4s+1.6)(s^2+3.5s+37)$

Other than some general knowledge about trends as the design parameter r is adjusted, the control system behavior is largely numerical based and the flight control engineer is left with little understanding. Common questions facing the designer include how do the individual weights affect particular modes, how do the control weights and airframe parameters combine to yield key closed-loop dynamic features, how do the properties change with flight condition, how do the sensor locations enter into the

characteristics, etc. Further, inevitable design modification will arise and assistance in implementing a tuning strategy that is short of a purely iterative approach is highly desirable. Answers to these issues could be obtained from a numerical-based sensitivity study. However, the conclusions would be problem specific, requiring additional calculations at other flight conditions, for example. Attention will now focus on analytical strategies for attacking these issues in Chapters III, IV and V.

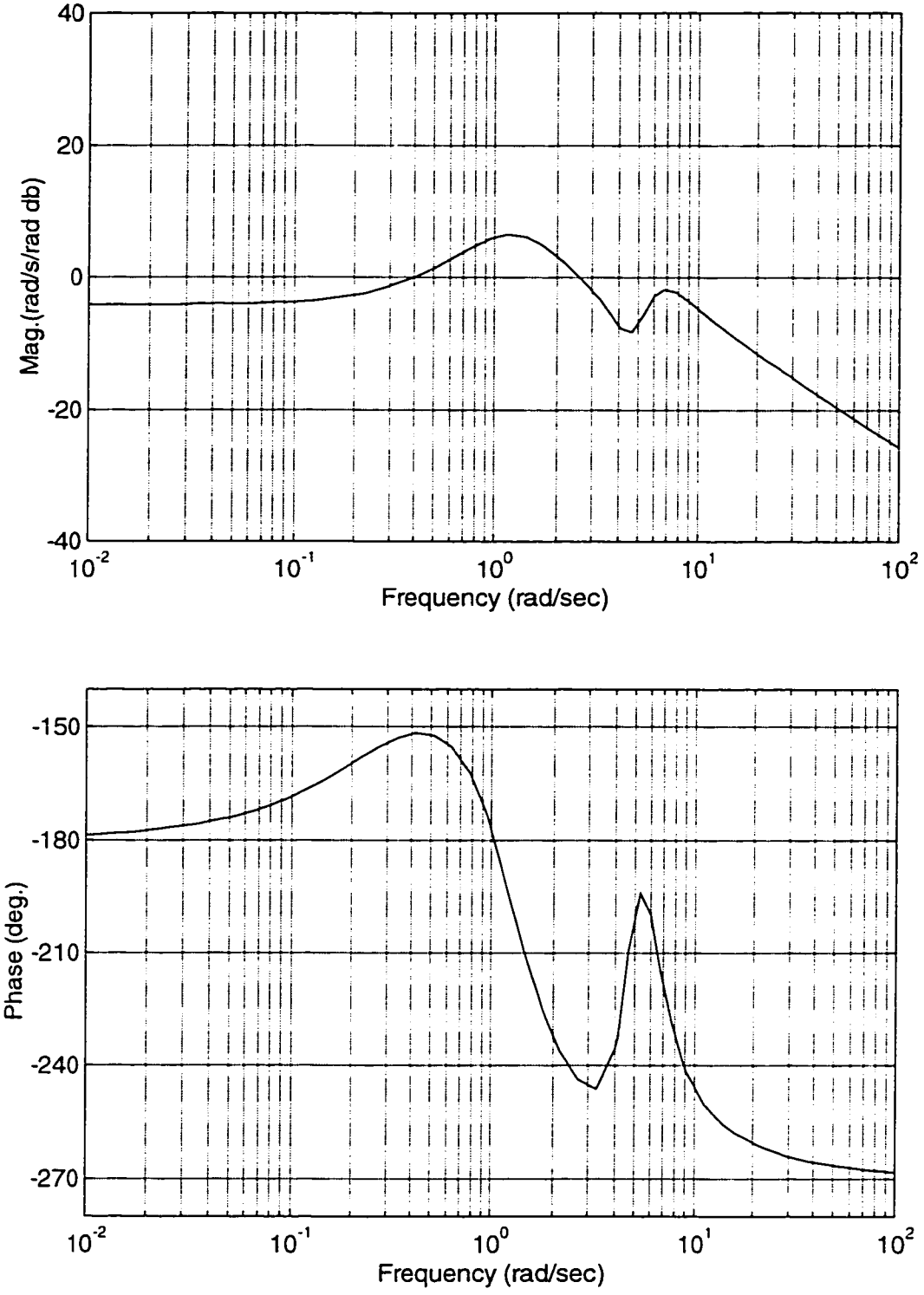

Figure 2.15 Closed-Loop Rigid Pitch Rate to Elevator Command Frequency Response

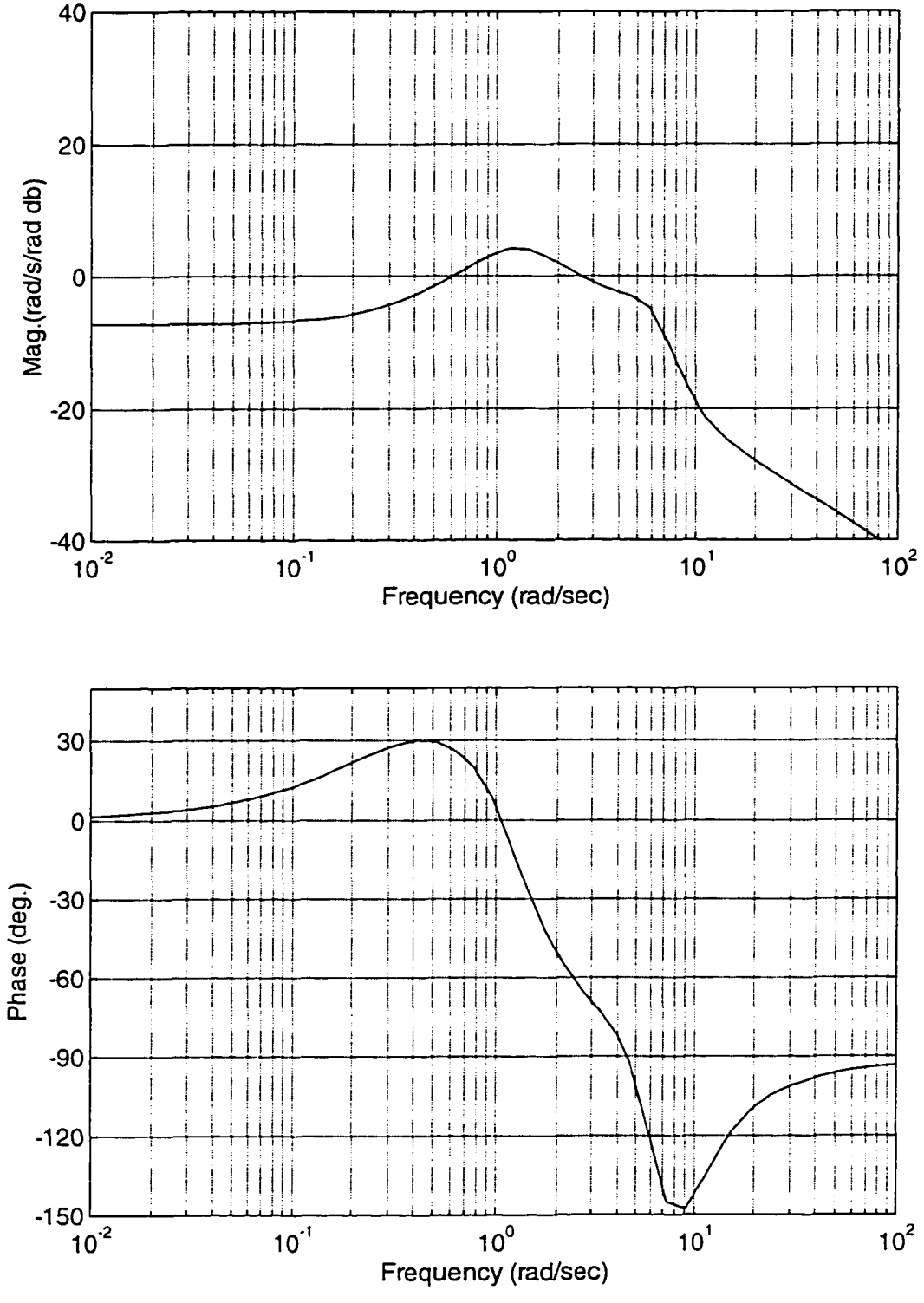

Figure 2.16 Closed-Loop Rigid Pitch Rate to Canard Command Frequency Response

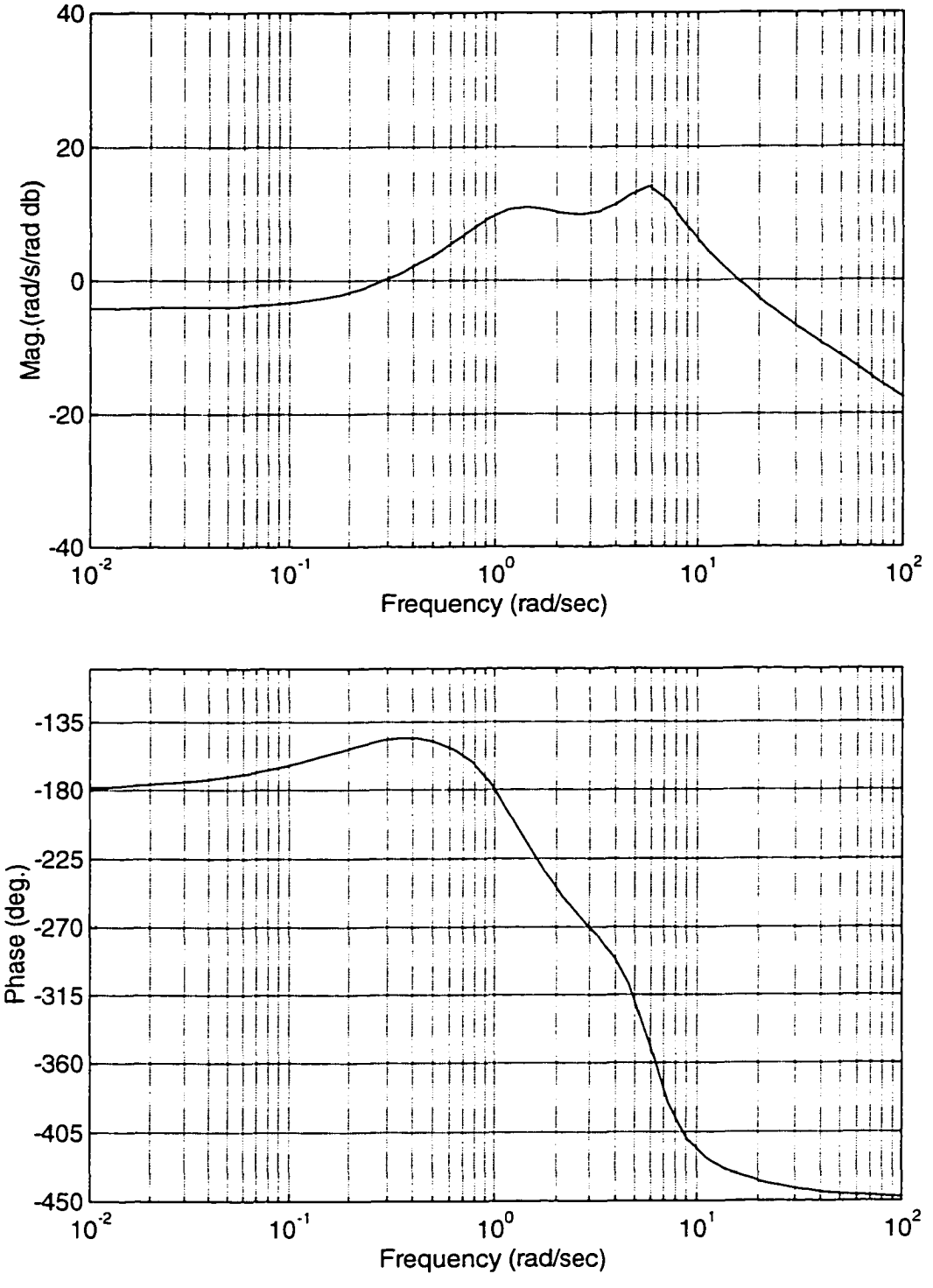

Figure 2.17 Closed-Loop Cockpit Pitch Rate to Elevator Command Frequency Response

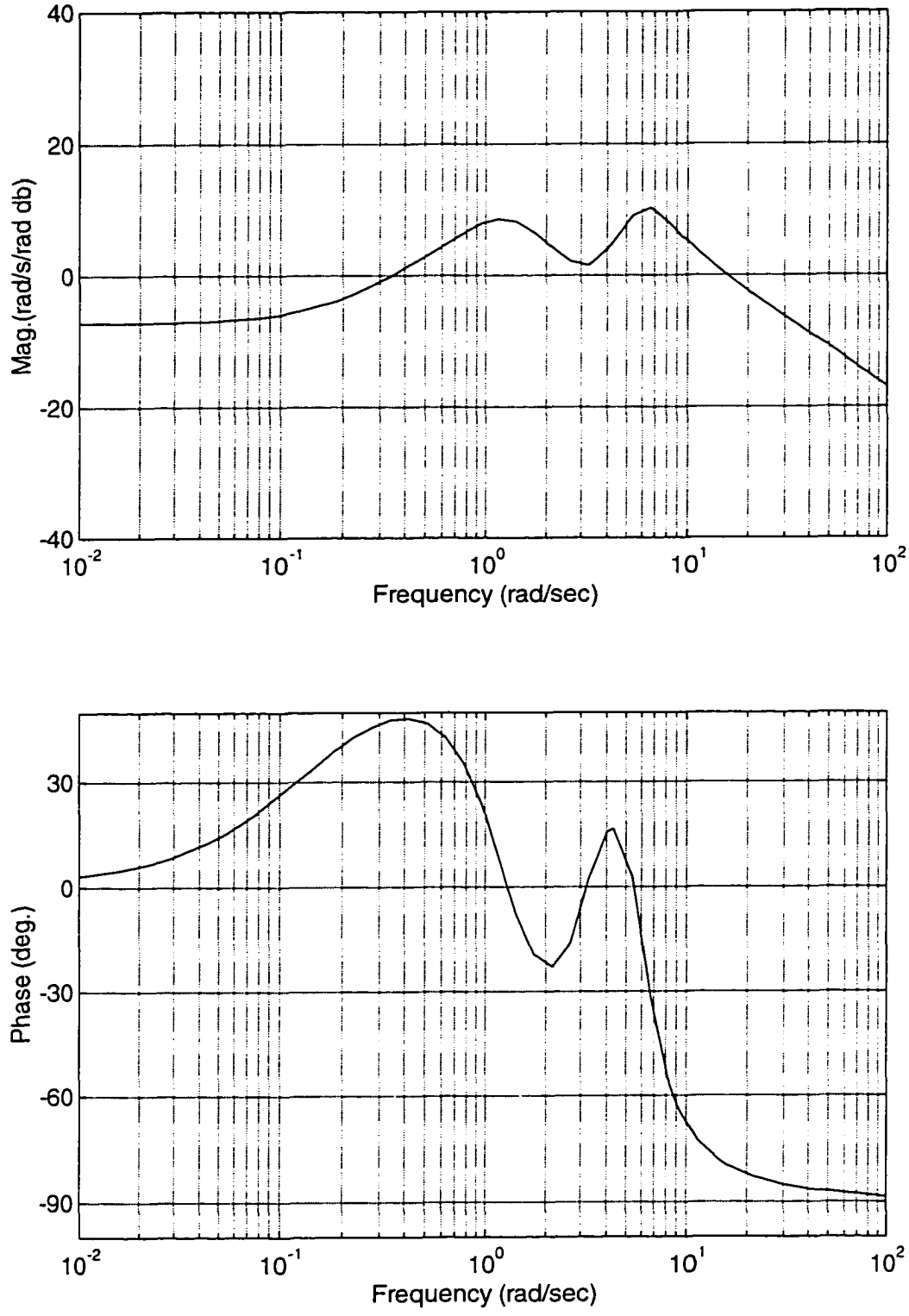

Figure 2.18 Closed-Loop Cockpit Pitch Rate to Canard Command Frequency Response

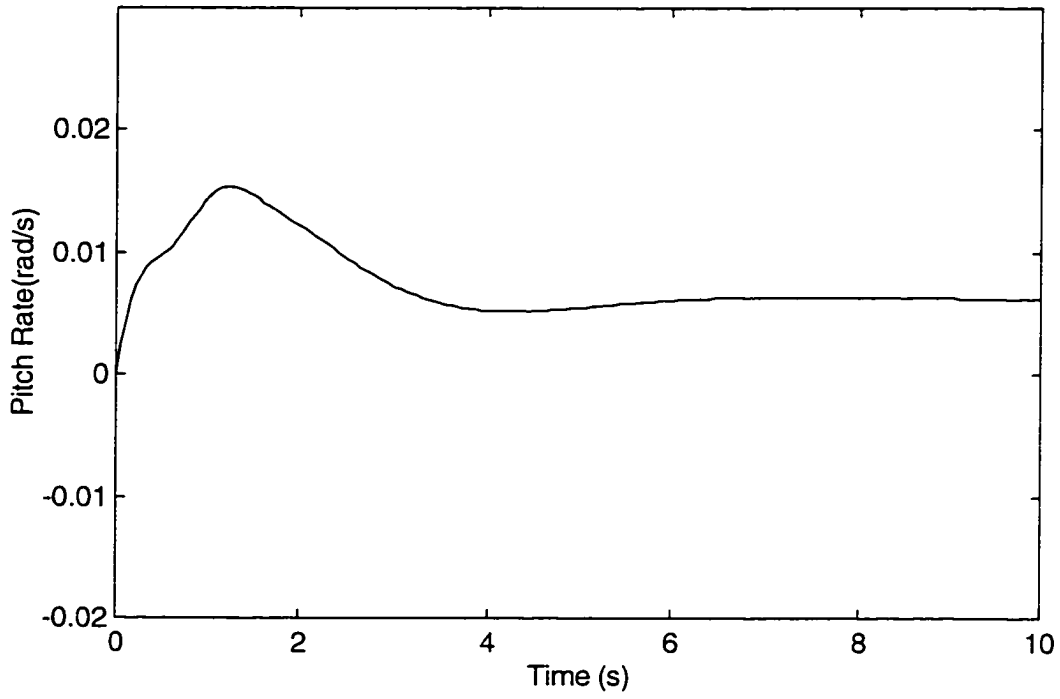

Figure 2.19 Closed-Loop Rigid Pitch Rate Time Response for Elevator Command Step

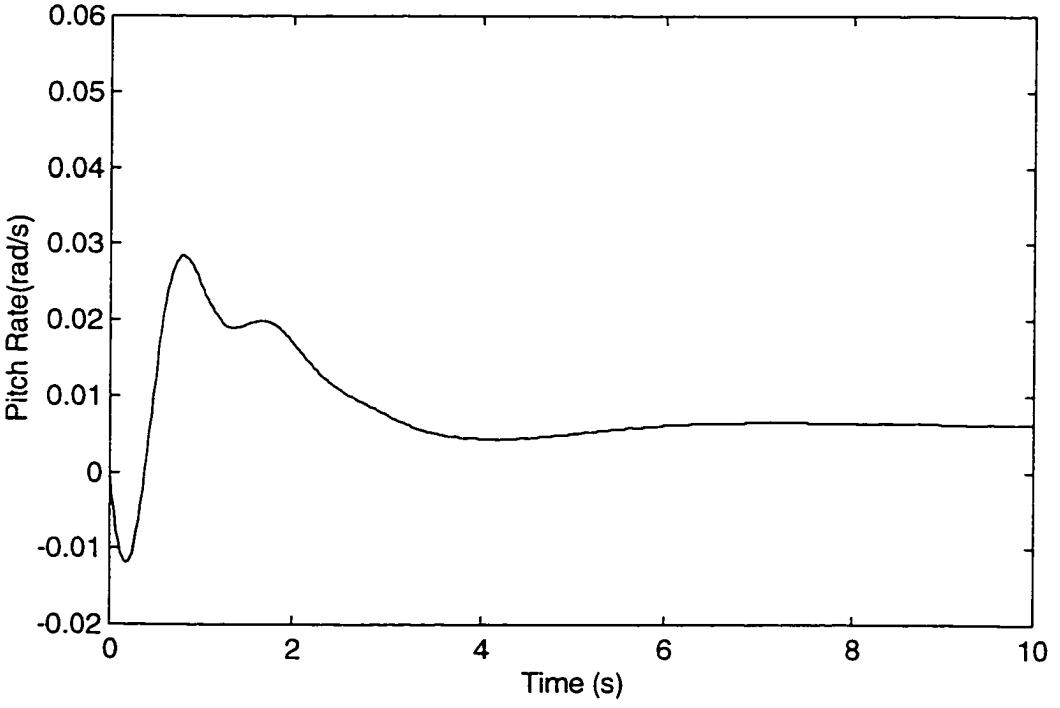

Figure 2.20 Closed-Loop Cockpit Pitch Rate Time Response for Elevator Command Step

CHAPTER III

DIRECT EIGEN-BASED TECHNIQUE

3.1 Overview

In this chapter, the Direct Eigen-Based Technique is presented for generating approximate analytical expressions for the closed-loop denominator factors resulting from the standard LQ state-feedback design strategy. The closed-loop characteristic polynomial from LQ root locus theory, which explicitly involves the cost weight matrices and vehicle transfer function matrix, is utilized as the base result. This polynomial, which involves the determinant function, is analytically factored, in an approximate sense, by an existing factoring technique for open-loop dynamic systems. In this technique, a truncated Taylor series is used to approximate the functional dependence of the polynomial factors on the polynomial coefficients. The technique is applied to a numerical flight control system for an aeroelastic vehicle. Tractable expressions which exhibit sufficient accuracy have been generated by this technique.

3.2 Preliminary Factors

Reconsider the LQ characteristic equation given in Equation (2.26). Upon expansion of this determinant for the 2x2 closed-loop aircraft system described in Chapter II, Equation (2.26) becomes Equation (3.1).

$$\phi = \frac{\det[R]}{(-1)^n}\delta\bar{\delta} = r^2(r_{11}r_{22} - r_{12}^2)d\bar{d}$$

$$+rq\{r_{11}q_{11}(n_{12}\bar{n}_{12})+r_{11}q_{12}(n_{12}\bar{n}_{22}+n_{22}\bar{n}_{12})+r_{11}q_{22}(n_{22}\bar{n}_{22})$$

$$-r_{12}q_{11}(n_{11}\bar{n}_{12}+n_{12}\bar{n}_{11})-r_{12}q_{12}(n_{11}\bar{n}_{22}+n_{12}\bar{n}_{21}+n_{21}\bar{n}_{12}+n_{22}\bar{n}_{11})-r_{12}q_{22}(n_{21}\bar{n}_{22}+n_{22}\bar{n}_{21})$$

$$+r_{22}q_{11}(n_{11}\bar{n}_{11})+r_{22}q_{12}(n_{11}\bar{n}_{21}+n_{21}\bar{n}_{11})+r_{22}q_{22}(n_{21}\bar{n}_{21})\} \tag{3.1}$$

$$+q^2(q_{11}q_{22}-q_{12}^2)\psi\bar{\psi}=0$$

In Equation (3.1), $\delta(s)$ denotes the left-half plane LQ characteristic polynomial (see Equation (2.29)) and the over-bar denotes evaluation at "- s". The polynomial $\phi(s)$ denotes a scaled variant of the left- and right-half plane LQ characteristic polynomial. Recall $d(s)$ and $n_{ij}(s)$ are the vehicle transfer function denominator and numerator polynomials, as defined in Equation (2.2). Equation (3.1) has also made use of the transmission zero polynomial[2.9] $\psi(s)$, or

$$\frac{(n_{11}n_{22}-n_{12}n_{21})}{d}=\psi \tag{3.2}$$

The aircraft numerator and denominator polynomials appearing in Equation (3.1) are easily generated by applying Cramer's rule to Equation (2.1). Suppose the vehicle polynomial matrix model in Equation (2.1) is re-expressed in general terms as

$$\underbrace{\begin{bmatrix} P(s) & 0 \\ -R(s) & I \end{bmatrix}}_{T}\begin{bmatrix} z(s) \\ y(s) \end{bmatrix}=\underbrace{\begin{bmatrix} Q(s) \\ W(s) \end{bmatrix}}_{S}u(s) \tag{3.3}$$

where $z(s)$ represents the system's degrees of freedom. The ij^{th} element of the transfer matrix $G(s)$ is

$$G_{ij}=\frac{n_{ij}(s)}{d(s)} \tag{3.4}$$

where the numerator and denominator polynomials $n_{ij}(s)$ and $d(s)$ are calculated as

$$n(s) = \det[T_{p+i} \mid S_j] = \sum_{k=1}^{(p+p_y)!} n_k(s) \tag{3.5}$$

$$d(s) = \det[T] = \sum_{k=1}^{(p+p_y)!} d_k(s) \tag{3.6}$$

In Equation (3.5) the notation $T_{p+i} \mid S_j$ represents the matrix T with the exception that the $p+i^{th}$ column of T is replaced with the j^{th} column of S, p is the number of degrees of freedom in the vector z, and p_y is the number of scalar responses in the vector y. The $n_k(s)$ and $d_k(s)$ component terms in Equations (3.5)-(3.6) consist of products of second order, first order, and constant polynomials with the basic aircraft parameters as coefficients, which appear as matrix elements within P(s), Q(s), R(s) and W(s) in Equation (3.3). As will be shown, the quasi-factored structure of these $n_k(s)$ and $d_k(s)$ component terms is key to obtaining preliminary approximations to the factors of $\delta(s)$ in Equation (3.1).[35]

Using Equations (3.1) and (3.5)-(3.6), $\phi(s)$ can also be expressed in expanded form as

$$\phi(s) = \phi_{2q}s^{2q} + \phi_{2q-2}s^{2q-2} + ... + \phi_2 s^2 + \phi_0 \tag{3.7}$$

ϕ_i denotes the polynomial coefficients in expanded form and q is the dynamic order of the system. Further, $\phi(s)$ can be expressed in factored form as

$$\phi(s) = \{k\prod_{i=1}^{q_r}[s + r_i]\prod_{i=1}^{q_c}[s^2 + (2\varsigma\omega)_i s + \omega_i^2]\}\{.....\} \tag{3.8}$$

where r_i, ω_i^2 and $(2\zeta\omega)_i$ are the LQ characteristic polynomial factors, and k is the polynomial gain. Note that q_r denotes the number of real factors and $2q_c$ denotes the number of complex conjugate factors ($q=q_r+2q_c$). In general, to know how many real and complex conjugate factors $\phi(s)$ has, as in Equation (3.8), the associated numerical model must already be factored. In Equation (3.8) the multiplying factor " $\{\ldots\}$ " denotes the symmetric right-half plane terms.

To obtain preliminary approximations for the factors in Equation (3.8), select one or more of the component terms within the $n_{ij}\bar{n}_{gh}$ and $d\bar{d}$ terms from Equation (3.1) which best satisfy the following two criteria:

1. The analytical expressions for the preliminary factors should have identical root constituency as that in Equation (3.8), and
2. The numerical values for the preliminary factors should be as close as possible to the numerical values for the exact factors in Equation (3.8).

As an illustrative example only, suppose Equation (3.1) has the structure

$$\begin{aligned}\phi &= d\bar{d} + rq(n_{ij}\bar{n}_{ij}) \\ &= \{[s+r_1][s+r_2][s^2+(2\varsigma\omega)s+\omega^2]\}\{\ldots\}\end{aligned} \tag{3.9}$$

where

$$d(s) = \det[T] = \det\begin{bmatrix} s+p_1 & p_9 & p_{10} \\ p_8 & s+p_2 & p_5 \\ p_{11}s+p_{12} & p_6 s+p_7 & s^2+p_3 s+p_4 \end{bmatrix} \tag{3.10}$$

$$= \underbrace{[s+p_1][s+p_2][s^2+p_3s+p_4]}_{d_1(s)} + \underbrace{[-p_5][[s+p_1][p_6s+p_7]}_{d_2(s)}$$
$$+ \underbrace{[-p_8p_9][s^2+p_3s+p_4]}_{d_3(s)} + \underbrace{[p_8p_{10}][p_6s+p_7]}_{d_4(s)}$$
$$+ \underbrace{[p_5p_9][p_{11}s+p_{12}]}_{d_5(s)} + \underbrace{[-p_{10}][s+p_2][p_{11}s+p_{12}]}_{d_6(s)}$$

and

$$n_{ij}(s) = \det[T_{p+i} \mid S_j] = \det\begin{bmatrix} s+p_1 & q_1 & p_{10} \\ p_8 & q_2 & p_5 \\ p_{11}s+p_{12} & q_3 & s^2+p_3s+p_4 \end{bmatrix} \tag{3.11}$$

$$= \underbrace{[q_2][s+p_1][s^2+p_3s+p_4]}_{n_1(s)} + \underbrace{[-q_3p_5][s+p_1]}_{n_2(s)}$$
$$+ \underbrace{[-q_1p_8][s^2+p_3s+p_4]}_{n_3(s)} + \underbrace{[q_3p_8p_{10}]}_{n_4(s)}$$
$$+ \underbrace{[q_1p_5][p_{11}s+p_{12}]}_{n_5(s)} + \underbrace{[-q_2p_{10}][p_{11}s+p_{12}]}_{n_6(s)}$$

In these equations p_i and q_i are the basic system parameters. Based upon criteria 1, there are only four choices for the preliminary factors when considering two component terms or less. These choices are

1. $d_1(s)\bar{d}_1(s) = \{[s+p_1][s+p_2][s^2+p_3s+p_4]\}\{...\}$ (3.12)

2. $d_1(s)\bar{d}_1(s) + d_3(s)\bar{d}_3(s) = \{[s+p_1][s+p_2][...] + [-p_8p_9][...]\}[s^2+p_3s+p_4][...]$

$$= \{[s^4 + \underbrace{(-p_1^2-p_2^2)}_{b}s^2 + \underbrace{(p_1p_2)^2+(p_8p_9)^2}_{c}]\}[s^2+p_3s+p_4][...]$$
$$= \{[s+\sqrt{\frac{-b+\sqrt{b^2-4c}}{2}}][s+\sqrt{\frac{-b-\sqrt{b^2-4c}}{2}}][s^2+p_3s+p_4]\}\{....\} \tag{3.13}$$

(assuming $b^2-4c \geq 0$)

3. $d_1(s)\bar{d}_1(s) + rqn_1(s)\bar{n}_1(s) = \{[s+p_1][s+p_2][s^2+p_3s+p_4]\}\{...\}$

$$+ rq\{[q_2][s+p_1][s^2+p_3s+p_4]\}\{...\} \tag{3.14}$$

$$= \{[s^4 + \underbrace{(-p_1^2 - p_2^2 + rqq_2^2)}_{b}s^2 + \underbrace{(p_1p_2)^2 - rq(p_1q_2)^2}_{c}]\}[s^2 + p_3s + p_4][...]$$

$$= \{[s + \sqrt{\frac{-b + \sqrt{b^2 - 4c}}{2}}][s + \sqrt{\frac{-b - \sqrt{b^2 - 4c}}{2}}][s^2 + p_3s + p_4]\}\{....\}$$

(assuming $b^2 - 4c \geq 0$)

4. $d_1(s)\bar{d}_1(s) + rqn_3(s)\bar{n}_3(s) = \{[s + p_1][s + p_2][s^2 + p_3s + p_4]\}\{...\}$

$$+ rq\{[-q_1p_8][s^2 + p_3s + p_4]\}\{...\} \qquad (3.15)$$

$$= \{[s^4 + \underbrace{(-p_1^2 - p_2^2)}_{b}s^2 + \underbrace{(p_1p_2)^2 + rq(p_8q_1)^2}_{c}]\}[s^2 + p_3s + p_4][...]$$

$$= \{[s + \sqrt{\frac{-b + \sqrt{b^2 - 4c}}{2}}][s + \sqrt{\frac{-b - \sqrt{b^2 - 4c}}{2}}][s^2 + p_3s + p_4]\}\{....\}$$

(assuming $b^2 - 4c \geq 0$)

With more than two component terms, combinations such as $d_1(s)\bar{d}_1(s) + d_3(s)\bar{d}_3(s) + rq[n_1(s)\bar{n}_1(s) + n_3(s)\bar{n}_3(s)]$ are also candidates for the preliminary factors. Among these choices, criteria 2 can be used to select the "best" preliminary factors.

Denote these preliminary factors as

$$\tilde{\phi}(s) = \{\tilde{k}\prod_{i=1}^{q_r}[s + \tilde{\xi}_i]\prod_{i=1}^{q_c}[s^2 + (2\tilde{\zeta}\tilde{\omega})_i s + \tilde{\omega}_i^2]\}\{.....\}$$

$$= \tilde{\phi}_{2q}s^{2q} + \tilde{\phi}_{2q-2}s^{2q-2} + ... + \tilde{\phi}_2 s^2 + \tilde{\phi}_0 \qquad (3.16)$$

It may turn out in specific problems that a complex conjugate preliminary factor may be a more accurate approximation, numerically (criteria 2.), to a pair of real factors than a pair of real preliminary factors, or vice versa. For example, consider the factors shown in Figure 3.1. Numerically, the complex conjugate preliminary factor is "closer" to the pair of exact real factors when compared with the pair of real preliminary factors. In

this example, using the complex conjugate preliminary factor might possibly lead to more accurate results, but with the added complexity of results expressed in terms of $r_1 r_2$ and $r_1 + r_2$ rather than in terms of r_1 and r_2 directly.

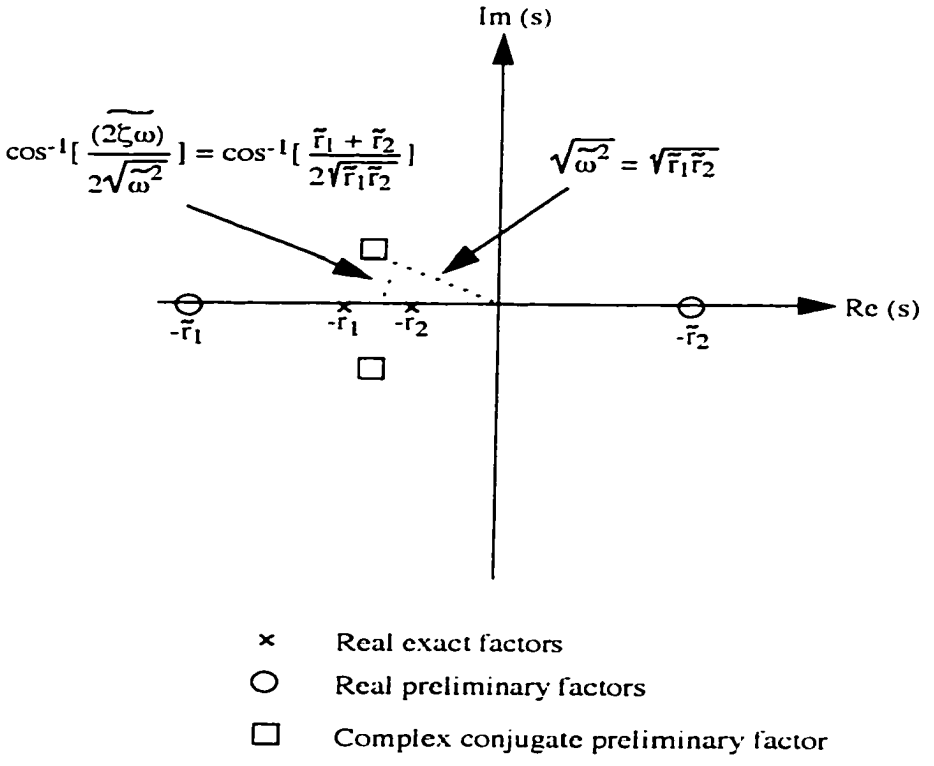

Figure 3.1 Example of Exact and Preliminary Factors

3.3 Taylor-Series Polynomial Expansion

Now focus on the technique that generates analytical corrections to the preliminary factors, thereby increasing the accuracy of the overall approximate symbolic expressions for the factors. The functional dependence of the polynomial coefficients

upon the polynomial factors is readily available by expanding Equation (3.8), and equating like powers of s with Equation (3.7), or

$$\phi_i = f_i[k, r_i, \omega_i^2, (2\varsigma\omega)_i] \tag{3.17}$$

where f_i is a continuous, nonlinear function consisting of addition and multiplication of the factors. For example, if

$$\phi(s) = \{[s + r_1][s + r_2][s^2 + (2\varsigma\omega)_1 s + \omega_1^2]\}\{....\} \tag{3.18}$$

then after expansion

$$\begin{aligned}\phi(s) = &\underbrace{\{1\}}_{\phi_3} s^3 + \underbrace{\{2(r_1r_2) + 2\omega_1^2 - (r_1 + r_2)^2 - (2\varsigma\omega)_1^2\}}_{\phi_2} s^6 \\ &+ \{(r_1r_2)^2 + \omega_1^4 + 4(r_1r_2)\omega_1^2 - 2(r_1r_2)(2\varsigma\omega)_1^2 \\ &\quad \underbrace{- 2\omega_1^2(r_1 + r_2)^2 + (r_1 + r_2)^2(2\varsigma\omega)_1^2\}}_{\phi_1} s^4 \\ &+ \underbrace{\{2(r_1r_2)^2\omega_1^2 + 2\omega_1^4(r_1r_2) - (r_1r_2)^2(2\varsigma\omega)_1^2 - \omega_1^4(r_1 + r_2)^2\}}_{\phi_2} s^2 \\ &+ \underbrace{\{(r_1r_2)^2\omega_1^4\}}_{\phi_0}\end{aligned} \tag{3.19}$$

Of more importance here, is the development of the functional dependence of the factors upon the coefficients, obtained by "inverting" Equation (3.17).

Consider expressing the continuous, functional dependence of the coefficients upon the factors, as given in Equation (3.17), in a Taylor series, or

$$\begin{aligned}\phi_i &= \phi_i\big|_0 + \left.\frac{\partial \phi_i}{\partial x}\right|_0 (x - x|_0) + \frac{1}{2}(x - x|_0)^T \left.\frac{\partial^2 \phi_i}{\partial x^2}\right|_0 (x - x|_0) + \cdots \\ &= \phi_i\big|_0 + \left.\frac{\partial \phi_i}{\partial x}\right|_0 \Delta x + \frac{1}{2}\Delta x^T \left.\frac{\partial^2 \phi_i}{\partial x^2}\right|_0 \Delta x + \cdots\end{aligned} \tag{3.20}$$

where the independent variables are the factors contained in the column vector x given as

$$x = [\, r_1 .... r_{q_r}\ \omega_1^2 .... \omega_{q_c}^2\ (2\varsigma\omega)_1 .... (2\varsigma\omega)_{q_c}\,]^T \tag{3.21}$$

Also, the first partial derivative $\frac{\partial \phi_i}{\partial x}$ is a row vector defined as

$$\frac{\partial \phi_i}{\partial x} = [\frac{\partial f_i}{\partial r_1} \cdots \frac{\partial f_i}{\partial r_{q_r}} \; \frac{\partial f_i}{\partial \omega_1^2} \cdots \frac{\partial f_i}{\partial \omega_{q_c}^2} \; \frac{\partial f_i}{\partial (2\varsigma\omega)_1} \cdots \frac{\partial f_i}{\partial (2\varsigma\omega)_{q_c}}] \tag{3.22}$$

the second partial derivative $\frac{\partial^2 \phi_i}{\partial x^2}$ is a matrix defined as

$$\frac{\partial^2 \phi_i}{\partial x^2} = \begin{bmatrix} \frac{\partial^2 f_i}{\partial r_1^2} & \cdots & \frac{\partial^2 f_i}{\partial r_1 \partial (2\varsigma\omega)_{q_c}} \\ \vdots & \ddots & \vdots \\ \frac{\partial^2 f_i}{\partial (2\varsigma\omega)_{q_c} \partial r_1} & \cdots & \frac{\partial^2 f_i}{\partial (2\varsigma\omega)_{q_c}^2} \end{bmatrix} \tag{3.23}$$

and the notation "$|_0$" denotes the nominal values about which the Taylor series is expanded. Also, Δx is defined as

$$\Delta x = x - x|_0 = [\Delta r_1 \cdots \Delta r_{q_r} \; \Delta\omega_1^2 \cdots \Delta\omega_{q_c}^2 \; \Delta(2\varsigma\omega)_1 \cdots \Delta(2\varsigma\omega)_{q_c}]^T \tag{3.24}$$

For a given numerical model, the basic system parameters appearing as matrix elements in P(s), Q(s), R(s), W(s), Q and R in Equations (3.3) and (2.27), and the corresponding polynomial coefficients, have specific numerical values associated with them. The functional dependence of the coefficients upon the factors can be expressed in a Taylor series expanded about these specific numerical values. However, a Taylor series, in particular Equation (3.20), is more general than this. The Taylor series in Equation (3.20) can be expanded about *any set* of numerical values for the basic system parameters.

In Equation (3.20), the nominal condition "$|_0$" is specified to be numerical values for the basic parameters which result in the preliminary factors given in Equation (3.16), or $\phi_i|_0 = \tilde{\phi}_i$. In other words, the system parameters appearing in the specific $n_k(s)$ and

$d_k(s)$ terms which form the preliminary factors, as well as the cost function weights appearing as overall coefficients, are evaluated at their given values, while the remaining system parameters are evaluated at zero, which, in general, is not necessarily their given values. When the system parameters are evaluated in this way, the $n_k(s)$ and $d_k(s)$ terms excluded from the preliminary factors must equal zero. This places a third criteria upon the selection of the preliminary factors:

3. The remaining $n_k(s)$ and $d_k(s)$ terms, and associated cost function weights, excluded from the preliminary factors must be a function of at least one system parameter which does not appear with the preliminary factor terms.

For example, reconsider the illustrative problem in Equations (3.12)-(3.15). For the preliminary factors selected in Equation (3.12), it is seen that the terms $d_2(s)$, $d_3(s)$, $d_4(s)$, $d_5(s)$, and $d_6(s)$ all become zero when the parameters p_5, p_6, p_7, p_8, p_9, p_{10}, p_{11}, and p_{12} are evaluated at zero.

3.4 Correction of the Preliminary Factors

If all the coefficient Taylor series in Equation (3.20) are combined and rearranged, a single vector Taylor series results, or

$$\Delta\phi = A\Delta x + \cdots \tag{3.25}$$

where $\Delta\phi$ and A are given as

$$\Delta\phi = [(\phi_0 - \phi_0|_0)(\phi_2 - \phi_2|_0)\ldots\ldots(\phi_{2q-2} - \phi_{2q-2}|_0)(\phi_{2q} - \phi_{2q}|_0)]^T \tag{3.26}$$

$$A = \left[\left.\frac{\partial \phi_0}{\partial x}\right|_0^T \quad \left.\frac{\partial \phi_2}{\partial x}\right|_0^T \quad \cdots\cdots \quad \left.\frac{\partial \phi_{2q-2}}{\partial x}\right|_0^T \quad \left.\frac{\partial \phi_{2q}}{\partial x}\right|_0^T \right]^T$$

Note that A is a square q+1 matrix.

The matrix A can be inverted analytically to obtain corrections to the preliminary factors, or

$$\Delta x \approx A^{-1}\Delta\phi \tag{3.27}$$

where the higher order terms in the series have been neglected. The matrix A will be invertible as long as it's determinant, when evaluated numerically, is nonzero. This "inversion" calculation requires the symbolic expressions for $\Delta\phi$ obtained from the difference between Equations (3.7) and (3.16), as well as the symbolic expressions for A obtained from differentiation of Equation (3.17), followed by evaluation at the " $|_0$ " condition. The overall approximate analytical expressions for the LQ characteristic polynomial factors are finally obtained by summing the preliminary factors in Equation (3.16) with their corrections in Equation (3.27), or

$$x \approx x|_0 + \Delta x \tag{3.28}$$

At this stage, the symbolic expressions for the factors, as functions of the basic system parameters, may be quite cumbersome for obtaining insight into key dynamic characteristics. By neglecting small terms based upon their relative numerical magnitude, the symbolic expressions can often be simplified to a level that is conducive to understanding "major players" in the dynamic characteristics.

3.5 Factoring Example

To demonstrate the approximate factoring technique presented above, reconsider the vehicle model presented in Equation (2.1). By applying Cramer's rule to Equation (2.1), the vehicle polynomials d(s) and $n_{ij}(s)$, with the component structure of Equations (3.5)-(3.6), (3.7) are generated as

$$\begin{aligned} d(s) = &-F_\alpha(1+\frac{Z_q}{V_T})s(M_\eta s + M_\eta) - F_\alpha(s^2 - M_q s)(\frac{Z_{\dot\eta}}{V_T}s + \frac{Z_\eta}{V_T}) \\ &- F_q s(s - \frac{Z_\alpha}{V_T})(M_\eta s + M_\eta) - F_q s M_\alpha(\frac{Z_\eta}{V_T}s + \frac{Z_\eta}{V_T}) \\ &+ \{s^2 + (2\zeta\omega - F_\eta)s + (\omega^2 - F_\eta)\}(s - \frac{Z_\alpha}{V_T})(s^2 - M_q s) \\ &- \{s^2 + (2\zeta\omega - F_\eta)s + (\omega^2 - F_\eta)\}(1 + \frac{Z_q}{V_T})sM_\alpha \end{aligned} \tag{3.29}$$

$$\begin{aligned} n_{11}(s) = &-s\{\frac{Z_{\delta_E}}{V_T}F_\alpha(-M_\eta s - M_\eta) - \frac{Z_{\delta_E}}{V_T}M_\alpha[s^2 + (2\zeta\omega - F_\eta)s + (\omega^2 - F_\eta)] \\ &- M_{\delta_E}(s - \frac{Z_\alpha}{V_T})[s^2 + (2\zeta\omega - F_\eta)s + (\omega^2 - F_\eta)] - M_{\delta_E}F_\alpha(-\frac{Z_\eta}{V_T}s - \frac{Z_\eta}{V_T}) \\ &+ F_{\delta_E}(s - \frac{Z_\alpha}{V_T})(-M_\eta s - M_\eta) + F_{\delta_E}M_\alpha(-\frac{Z_\eta}{V_T}s - \frac{Z_\eta}{V_T})\} \end{aligned} \tag{3.30}$$

$$\begin{aligned} n_{12}(s) = &-s\{Z_{\delta_C}F_\alpha(-M_\eta s - M_\eta) - \frac{Z_{\delta_C}}{V_T}M_\alpha[s^2 + (2\zeta\omega - F_\eta)s + (\omega^2 - F_\eta)] \\ &- M_{\delta_C}(s - \frac{Z_\alpha}{V_T})[s^2 + (2\zeta\omega - F_\eta)s + (\omega^2 - F_\eta)] - M_{\delta_C}F_\alpha(-\frac{Z_\eta}{V_T}s - \frac{Z_\eta}{V_T}) \\ &+ F_{\delta_C}(s - \frac{Z_\alpha}{V_T})(-M_\eta s - M_\eta) + F_{\delta_C}M_\alpha(-\frac{Z_\eta}{V_T}s - \frac{Z_\eta}{V_T})\} \end{aligned} \tag{3.31}$$

$$
\begin{aligned}
n_{21}(s) = -\{ & s\frac{Z_{\delta_E}}{V_T}F_\alpha(-M_\eta s - M_\eta) - \frac{Z_{\delta_E}}{V_T}sM_\alpha[s^2 + (2\varsigma\omega - F_\eta)s + (\omega^2 - F_\eta)] \\
& + s\frac{Z_{\delta_E}}{V_T}\phi' F_\alpha(s^2 - M_q s) + \frac{Z_{\delta_E}}{V_T}\phi' s^2 M_\alpha F_q \\
& - M_{\delta_E} s(s - \frac{Z_\alpha}{V_T})[s^2 + (2\varsigma\omega - F_\eta)s + (\omega^2 - F_\eta)] - M_{\delta_E} sF_\alpha(-\frac{Z_\eta}{V_T}s - \frac{Z_\eta}{V_T}) \\
& + M_{\delta_E}\phi' s^2 F_q(s - \frac{Z_\alpha}{V_T}) + M_{\delta_E}\phi' s^2 F_\alpha(1 + \frac{Z_q}{V_T}) \\
& + F_{\delta_E} s(s - \frac{Z_\alpha}{V_T})(-M_\eta s - M_\eta) + F_{\delta_E} sM_\alpha(-\frac{Z_\eta}{V_T}s - \frac{Z_\eta}{V_T}) \\
& + F_{\delta_E}\phi' s(s - \frac{Z_\alpha}{V_T})(s^2 - M_q s) - F_{\delta_E}\phi' s^2 M_\alpha(1 + \frac{Z_q}{V_T})\}
\end{aligned}
\tag{3.32}
$$

$$
\begin{aligned}
n_{22}(s) = -\{ & s\frac{Z_{\delta_C}}{V_T}F_\alpha(-M_\eta s - M_\eta) - \frac{Z_{\delta_C}}{V_T}sM_\alpha[s^2 + (2\varsigma\omega - F_\eta)s + (\omega^2 - F_\eta)] \\
& + s\frac{Z_{\delta_C}}{V_T}\phi' F_\alpha(s^2 - M_q s) + \frac{Z_{\delta_C}}{V_T}\phi' s^2 M_\alpha F_q \\
& - M_{\delta_C} s(s - \frac{Z_\alpha}{V_T})[s^2 + (2\varsigma\omega - F_\eta)s + (\omega^2 - F_\eta)] - M_{\delta_C} sF_\alpha(-\frac{Z_\eta}{V_T}s - \frac{Z_\eta}{V_T}) \\
& + M_{\delta_C}\phi' s^2 F_q(s - \frac{Z_\alpha}{V_T}) + M_{\delta_C}\phi' s^2 F_\alpha(1 + \frac{Z_q}{V_T}) \\
& + F_{\delta_C} s(s - \frac{Z_\alpha}{V_T})(-M_\eta s - M_\eta) + F_{\delta_C} sM_\alpha(-\frac{Z_\eta}{V_T}s - \frac{Z_\eta}{V_T}) \\
& + F_{\delta_C}\phi' s(s - \frac{Z_\alpha}{V_T})(s^2 - M_q s) - F_{\delta_C}\phi' s^2 M_\alpha(1 + \frac{Z_q}{V_T})\}
\end{aligned}
\tag{3.33}
$$

These polynomials combine according to Equation (3.1) to form the LQ characteristic polynomial. The exact numerical solution for this closed-loop is

$$\phi(s) = \{71s(s^2 + 1.4s + 1.6)(s^2 + 3.5s + 37)\}\{\cdots\} \tag{3.34}$$

This polynomial is represented analytically as

$$\begin{aligned}\phi(s) &= \{ks(s^2+(2\zeta\omega)_1 s+\omega_1^2)(s^2+(2\zeta\omega)_2 s+\omega_2^2)\}\{\cdots\} \\ &= \phi_{10}s^{10}+\phi_8 s^8+\phi_6 s^6+\phi_4 s^4+\phi_2 s^2\end{aligned} \tag{3.35}$$

where the first quadratic factor denoted by subscript 1 represents the augmented short period mode, and the second factor denoted by subscript 2 indicates the augmented aeroelastic mode.

Out of all possible combinations of the factored terms in Equation (3.1), which factor symbolically into one real root at the origin and two complex conjugate roots (criteria 1), and are as close to the exact numerical values as possible (criteria 2), the following terms are selected as the preliminary factors.

$$\begin{aligned}\tilde{\phi}(s) &= \{r(r_{11}r_{22})^{1/2}s[s^2+(-\frac{Z_\alpha}{V_T}-M_q)s+(\frac{Z_\alpha}{V_T}M_q-(1+\frac{Z_q}{V_T})M_\alpha)] \\ &\times[s^2+(2\zeta\omega-F_\eta)s+(\omega^2-F_\eta)]\}\{\cdots\} = \{71s(s^2+1.2s+3.8)(s^2+0.62s+35)\}\{\cdots\}\end{aligned} \tag{3.36}$$

Note the factors in Equation (3.36) originate from the last two of the six components within the bare airframe denominator polynomial d(s) in Equation (3.29). Comparison of Equations (3.34) and (3.36) indicate the preliminary factors are not, by themselves, sufficiently accurate, implying corrections are needed. Specifically, ω_1^2 (1.6 vs. 3.8) and $(2\zeta\omega)_2$ (3.5 vs. 0.62) indicate large discrepancies. With review of the basic parameters, it can be verified that criterion 3 is met for the above selection.

Before moving on to the correction terms, a slight modification to the strategy is considered. In Equation (3.1), the r^2 term denotes the open-loop root locations, while the rq and q^2 terms represent the feedback effects that modify the open-loop roots into closed-loop roots. Note the chosen preliminary factors in Equation (3.36) are the classic short period and aerodynamically damped pure vibration factors, arising solely from the r^2

term. Numerically speaking, the preliminary factors are not a sufficient approximation to even the bare airframe poles in Table 2.2 (see d(s)). As proposed, the factoring technique would attempt to correct for errors originating from both open-loop and closed-loop sources in *one-step*. Better accuracy can be had if the problem is broken down into a *two-step* procedure, first correcting for the open-loop errors, and second for the feedback errors. The first step was the subject of Ref. 35 and the results are applicable here (see Table 2.3). These results consist of the preliminary factors and their corrections for the bare airframe. These results will be interpreted as the preliminary factors for the second step, which is the subject of this dissertation. Therefore, the expressions for these new "preliminary" factors become

$$\tilde{k} = r(r_{11}r_{22})^{1/2} = 71$$

$$\tilde{\omega}_1^2 \approx \frac{Z_\alpha}{V_T} M_q - (1+\frac{Z_q}{V_T})M_\alpha - \frac{(1+\frac{Z_q}{V_T})M_\eta F_\alpha}{(\omega^2 - F_\eta)} = 1.8$$

$$(2\tilde{\zeta}\tilde{\omega})_1 \approx -\frac{Z_\alpha}{V_T} - M_q - \frac{[\frac{Z_\eta}{V_T} + (1+\frac{Z_q}{V_T})M_\eta]F_\alpha + M_\eta F_q}{(\omega^2 - F_\eta)} = 0.90 \qquad (3.37)$$

$$\tilde{\omega}_2^2 \approx (\omega^2 - F_\eta) + \frac{(1+\frac{Z_q}{V_T})M_\eta F_\alpha}{(\omega^2 - F_\eta)} = 37$$

$$(2\tilde{\zeta}\tilde{\omega})_2 \approx (2\zeta\omega - F_\eta) + \frac{[\frac{Z_\eta}{V_T} + (1+\frac{Z_q}{V_T})M_\eta]F_\alpha + M_\eta F_q}{(\omega^2 - F_\eta)} = 0.97$$

These modified preliminary factors provide a much better approximation to the airframe poles in Table 2.2. To account for the effect of feedback augmentation upon the root locations, corrections to these factors will now be considered, where only the rq and q^2 terms in Equation (3.1) are utilized.

To construct the symbolic Taylor series for the polynomial coefficients, consider equating like powers of s between the two forms given in Equation (3.35). The functional dependence of the polynomial coefficients upon the polynomial factors from these calculations is

$$\begin{aligned}
\phi_2 &= -k^2\{\omega_1^4\omega_2^4\} \\
\phi_4 &= -k^2\{2\omega_1^4\omega_2^2 + 2\omega_2^4\omega_1^2 - \omega_1^4(2\varsigma\omega)_2^2 - \omega_2^4(2\varsigma\omega)_1^2\} \\
\phi_6 &= -k^2\{\omega_1^4 + \omega_2^4 + 4\omega_1^2\omega_2^2 - 2\omega_1^2(2\varsigma\omega)_2^2 - 2\omega_2^2(2\varsigma\omega)_1^2 + (2\varsigma\omega)_1^2(2\varsigma\omega)_2^2\} \\
\phi_8 &= -k^2\{2\omega_1^2 + 2\omega_2^2 - (2\varsigma\omega)_1^2 - (2\varsigma\omega)_2^2\} \\
\phi_{10} &= -k^2
\end{aligned} \tag{3.38}$$

From Equation (3.38) an exact expression for k in closed-form is available. Thus, no correction is required for k and the corresponding row and column for ϕ_{10} in the Taylor series can be dropped and A becomes 4x4.

After calculating the appropriate partial derivatives of ϕ_i, the matrix A is expressed as in Equation (3.39).

$$A = -2\tilde{k}^2\begin{bmatrix} \tilde{\omega}_2^4\tilde{\omega}_1^2 & 0 & \tilde{\omega}_1^4\tilde{\omega}_2^2 & 0 \\ \tilde{\omega}_2^4 + \{2\tilde{\omega}_2^2 - (2\xi\tilde{\omega})_2^2\}\tilde{\omega}_1^2 & -\tilde{\omega}_2^4(2\xi\tilde{\omega})_1 & \tilde{\omega}_1^4 + \{2\tilde{\omega}_1^2 - (2\xi\tilde{\omega})_1^2\}\tilde{\omega}_2^2 & -\tilde{\omega}_1^4(2\xi\tilde{\omega})_2 \\ 2\tilde{\omega}_2^2 + \tilde{\omega}_1^2 - (2\xi\tilde{\omega})_2^2 & -\{2\tilde{\omega}_2^2 - (2\xi\tilde{\omega})_2^2\}(2\xi\tilde{\omega})_1 & 2\tilde{\omega}_1^2 + \tilde{\omega}_2^2 - (2\xi\tilde{\omega})_1^2 & -\{2\tilde{\omega}_1^2 - (2\xi\tilde{\omega})_1^2\}(2\xi\tilde{\omega})_2 \\ 1 & -(2\xi\tilde{\omega})_1 & 1 & -(2\xi\tilde{\omega})_2 \end{bmatrix} \tag{3.39}$$

After some effort, this A matrix can be inverted analytically. With the goal of *simple* and *useful* expressions, A^{-1} has far too many terms to retain. For example, the 1,1 element of A^{-1} is given as

$$A_{11}^{-1} = \frac{\begin{array}{l} 8\{-\tilde{\omega}_2^6(2\tilde{\zeta}\tilde{\omega})_1(2\tilde{\zeta}\tilde{\omega})_2 + [-3\tilde{\omega}_1^4 - (2\tilde{\zeta}\tilde{\omega})_1^4 + 4\tilde{\omega}_1^2(2\tilde{\zeta}\tilde{\omega})_1^2]\tilde{\omega}_2^2(2\tilde{\zeta}\tilde{\omega})_1(2\tilde{\zeta}\tilde{\omega})_2 \\ -[-2\tilde{\omega}_1^2 + (2\tilde{\zeta}\tilde{\omega})_1^2][2\tilde{\omega}_2^2(2\tilde{\zeta}\tilde{\omega})_1 - (2\tilde{\zeta}\tilde{\omega})_2^2(2\tilde{\zeta}\tilde{\omega})_1]\tilde{\omega}_2^2(2\tilde{\zeta}\tilde{\omega})_2\} \end{array}}{\begin{array}{l} 16\tilde{k}^2\tilde{\omega}_1^2\tilde{\omega}_2^2(2\tilde{\zeta}\tilde{\omega})_1(2\tilde{\zeta}\tilde{\omega})_2\{\tilde{\omega}_1^8 + \tilde{\omega}_2^8 + 6\tilde{\omega}_1^4\tilde{\omega}_2^4 - [\tilde{\omega}_2^4 + \tilde{\omega}_1^4]4\tilde{\omega}_1^2\tilde{\omega}_2^2 \\ + \tilde{\omega}_2^4(2\tilde{\zeta}\tilde{\omega})_1^4 + \tilde{\omega}_1^4(2\tilde{\zeta}\tilde{\omega})_2^4 - [\tilde{\omega}_2^2(2\tilde{\zeta}\tilde{\omega})_1^2 + \tilde{\omega}_1^2(2\tilde{\zeta}\tilde{\omega})_2^2]4\tilde{\omega}_1^2\tilde{\omega}_2^2 \\ + [2\tilde{\omega}_2^2 - (2\tilde{\zeta}\tilde{\omega})_2^2]\tilde{\omega}_1^4(2\tilde{\zeta}\tilde{\omega})_1^2 + [2\tilde{\omega}_1^2 - (2\tilde{\zeta}\tilde{\omega})_1^2]\tilde{\omega}_2^4(2\tilde{\zeta}\tilde{\omega})_2^2 + 2\tilde{\omega}_2^6(2\tilde{\zeta}\tilde{\omega})_1^2 + 2\tilde{\omega}_1^6(2\tilde{\zeta}\tilde{\omega})_2^2\} \end{array}} \quad (3.40)$$

However, if small numerical terms are neglected, the 1,1 element in A^{-1}, as well as all other elements can be reasonably approximated by Equation (3.41).

$$A^{-1} = \frac{1}{\Gamma}\begin{bmatrix} -(4\tilde{\omega}_1^2 - \tilde{\omega}_2^2)\tilde{\omega}_2^2(2\tilde{\zeta}\tilde{\omega})_1(2\tilde{\zeta}\tilde{\omega})_2 & 2\tilde{\omega}_1^4\tilde{\omega}_2^2(2\tilde{\zeta}\tilde{\omega})_1(2\tilde{\zeta}\tilde{\omega})_2 & -\tilde{\omega}_1^4\tilde{\omega}_2^2(2\tilde{\zeta}\tilde{\omega})_1(2\tilde{\zeta}\tilde{\omega})_2 & 2\tilde{\omega}_1^6\tilde{\omega}_2^2(2\tilde{\zeta}\tilde{\omega})_1(2\tilde{\zeta}\tilde{\omega})_2 \\ -(4\tilde{\omega}_1^2 - \tilde{\omega}_2^2)\tilde{\omega}_2^2(2\tilde{\zeta}\tilde{\omega})_2 & -2\tilde{\omega}_1^4\tilde{\omega}_1^2(2\tilde{\zeta}\tilde{\omega})_2 & \tilde{\omega}_1^4\tilde{\omega}_2^2(2\tilde{\zeta}\tilde{\omega})_2 & -(\tilde{\omega}_1^2 - 3(2\tilde{\zeta}\tilde{\omega})_1^2)\tilde{\omega}_1^4\tilde{\omega}_2^2(2\tilde{\zeta}\tilde{\omega})_2 \\ 2\tilde{\omega}_1^2\tilde{\omega}_2^2(2\tilde{\zeta}\tilde{\omega})_1(2\tilde{\zeta}\tilde{\omega})_2 & -2\tilde{\omega}_1^2\tilde{\omega}_2^4(2\tilde{\zeta}\tilde{\omega})_1(2\tilde{\zeta}\tilde{\omega})_2 & \tilde{\omega}_2^2\tilde{\omega}_1^2(2\tilde{\zeta}\tilde{\omega})_1(2\tilde{\zeta}\tilde{\omega})_2 & -2\tilde{\omega}_2^2\tilde{\omega}_1^4(2\tilde{\zeta}\tilde{\omega})_1(2\tilde{\zeta}\tilde{\omega})_2 \\ -(2\tilde{\omega}_1^2 - \tilde{\omega}_2^2)\tilde{\omega}_1^2(2\tilde{\zeta}\tilde{\omega})_1 & -2\tilde{\omega}_1^2\tilde{\omega}_2^4(2\tilde{\zeta}\tilde{\omega})_1 & \tilde{\omega}_2^2\tilde{\omega}_1^2(2\tilde{\zeta}\tilde{\omega})_1 & (4\tilde{\omega}_1^2 - \tilde{\omega}_2^2)\tilde{\omega}_2^2\tilde{\omega}_1^2(2\tilde{\zeta}\tilde{\omega})_1 \end{bmatrix}$$

$$= \begin{bmatrix} -1.2\times10^{-8} & -1.8\times10^{-8} & 3.1\times10^{-7} & -2.3\times10^{-6} \\ -1.0\times10^{-8} & 6.6\times10^{-8} & -2.5\times10^{-7} & -2.2\times10^{-7} \\ -4.7\times10^{-9} & 1.6\times10^{-7} & -2.9\times10^{-6} & 2.2\times10^{-5} \\ -3.0\times10^{-9} & 1.3\times10^{-7} & -4.6\times10^{-6} & 9.1\times10^{-5} \end{bmatrix}, \Gamma = -2\tilde{k}^2\tilde{\omega}_2^4\tilde{\omega}_1^2(2\tilde{\zeta}\tilde{\omega})_1(2\tilde{\zeta}\tilde{\omega})_2 \quad (3.41)$$

Moving on to the calculation for the excluded terms not selected in the preliminary factors, $\Delta\phi$ consists of the rq and q^2 terms in Equation (3.1), broken down into coefficients for the relevant powers of s. Recall that terms originating from the r^2 set are *not* included in $\Delta\phi$ for the modified two-step strategy. When fully expanded, expressions for $\Delta\phi_i$ are extremely long and unsatisfactory for obtaining insight. After retaining only the dominant terms, similar to the transition step from Equation (3.40) to (3.41), $\Delta\phi$ is approximately

$$\Delta\phi_2 \approx rq\{-r_{11}q_{22}(-\frac{Z_\alpha}{V_T}M_\eta F_{\delta_C})^2$$
$$-r_{22}(q_{11}+q_{22})(-\frac{Z_\alpha}{V_T}M_\eta F_{\delta_E}-\frac{Z_\alpha}{V_T}M_{\delta_E}(\omega^2-F_\eta))^2\} = -4.4\times10^5$$

$$\Delta\phi_4 \approx rq\{r_{11}q_{22}(M_\eta F_{\delta_C}+M_{\delta_C}(\omega^2-F_\eta)+(1+\frac{Z_q}{V_T})M_\alpha F_{\delta_C}\phi')^2 \quad (3.42)$$
$$+r_{22}q_{22}(M_{\delta_E}(\omega^2-F_\eta))^2\} = 5.8\times10^6$$

$$\Delta\phi_6 \approx rq\{-r_{11}q_{22}2F_{\delta_C}\phi'(M_\eta F_{\delta_C}+M_{\delta_C}(\omega^2-F_\eta)+(1+\frac{Z_q}{V_T})M_\alpha F_{\delta_C}\phi')$$
$$+r_{22}q_{22}2(M_{\delta_E}-F_{\delta_E}\phi')M_{\delta_E}(\omega^2-F_\eta)\} = 1.4\times10^5$$

$$\Delta\phi_8 \approx rq\{r_{11}q_{22}(-F_{\delta_C}\phi')^2+r_{22}q_{22}(M_{\delta_E}-F_{\delta_E}\phi')^2\} = 5.2\times10^4$$

The corrections to the preliminary factors Δx are obtained by forming the product of A^{-1} and $\Delta\phi$. This product yields four terms for each element of Δx. Again, keeping only the dominant terms, the corrections for the preliminary factors are

$$\Delta\omega_1^2 \approx \frac{\tilde{\omega}_1^2}{-\tilde{k}^2\tilde{\omega}_2^6}(\Delta\phi_4+\tilde{\omega}_1^2\tilde{\omega}_2^2\Delta\phi_8) = -0.22$$

$$\Delta(2\zeta\omega)_1 \approx \frac{1}{2\tilde{k}^2\tilde{\omega}_2^4(2\tilde{\zeta}\tilde{\omega})_1}\Delta\phi_4 = 0.38$$

$$\Delta\omega_2^2 \approx \frac{1}{\tilde{k}^2\tilde{\omega}_2^4}(\Delta\phi_4+\tilde{\omega}_1^2\tilde{\omega}_2^2\Delta\phi_8) = 2.1 \quad (3.43)$$

$$\Delta(2\zeta\omega)_2 \approx \frac{4\tilde{\omega}_1^2-\tilde{\omega}_2^2}{-2\tilde{k}^2\tilde{\omega}_2^2(2\tilde{\zeta}\tilde{\omega})_2}\Delta\phi_8 = 4.8$$

The pinnacle result from the above steps is now available. Approximate analytical expressions for the LQ characteristic polynomial factors are

$$\omega_1^2 \approx \tilde{\omega}_1^2+\Delta\omega_1^2 = 1.5$$

$$(2\varsigma\omega)_1 \approx (2\tilde{\zeta}\tilde{\omega})_1 + \Delta(2\varsigma\omega)_1 = 1.3$$

$$\omega_2^2 \approx \tilde{\omega}_2^2 + \Delta\omega_2^2 = 39 \qquad (3.44)$$

$$(2\varsigma\omega)_2 \approx (2\tilde{\zeta}\tilde{\omega})_2 + \Delta(2\varsigma\omega)_2 = 5.7$$

where ultimately, every term has been traced back to a function of the basic vehicle parameters and cost function weightings using Equations (3.37), (3.42) and (3.43). Table 3.1 contains the expanded results. In addition, Table 3.2 compares the numerical accuracy from the approximate expressions with the exact values. In each case, the accuracy is judged to be sufficient for portraying the relationships between closed-loop factors and design parameters. Additionally, Figures 3.2-3.5 show the closed-loop frequency responses computed by "exact" numerical techniques and from the approximate expressions. Note that since the Direct Eigen-Based Technique did not provide analytical results for the numerator factors, exact numerical data was substituting in their place to generate Figures 3.2-3.5. Again, the accuracy of the approximations is sufficient. Utilization of these expressions to explore the relationships they represent is deferred until Chapter VI.

Table 3.1 Analytical Expressions for LQ Eigenvalues

$$\omega_1^2 \approx \frac{Z_\alpha}{V_T} M_q - (1 + \frac{Z_q}{V_T}) M_\alpha - \frac{(1 + \frac{Z_q}{V_T}) M_\eta F_\alpha}{(\omega^2 - F_\eta)}$$

$$+ \frac{\tilde{\omega}_1^2}{-\tilde{k}^2 \tilde{\omega}_2^6}$$

$$[rq\{r_{11} q_{22} (M_\eta F_{\delta_c} + M_{\delta_c} (\omega^2 - F_\eta) + (1 + \frac{Z_q}{V_T}) M_\alpha F_{\delta_c} \phi')^2 + r_{22} q_{22} (M_{\delta_\varepsilon} (\omega^2 - F_\eta))^2\}$$

$$+\tilde{\omega}_1^2\tilde{\omega}_2^2 rq\{r_{11}q_{22}(-F_{\delta_C}\phi')^2 + r_{22}q_{22}(M_{\delta_E} - F_{\delta_E}\phi')^2\}]$$

$$(2\zeta\omega)_1 \approx -\frac{Z_\alpha}{V_T} - M_q - \frac{[\frac{Z_\eta}{V_T} + (1+\frac{Z_q}{V_T})M_\eta]F_\alpha + M_\eta F_q}{(\omega^2 - F_\eta)}$$

$$+\frac{1}{2\tilde{k}^2\tilde{\omega}_2^4(2\tilde{\zeta}\tilde{\omega})_1} rq\{r_{11}q_{22}(M_\eta F_{\delta_C} + M_{\delta_C}(\omega^2 - F_\eta) + (1+\frac{Z_q}{V_T})M_\alpha F_{\delta_C}\phi')^2$$

$$+ r_{22}q_{22}(M_{\delta_E}(\omega^2 - F_\eta))^2\}$$

$$\omega_2^2 \approx (\omega^2 - F_\eta) + \frac{(1+\frac{Z_q}{V_T})M_\eta F_\alpha}{(\omega^2 - F_\eta)}$$

$$+\frac{1}{\tilde{k}^2\tilde{\omega}_2^4}$$

$$[rq\{r_{11}q_{22}(M_\eta F_{\delta_C} + M_{\delta_C}(\omega^2 - F_\eta) + (1+\frac{Z_q}{V_T})M_\alpha F_{\delta_C}\phi')^2 + r_{22}q_{22}(M_{\delta_E}(\omega^2 - F_\eta))^2\}$$

$$+\tilde{\omega}_1^2\tilde{\omega}_2^2 rq\{r_{11}q_{22}(-F_{\delta_C}\phi')^2 + r_{22}q_{22}(M_{\delta_E} - F_{\delta_E}\phi')^2\}]$$

$$(2\zeta\omega)_2 \approx (2\zeta\omega - F_\eta) + \frac{[\frac{Z_\eta}{V_T} + (1+\frac{Z_q}{V_T})M_\eta]F_\alpha + M_\eta F_q}{(\omega^2 - F_\eta)}$$

$$+\frac{4\tilde{\omega}_1^2 - \tilde{\omega}_2^2}{-2\tilde{k}^2\tilde{\omega}_2^2(2\tilde{\zeta}\tilde{\omega})_2} rq\{r_{11}q_{22}(-F_{\delta_C}\phi')^2 + r_{22}q_{22}(M_{\delta_E} - F_{\delta_E}\phi')^2\}$$

Table 3.2 Accuracy of Analytical Expressions for LQ Eigenvalues

LQ Factors		Exact	Approximate Symbolic
ω_1^2	$1/s^2$	1.6	1.5
$(2\zeta\omega)_1$	1/s	1.4	1.3
ω_2^2	$1/s^2$	37	39
$(2\zeta\omega)_2$	1/s	3.5	5.7

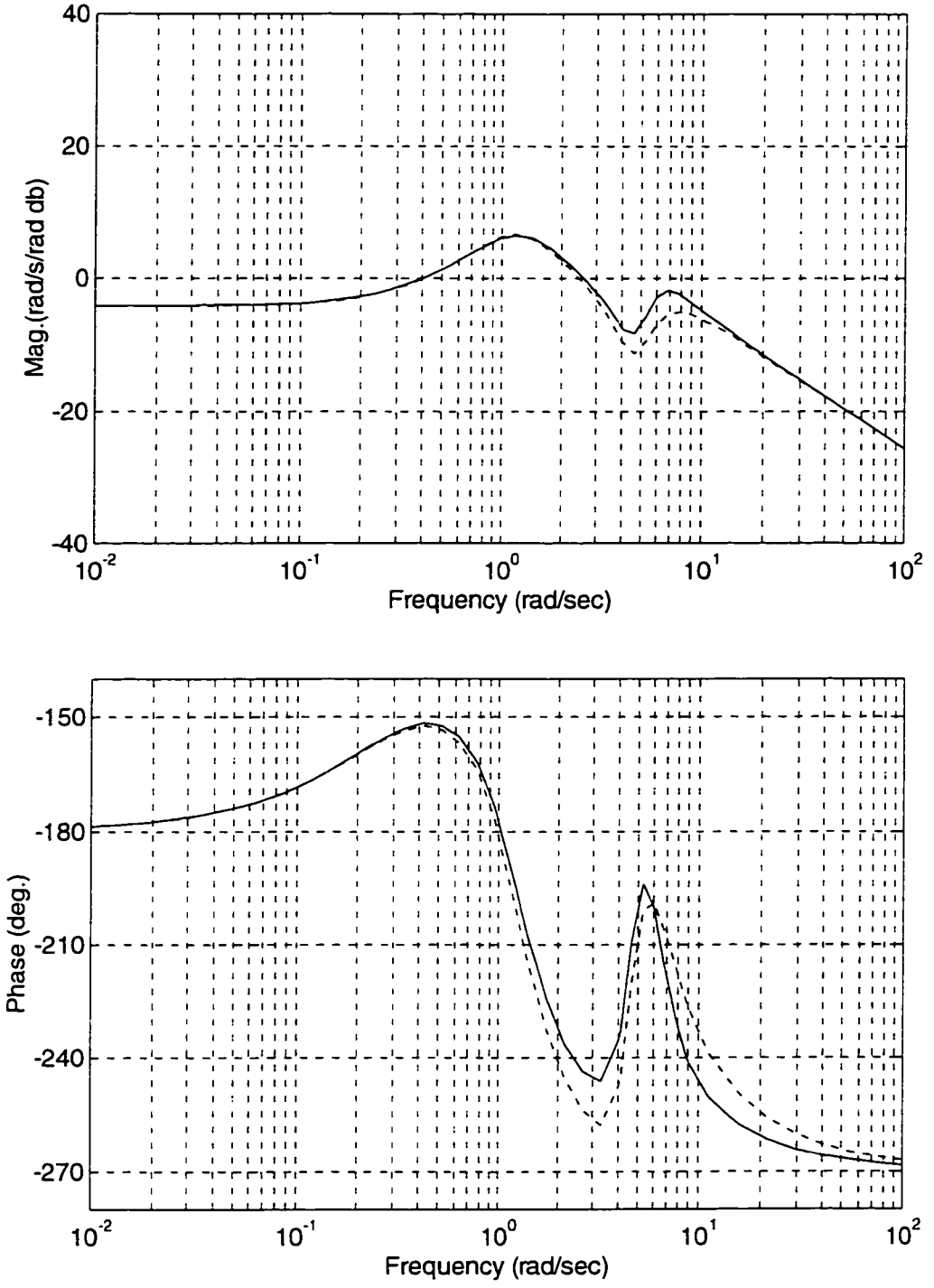

Figure 3.2 Comparison of q/δ_E Closed-Loop Frequency Responses Using the Approximate Symbolic Calculations

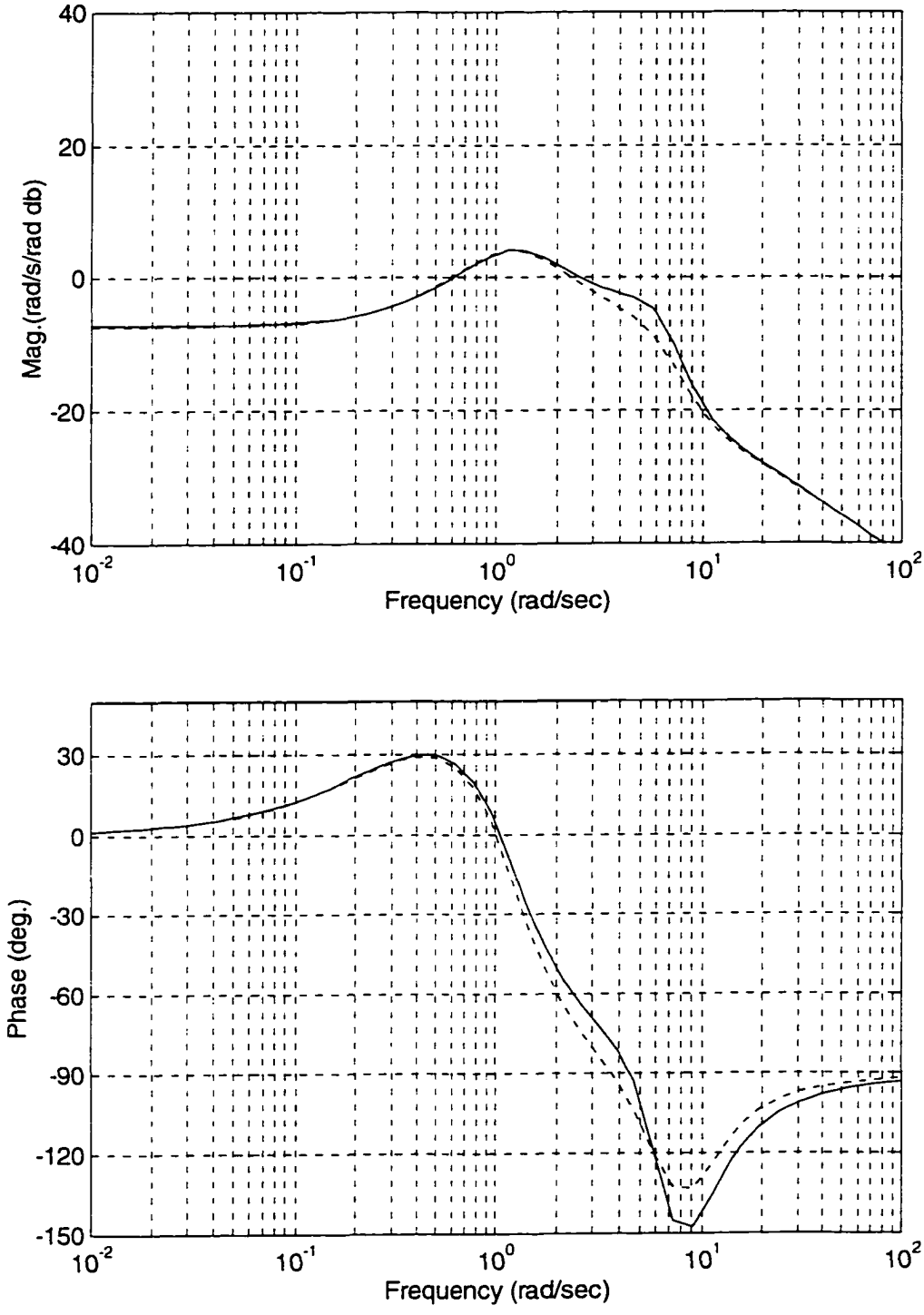

Figure 3.3 Comparison of q/δ_c Closed-Loop Frequency Responses Using the Approximate Symbolic Calculations

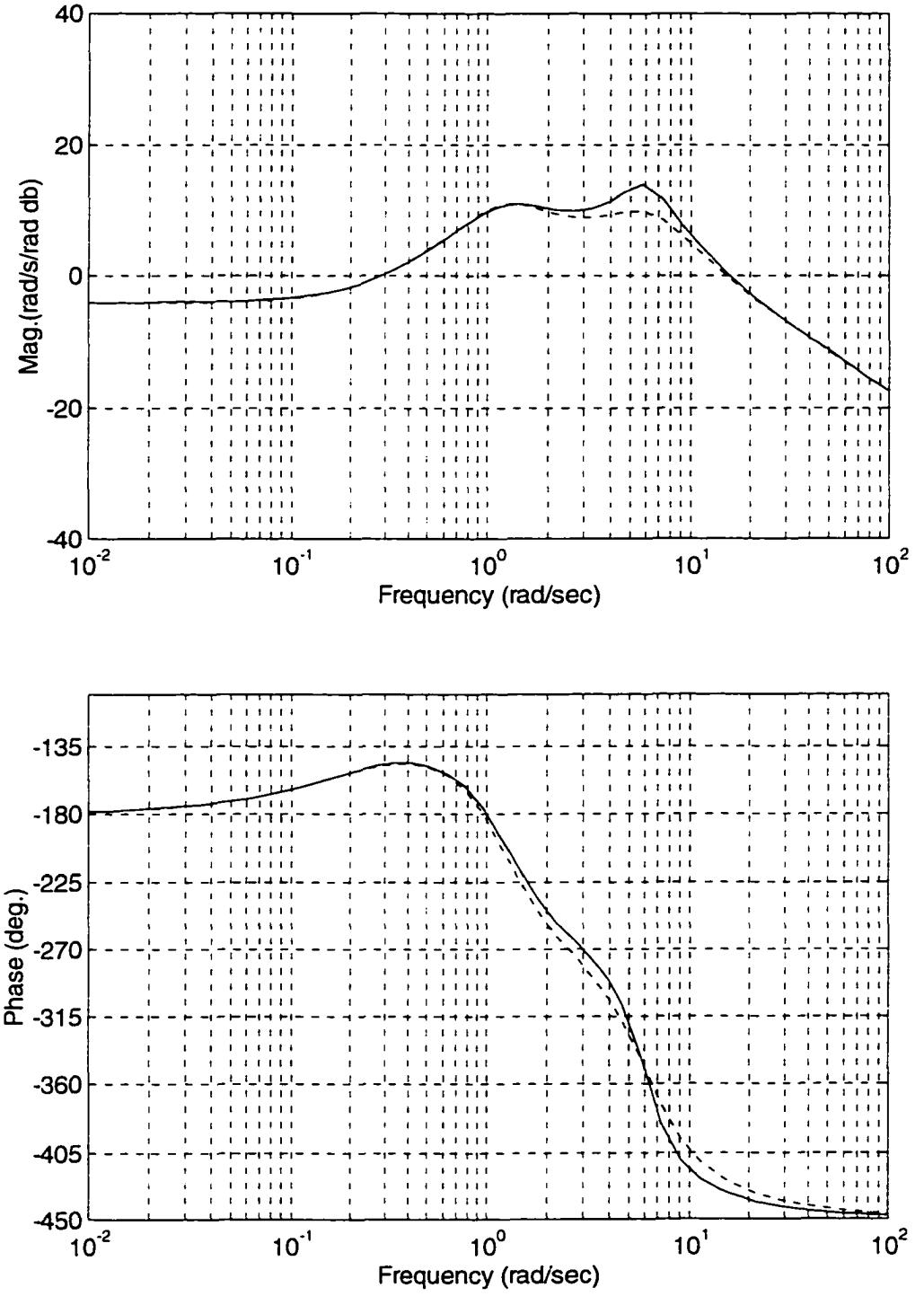

Figure 3.4 Comparison of q'/δ_E Closed-Loop Frequency Responses Using the Approximate Symbolic Calculations

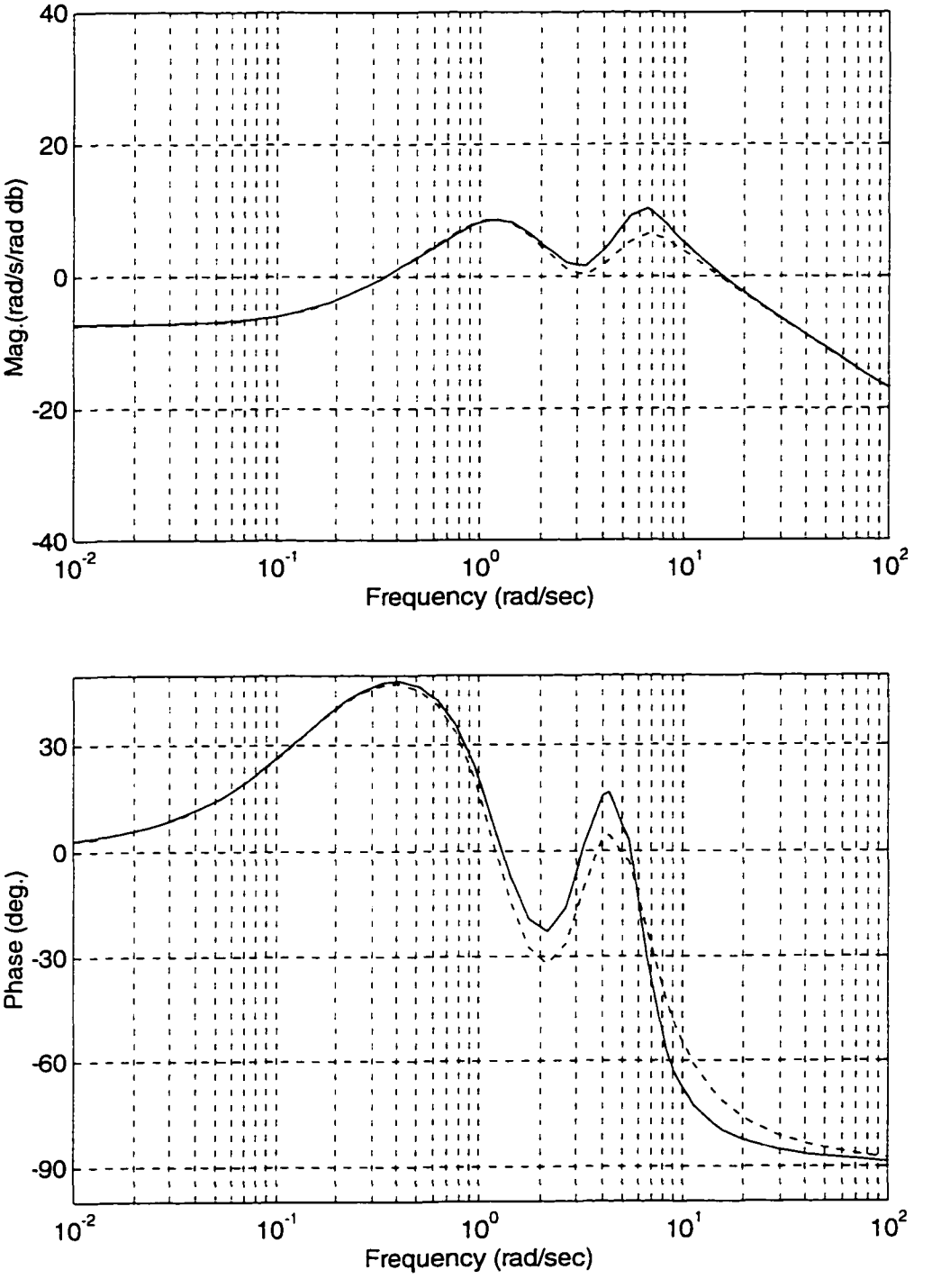

Figure 3.5 Comparison of q'/δ_c Closed-Loop Frequency Responses Using the Approximate Symbolic Calculations

CHAPTER IV

ORDER OF MAGNITUDE TECHNIQUE

4.1 Overview

In this chapter, the Order of Magnitude Technique is presented for generating approximate analytical expressions for the closed-loop denominator and numerator factors resulting from the standard LQ state feedback design strategy. The relationship between the closed-loop factors and the cost function weights is *indirect*, with the Riccati equation solution and/or feedback gain matrix acting as an intermediate variable. By applying an order of magnitude analysis to the basic system parameters, the Riccati equation can be reduced to a set of simple approximate equations which can be solved in closed-form. After forming the closed-loop transfer functions polynomials from the vehicle state-space matrices and the gain matrix, another order of magnitude simplification is considered to analytically factor these polynomials, in an approximate sense. This technique is applied to a numerical flight control system for an aeroelastic vehicle. The technique has yielded expressions which are amendable for understanding relationships and still provide sufficient accuracy.

4.2 Riccati Equation Solution

The initial step in the technique is to perform a classification of the matrix elements appearing in the Riccati equation (Equation (2.20)) for the purpose of tracking numerically large vs. small parameters throughout the solution procedure. These matrices

include the vehicle state space matrices A, B and C (Equation (2.6)), the cost function weight matrices Q and R (Equation (2.7)), and Riccati solution matrix P (Equation (2.20)). The classification is based on the numerical magnitudes of the individual elements within these matrices and is implemented by "tagging" all parameters with an extra symbolic tracking parameter ε. The classification is somewhat arbitrary, but would typically be based on powers of 10 (i.e., 0.1, 1, 10, etc.). As will be shown, the tracking parameter ε allows separation of dominant and negligible terms in a nonlinear equality such as the Riccati equation. By exploiting this separation, simplifications can be made to obtain approximate closed-loop solutions. The tracking parameter does not affect the numerics as it can be assigned a unity value.

A simple example is considered to further explain this classification of the matrix elements. Suppose the matrices A, P and Q are given as

$$A = \begin{bmatrix} a_{11} & a_{12} \\ a_{21} & a_{22} \end{bmatrix} = \begin{bmatrix} 6.0 & 1.1 \\ 0.2 & 1.0 \end{bmatrix}$$

$$P = \begin{bmatrix} p_{11} & p_{12} \\ p_{12} & p_{22} \end{bmatrix} = \begin{bmatrix} -0.10 & 0.30 \\ 0.30 & -10 \end{bmatrix} \tag{4.1}$$

$$Q = \begin{bmatrix} q_{11} & q_{12} \\ q_{12} & q_{22} \end{bmatrix} = \begin{bmatrix} 1.0 & 0.10 \\ 0.10 & 20 \end{bmatrix}$$

Note the matrix elements range from an order of magnitude of near 10^1 down to an order of magnitude near 10^{-1}. Each element is "tagged" with ε according to its power of 10. Thus, a_{11} would be tagged with ε^1, a_{12} with ε^0, and a_{21} with ε^{-1}, for example. After performing similar assignments for all the elements, the matrices in Equation (4.1) would

be replaced with matrices in Equation (4.2). With $\varepsilon = 1$, this substitution is transparent to further manipulation and the final results.

$$A = \begin{bmatrix} a_{11}\varepsilon^{1} & a_{12}\varepsilon^{0} \\ a_{21}\varepsilon^{-1} & a_{22}\varepsilon^{0} \end{bmatrix}$$

$$P = \begin{bmatrix} p_{11}\varepsilon^{-1} & p_{12}\varepsilon^{-1} \\ p_{12}\varepsilon^{-1} & p_{22}\varepsilon^{1} \end{bmatrix} \qquad (4.2)$$

$$Q = \begin{bmatrix} q_{11}\varepsilon^{0} & q_{12}\varepsilon^{-1} \\ q_{12}\varepsilon^{-1} & q_{22}\varepsilon^{1} \end{bmatrix}$$

The matrices which have been classified at the element level by the symbol ε are now substituted into the Riccati equation. After carrying out all necessary multiplications and additions in symbolic form, scalar equalities result for each element of the matrix Riccati equation. These equations are then decomposed into orders of magnitude based on the tracking parameters ε. A representative equality from this process for the ij element within the Riccati equation appears as

$$\{f_{ij_n}(A,B,C,Q,R,P)\}\varepsilon^{n} + \{f_{ij_{n-1}}(A,B,C,Q,R,P)\}\varepsilon^{n-1} + \ldots\ldots = 0 \qquad (4.3)$$

The leading term in this decomposition contains the collection of matrix elements corresponding to the largest numerical magnitudes. These magnitude values are on the order of 10^{n}. The second term in Equation (4.3) is of order of 10^{n-1} and so forth where n denotes and integer.

An approximate closed-form solution to the Riccati equation is obtained by extracting a dominant subset from the full expression in Equation (4.3). The exact Riccati equation can thus be replaced by the approximation

$$\{f_{ij_n}(A,B,C,Q,R,P)\} \approx 0 \qquad (4.4)$$

after neglecting the "small" terms. The simplified structure represented by Equation (4.4) facilitates an approximate closed-form solution for the Riccati matrix P, although solvability is not guaranteed in all problems due to the coupled nonlinear algebraic structure. A larger or smaller subset of terms from Equation (4.3) could be retained to possibly circumvent this potential problem, or to increase accuracy. However, when extracting the simplified subset, one must strike a balance between solvability of the equations (typically fewer terms) and numerical accuracy (more terms).

To illustrate the simplification of the Riccati equation, reconsider the example matrices in Equations (4.2). Further, assume here that C = I and R is infinite. In this case, the Riccati equation is,

$$PA + A^T P + Q = 0 \tag{4.5}$$

The numerical value for P in Equation (4.1) is precisely the solution which satisfies Equation (4.5) for the given A and Q values. Substitution of Equation (4.2) into Equation (4.5) leads to the following three scalar equations.

$$\begin{aligned}
&(2p_{11}a_{11} + q_{11})\varepsilon^0 + 2p_{12}a_{21}\varepsilon^{-2} = 0 \\
&(p_{11}a_{12} + p_{12}a_{22})\varepsilon^0 + (p_{12}a_{11} + p_{22}a_{21} + q_{12})\varepsilon^{-1} = 0 \\
&(2p_{22}a_{22} + q_{22})\varepsilon^1 + 2p_{12}a_{12}\varepsilon^{-1} = 0
\end{aligned} \tag{4.6}$$

Note the terms in Equation (4.6) have been grouped according to the tracking parameter ε. Retaining only the ε^0 terms which correspond to order of 1 for the first and second equations, and terms of order of 10 (ε^1) for the third equation, yields

$$\begin{aligned}
&2p_{11}a_{11} + q_{11} \approx 0 \\
&p_{11}a_{12} + p_{12}a_{22} \approx 0 \\
&2p_{22}a_{22} + q_{22} \approx 0
\end{aligned} \tag{4.7}$$

Even though Equation (4.5) can be solved in closed-form, for the sake of illustration, Equation (4.7) represents the simplified structure that would allow approximate closed-form solutions in a more general case.

4.3 Feedback Gain Calculation

Now focus on the technique to generate expressions for the feedback gain matrix. Equation (2.16) provides an explicit, closed-form solution for the gains as a simple multiplication function of several matrices including the Riccati solution from the previous section. This explicit structure makes the solution for the gains fundamentally easier when compared to the Riccati solution. With this explicit structure, application of the tracking parameter ε to the gain matrix is unnecessary.

The first step is to substitute the "tagged" matrices R, B and P from Section 4.2 into Equation (2.16). After carrying out the multiplications and decomposing the results based on the parameter ε, the ij element of the gain matrix appears as

$$K_{R_{ij}} = \{K_{R_{ij_n}}(B,R,P)\}\varepsilon^n + \{K_{R_{ij_{n-1}}}(B,R,P)\}\varepsilon^{n-1} + \ldots\ldots \tag{4.8}$$

If all terms were retained in Equation (4.8), and if the exact analytical solution for P were somehow available, then an exact analytical solution for K_R would be attainable.

The objective of this dissertation, however, is to develop simple relationships which will be useful for obtaining insight. Thus, consider retaining only the critical terms from the full expression in Equation (4.8). Again for illustrative purposes only, consider retaining the ε^n terms. The resulting expression is

$$K_{R_{ij}} \approx K_{R_{ij_n}}(B,R,P) \tag{4.9}$$

Equation (4.9) is an approximate equality, not only because higher order terms have been neglected, but also because the exact solution for P is unavailable. When computing K_R from Equation (4.9), the approximate solution for P from the previous section must be utilized. No other choice is available.

4.4 Transfer Function Polynomial Construction

With the feedback matrix available, the closed-loop transfer function polynomials are to be considered. Using the state-space closed-loop matrices in Equation (2.18), the transfer matrix can be computed as

$$G_{cl}(s) = C(sI - A + BK_R)^{-1}B \tag{4.10}$$

If the numerator and denominator polynomials are denoted as in Equation (2.29), then

$$\begin{aligned} \delta(s) &= \det[sI - A + BK_R] \\ N_{cl}(s) &= C\,\mathrm{adj}[sI - A + BK_R]B \end{aligned} \tag{4.11}$$

Up to this point, the matrix K_R has not been applied with the tracking parameter ε. However, this process is required to carry out further manipulations of the right-hand side of Equation (4.11). Following previous guidelines, ε is applied to the matrix K_R.

Carrying out the matrix operations indicated in Equation (4.11) leads to the transfer function polynomials expressed in coefficient form, or

$$\begin{aligned} \delta(s) &= s^q + \delta_{q-1}s^{q-1} + \ldots + \delta_1 s + \delta_0 \\ \eta_{ij}(s) &= \eta_{ij_p}s^p + \eta_{ij_{p-1}}s^{p-1} + \ldots + \eta_{ij_1}s + \eta_{ij_0} \end{aligned} \tag{4.12}$$

In Equation (4.12), q and p denote the polynomial orders. The polynomial coefficients in Equation (4.12) depend on the system matrices A, B, C and K_R as shown in Equation

(4.11). Utilizing the tracking parameter ε associated with these matrices, the polynomial coefficients can be decomposed according to orders of magnitude as

$$\begin{aligned}\delta_k &= \{\delta_{k_n}(A,B,K_R)\}\varepsilon^n + \{\delta_{k_{n-1}}(A,B,K_R))\}\varepsilon^{n-1} + \ldots\ldots \\ \eta_{ij_k} &= \{\eta_{ij_{k_n}}(A,B,C,K_R)\}\varepsilon^n + \{\eta_{ij_{k_{n-1}}}(A,B,C,K_R))\}\varepsilon^{n-1} + \ldots\ldots\end{aligned} \tag{4.13}$$

The relationships in Equation (4.13) are strict equalities only if the exact analytical solution for K_R is available. Extracting the dominant subset from Equation (4.13) for the purpose of retaining only the key effects in the relationships leads to

$$\begin{aligned}\delta_k &\approx \delta_{k_n}(A,B,K_R) \\ \eta_{ij_k} &\approx \eta_{ij_{k_n}}(A,B,C,K_R)\end{aligned} \tag{4.14}$$

Approximate equivalence in Equation (4.14) is again due to neglection of higher order decomposition terms and use of the approximate expressions for K_R.

4.5 Transfer Function Factoring

The final step in the Order of Magnitude Technique described in this chapter is the process of analytically factoring the closed-loop transfer function polynomials, in an approximate sense. Suppose the polynomials from Equation (2.29) are expressed in factored form

$$\begin{aligned}\delta(s) &= \prod_{m=1}^{q_r}[s+r_m]\prod_{m=1}^{q_c}[s+\alpha_m - i\beta_m][s+\alpha_m + i\beta_m] \\ \eta_{ij}(s) &= k_{ij}\prod_{m=1}^{p_r}[s+r_{ij_m}]\prod_{m=1}^{p_c}[s+\alpha_{ij_m} - i\beta_{ij_m}][s+\alpha_{ij_m} + i\beta_{ij_m}]\end{aligned} \tag{4.15}$$

where q_r and p_r denote the number of real factors while q_c and p_c denote the number of complex conjugate factors ($q=q_r+2q_c$, $p=p_r+2p_c$). Expanding Equation (4.15) and equating to Equation (4.12) leads to

$$\begin{aligned}\delta_k &= g_k(r_m, \alpha_m, \beta_m) \\ \eta_{ij_k}(s) &= h_k(k_{ij}, r_{ij_m}, \alpha_{ij_m}, \beta_{ij_m})\end{aligned} \tag{4.16}$$

The polynomial factors in Equation (4.16) must be "tagged" with the tracking parameter ε. Based on the numerical values of the factors in terms of powers of 10, this procedure is straight forward as outlined previously. After this step, the right-hand side of Equation (4.16) can be separated out into orders of magnitude as

$$\begin{aligned}\delta_k &= \{g_{k_n}(r_m, \alpha_m, \beta_m)\}\varepsilon^n + \{g_{k_{n-1}}(r_m, \alpha_m, \beta_m)\}\varepsilon^{n-1} + \ldots\ldots \\ \eta_{ij_k}(s) &= \{h_{k_n}(k_{ij}, r_{ij_m}, \alpha_{ij_m}, \beta_{ij_m})\}\varepsilon^n + \{h_{k_{n-1}}(k_{ij}, r_{ij_m}, \alpha_{ij_m}, \beta_{ij_m})\}\varepsilon^{n-1} + \ldots\ldots\end{aligned} \tag{4.17}$$

The strict equality in Equation (4.17) only holds when all terms are retained and exact expressions for δ_k and η_{ij_k} are available. Keeping the same assumptions as before, the dominant subset from Equation (4.17) would appear as

$$\begin{aligned}\delta_k &\approx g_{k_n}(r_m, \alpha_m, \beta_m) \\ \eta_{ij_k}(s) &\approx h_{k_n}(k_{ij}, r_{ij_m}, \alpha_{ij_m}, \beta_{ij_m})\end{aligned} \tag{4.18}$$

The noted simplifications in Equation (4.18) again facilitate approximate closed-form solutions to these coupled, nonlinear algebraic expressions. These solutions provide the final link between the closed-loop transfer function factors and the basic system parameters

4.6 Example

To demonstrate the procedure by applying it to the flight dynamics and control system from Chapter II, consider the vehicle state space matrices in Equation (2.6). By utilizing the information in Equation (2.1), these matrices are

$$A=\begin{bmatrix} \frac{Z_\alpha}{V_T} & 1+\frac{Z_q}{V_T} & \frac{Z_\eta}{V_T} & \frac{Z_\eta}{V_T} \\ M_\alpha & M_q & M_\eta & M_\eta \\ F_\alpha & F_q & -(2\varsigma\omega - F_\eta) & -(\omega^2 - F_\eta) \\ 0 & 0 & 1 & 0 \end{bmatrix} \cdot B=\begin{bmatrix} \frac{Z_{\delta_E}}{V_T} & \frac{Z_{\delta_C}}{V_T} \\ M_{\delta_E} & M_{\delta_C} \\ F_{\delta_E} & F_{\delta_C} \\ 0 & 0 \end{bmatrix} \cdot C=\begin{bmatrix} 0 & 1 & 0 & 0 \\ 0 & 1 & -\phi' & 0 \end{bmatrix} \quad (4.19)$$

where the state vector x is ordered as

$$x=[\alpha \quad q \quad \dot{\eta} \quad \eta]^T \quad (4.20)$$

Numerical values for the element parameters in Equation (4.19) can be found in Table 2.1. The cost function weighting matrices from Equation (2.27) are re-expressed as

$$Q=\begin{bmatrix} q_1 & 0 \\ 0 & q_3 \end{bmatrix} \quad , \quad R=\begin{bmatrix} r_1 & 0 \\ 0 & r_3 \end{bmatrix} \quad (4.21)$$

where numerical values can be backed out from Equation (2.28) with r=50 $1/rad^2$. Finally, the Riccati equation solution is represented analytically as

$$P=\begin{bmatrix} p_1 & p_2 & p_3 & p_4 \\ p_2 & p_5 & p_6 & p_7 \\ p_3 & p_6 & p_8 & p_9 \\ p_4 & p_7 & p_9 & p_{10} \end{bmatrix} \quad (4.22)$$

For the specific design considered in Chapter II, the corresponding numerical values are

$$P=\begin{bmatrix} 7.1\frac{1}{rad^2} & 1.4\frac{s}{rad^2} & -0.0075\frac{s}{rad^2} & 0.15\frac{1}{rad^2} \\ 1.4\frac{s}{rad^2} & 2.8\frac{s^2}{rad^2} & -0.0036\frac{s^2}{rad^2} & 0.073\frac{s}{rad^2} \\ -0.0075\frac{s}{rad^2} & -0.0036\frac{s^2}{rad^2} & 0.00016\frac{s^2}{rad^2} & -0.00016\frac{s}{rad^2} \\ 0.15\frac{1}{rad^2} & 0.073\frac{s}{rad^2} & -0.00016\frac{s}{rad^2} & 0.0056\frac{1}{rad^2} \end{bmatrix} \tag{4.23}$$

By assessing the magnitudes of the elements of these matrices relative to powers of 10, they can be grouped into sets based on their magnitude order. For example, $1+\frac{Z_q}{V_T}$ is of order 10^0 while $\frac{Z_{\delta_e}}{V_T}$ is of order 10^{-1}. Therefore, $1+\frac{Z_q}{V_T}$ would be tagged with the tracking parameter ε^0 and $\frac{Z_{\delta_e}}{V_T}$ would be assigned the parameter ε^{-1}. In this manner the matrices are given ε assignments as

$$A=\begin{bmatrix} \frac{Z_\alpha}{V_T}\varepsilon^{-1} & (1+\frac{Z_q}{V_T})\varepsilon^0 & \frac{Z_\eta}{V_T}\varepsilon^{-4} & \frac{Z_\eta}{V_T}\varepsilon^{-3} \\ M_\alpha\varepsilon^0 & M_q\varepsilon^0 & M_\eta\varepsilon^{-3} & M_\eta\varepsilon^{-2} \\ F_\alpha\varepsilon^3 & F_q\varepsilon^2 & -(2\varsigma\omega-F_{\dot\eta})\varepsilon^0 & -(\omega^2-F_\eta)\varepsilon^1 \\ 0 & 0 & 1 & 0 \end{bmatrix}$$

$$B=\begin{bmatrix} \frac{Z_{\delta_e}}{V_T}\varepsilon^{-1} & \frac{Z_{\delta_c}}{V_T}\varepsilon^{-2} \\ M_{\delta_e}\varepsilon^0 & M_{\delta_c}\varepsilon^0 \\ F_{\delta_e}\varepsilon^3 & F_{\delta_c}\varepsilon^3 \\ 0 & 0 \end{bmatrix}, \quad C=\begin{bmatrix} 0 & 1 & 0 & 0 \\ 0 & 1 & -\phi'\varepsilon^{-2} & 0 \end{bmatrix}$$

$$P=\begin{bmatrix} p_1\varepsilon^{1} & p_2\varepsilon^{0} & p_3\varepsilon^{-2} & p_4\varepsilon^{-1} \\ p_2\varepsilon^{0} & p_5\varepsilon^{0} & p_6\varepsilon^{-3} & p_7\varepsilon^{-1} \\ p_3\varepsilon^{-2} & p_6\varepsilon^{-3} & p_8\varepsilon^{-4} & p_9\varepsilon^{-4} \\ p_4\varepsilon^{-1} & p_7\varepsilon^{-1} & p_9\varepsilon^{-4} & p_{10}\varepsilon^{-3} \end{bmatrix}, \quad Q=\begin{bmatrix} q_1\varepsilon^{0} & 0 \\ 0 & q_3\varepsilon^{0} \end{bmatrix}, \quad R=\begin{bmatrix} r_1\varepsilon^{2} & 0 \\ 0 & r_3\varepsilon^{1} \end{bmatrix} \tag{4.24}$$

Some assignments are subjective when the numerical values fall half way between two magnitude orders. Recall ε is utilized to track large vs. small parameters such that dominant relationships can be extracted from the unsolvable full expressions. This parameter also drops out of the results in a transparent way and it does not affect the numerics as it can be assigned the value of 1.

Substituting Equation (4.24) into the Riccati equation and neglecting higher order terms in ε gives the simplified equations in Table 4.1. These equations would correspond to Equation (4.4) in the general framework. Note the following abbreviations have been used to simplify the appearance of these relationships.

$$\tilde{Z}_\alpha=\frac{Z_\alpha}{V_T}, \quad \tilde{Z}_q=1+\frac{Z_q}{V_T}, \quad \tilde{Z}_\eta=\frac{Z_\eta}{V_T}, \quad \tilde{Z}_{\dot{\eta}}=\frac{Z_{\dot{\eta}}}{V_T}, \quad \tilde{Z}_{\delta_E}=\frac{Z_{\delta_E}}{V_T}$$

$$\tilde{Z}_{\delta_c}=\frac{Z_{\delta_c}}{V_T}, \quad \tilde{F}_\eta=2\zeta\omega-F_\eta, \quad \tilde{F}_\eta=\omega^2-F_\eta$$

These equations can be solved by simple substitution techniques and the results are listed in Table 4.2. These results are approximate analytical expressions for the Riccati solution in terms of aircraft and cost weight parameters. To assess the accuracy of the approximate expressions for p_i, consider Table 4.3, which contrasts exact numerical values with those for the symbolic expressions. In each element of P, the accuracy is quite acceptable

indicating the feedback gain can now be computed from these expressions without introducing significant errors.

Table 4.1 Simplified Riccati Equations

$$M_\alpha p_2 + F_\alpha p_3 + \tilde{Z}_\alpha p_1 \approx 0$$

$$M_\alpha p_5 + F_\alpha p_6 + (M_q + \tilde{Z}_\alpha)p_2 + \tilde{Z}_q p_1 \approx 0$$

$$p_4 + M_\alpha p_6 + F_\alpha p_8 + (-\tilde{F}_\eta + \tilde{Z}_\alpha)p_3 \approx 0$$

$$M_\eta p_2 - \tilde{F}_\eta p_3 + M_\alpha p_7 + F_\alpha p_9 + \tilde{Z}_\alpha p_4 + \tilde{Z}_\eta p_1 - \frac{M_{\delta_E}^2 p_2 p_7}{r_1} \approx 0$$

$$q_1 + q_3 + 2(\tilde{Z}_q p_2 + M_q p_5 + F_q p_6) - \frac{M_{\delta_E}^2 p_5^2}{r_1} \approx 0$$

$$p_7 + F_q p_8 + \tilde{Z}_q p_3 - \phi' q_3 + M_\eta p_5 \approx 0$$

$$M_\eta p_5 - \tilde{F}_\eta p_6 + M_q p_7 + F_q p_9 + \tilde{Z}_q p_4 - \frac{M_{\delta_E}^2 p_5 p_7}{r_1} \approx 0$$

$$2p_9 - 2\tilde{F}_\eta p_8 + \phi'^2 q_3 - \left(\frac{F_{\delta_E}^2}{r_1} + \frac{F_{\delta_C}^2}{r_3}\right)p_8^2 \approx 0 \qquad (p_9 \approx -p_8)$$

$$p_{10} - \tilde{F}_\eta p_8 \approx 0$$

$$2M_\eta p_7 - 2\tilde{F}_\eta p_9 - \frac{M_{\delta_E}^2 p_7^2}{r_1} - \frac{F_{\delta_E}^2 p_9^2}{r_1} \approx 0$$

Table 4.2 Symbolic Expressions for Riccati Matrix Elements

$$p_8 \approx \frac{-r_3 r_1 + \phi'\sqrt{F_{\delta_E}^2 q_3 r_1^2 r_3 + F_{\delta_C}^2 q_3 r_3^2 r_1}}{(F_{\delta_E}^2 r_1 + F_{\delta_C}^2 r_3)}$$

$$p_9 \approx -p_8$$

$$p_{10} \approx \tilde{F}_\eta p_8$$

$$p_7 \approx \frac{M_\eta r_1^2 F_{\delta_E}^2}{2M_{\delta_E}^2 (r_3 F_{\delta_C}^2 + r_1 F_{\delta_E}^2)} + \frac{\sqrt{\tilde{F}_\eta r_1 \phi' \sqrt{q_3 r_3 r_1}}}{M_{\delta_E}^2 \sqrt[4]{(r_3 F_{\delta_C}^2 + r_1 F_{\delta_E}^2)}}$$

$$p_2 \approx \frac{(M_\eta r_1 - M_{\delta_E}^2 p_7)(\tilde{Z}_\alpha + 1) F_\alpha p_8}{M_\eta (M_\eta r_1 - 2M_{\delta_E}^2 p_7)}$$

$$p_3 \approx \frac{M_\eta r_1 (2\tilde{F}_\eta \tilde{Z}_\alpha^2 - \tilde{Z}_q F_\alpha M_\eta)(\tilde{Z}_\alpha + 1) p_8}{M_\eta (M_\eta r_1 - 2M_{\delta_E}^2 p_7) \tilde{Z}_q \tilde{Z}_\alpha}$$

$$p_5 \approx -\frac{-\tilde{Z}_q p_3 + p_7 + F_q p_8 - q_3 \phi'}{M_\eta - \frac{M_{\delta_E} F_{\delta_E} p_8}{r_1}}$$

$$p_4 \approx -\frac{M_\eta p_2 r_1 - F_\alpha p_8 r_1 - M_{\delta_E}^2 p_2 p_7}{r_1 \tilde{Z}_\alpha}$$

$$p_1 \approx -\frac{r_1 (M_\alpha p_2 - F_\alpha p_3) - M_{\delta_E}^2 p_2^2}{r_1 \tilde{Z}_\alpha}$$

$$p_6 \approx -\frac{2(M_\eta r_1 - M_{\delta_E}^2 p_7)(\tilde{Z}_\alpha + 1)(\tilde{Z}_\alpha + M_q) p_8}{M_\eta (M_\eta r_1 - 2M_{\delta_E}^2 p_7)}$$

Table 4.3 Accuracy of the Symbolic Expressions for the Riccati Matrix

Riccati Solution	Exact	Approximate Symbolic
p_1	7.1	7.9
p_2	1.4	1.2
p_3	-0.0075	-0.0075
p_4	0.15	0.16
p_5	2.8	2.4
p_6	-0.0036	-0.0030
p_7	0.073	0.066

p_8	0.00016	0.00016
p_9	-0.00016	-0.00016
p_{10}	0.0056	0.0057

The feedback gain matrix is represented analytically as

$$K_R = \begin{bmatrix} k_1 & k_2 & k_3 & k_4 \\ k_5 & k_6 & k_7 & k_8 \end{bmatrix} \tag{4.25}$$

Using the design from Chapter II, the numerical values correspond to Equation (4.25) are

$$K_R = \begin{bmatrix} -0.010 & -0.11\,s & -0.0012\,s & -0.0024 \\ 0.11 & 0.091\,s & -0.0021\,s & 0.0032 \end{bmatrix} \tag{4.26}$$

Substituting Equation (4.24) into the feedback gain expression (Equation (2.16)), and neglecting the higher order terms in ε, yields the approximate analytical expressions for the gain matrix listed in Table 4.4. The expressions are in terms of basic aircraft parameters and the Riccati equation solution. Using Table 4.2, these latter variables can ultimately be expressed in terms of the aircraft and weighting parameters. The results in Table 4.4 correspond to Equation (4.9) in the general framework. Finally, Table 4.5 assesses the accuracy of these approximate expressions. The accuracy is quite sufficient for the purposes of this dissertation.

Table 4.4 Symbolic Expressions for the Gain Matrix

$k_1 \approx \dfrac{\tilde{Z}_{\delta_E} p_1 + M_{\delta_E} p_2 + F_{\delta_E} p_3}{r_1}$
$k_2 \approx \dfrac{M_{\delta_E} p_5 + F_{\delta_E} p_6}{r_1}$

$$k_3 \approx \frac{M_{\delta_E} p_6 + F_{\delta_E} p_8}{r_1}$$

$$k_4 \approx \frac{M_{\delta_E} p_7 + F_{\delta_E} p_9}{r_1}$$

$$k_5 \approx \frac{M_{\delta_C} p_2 + F_{\delta_C} p_3}{r_3}$$

$$k_6 \approx \frac{M_{\delta_C} p_5 + F_{\delta_C} p_6}{r_3}$$

$$k_7 \approx \frac{F_{\delta_C} p_8}{r_3}$$

$$k_8 \approx \frac{\tilde{Z}_{\delta_C} p_4 + M_{\delta_C} p_7 + F_{\delta_C} p_9}{r_3}$$

Table 4.5 Accuracy of the Symbolic Expressions for the Gain Matrix

Feedback Gain	Exact	Approximate Symbolic
k_1	-0.010	-0.012
k_2	-0.11	-0.11
k_3	-0.0012	-0.0012
k_4	-0.0024	-0.0023
k_5	0.11	0.12
k_6	0.091	0.091
k_7	-0.0021	-0.0020
k_8	0.0032	0.0031

Although not needed for the previous step, the gain matrix elements must be tagged with ε for the transfer function calculations. Based on the numerical data in Equation (4.26), the gain matrix is given ε assignments as

$$K_R = \begin{bmatrix} k_1\varepsilon^{-2} & k_2\varepsilon^{-1} & k_3\varepsilon^{-3} & k_4\varepsilon^{-3} \\ k_5\varepsilon^{-1} & k_6\varepsilon^{-1} & k_7\varepsilon^{-3} & k_8\varepsilon^{-3} \end{bmatrix} \tag{4.27}$$

Further, the closed-loop numerator and denominator polynomials in coefficient form are denoted analytically as

$$\begin{aligned} \delta(s) &= 1s^4 + \delta_3 s^3 + \delta_2 s^2 + \delta_1 s + \delta_0 \\ \eta_{11}(s) &= \eta_{113} s^3 + \eta_{112} s^2 + \eta_{111} s + \eta_{110} \\ \eta_{12}(s) &= \eta_{123} s^3 + \eta_{122} s^2 + \eta_{121} s + \eta_{120} \\ \eta_{21}(s) &= \eta_{213} s^3 + \eta_{212} s^2 + \eta_{211} s + \eta_{210} \\ \eta_{22}(s) &= \eta_{223} s^3 + \eta_{222} s^2 + \eta_{221} s + \eta_{220} \end{aligned} \tag{4.28}$$

By expanding the data of Table 2.5, these coefficients have the following numerical values.

$$\begin{aligned} \delta(s) &= s^4 + 4.9s^3 + 44s^2 + 57s + 58 \\ \eta_{11}(s) &= -5.1s^3 - 10s^2 - 110s - 36 \\ \eta_{12}(s) &= 0.81s^3 + 8.2s^2 + 82s + 25 \\ \eta_{21}(s) &= 13s^3 + 10s^2 - 150s - 36 \\ \eta_{22}(s) &= 14s^3 + 35s^2 + 150s + 25 \end{aligned} \tag{4.29}$$

The coefficients in Equation (4.28) are complex functions of the feedback gains and aircraft parameters and will require further simplification if they are to be used for obtaining insight. For example, substitution of Equation (4.24) and (4.27) into Equation (4.11) leads to the following expression for coefficient δ_2

$$\delta_2 = \tilde{F}_\eta \varepsilon^1 + (F_{\delta_C} k_8 - M_q F_{\delta_C} k_7 - M_q \tilde{F}_\eta - M_\alpha \tilde{Z}_q + F_{\delta_E} k_4 - M_q F_{\delta_E} k_3)\varepsilon^0 + (M_{\delta_C} k_5 \tilde{Z}_\alpha + F_{\delta_C} k_6 M_{\dot{\eta}} + F_\alpha \tilde{Z}_{\delta_E} k_{33} - F_q M_{\dot{\eta}} + F_\alpha \tilde{Z}_{\delta_E} k_3 - F_{\delta_E} k_2 M_{\delta_C} k_7 + F_{\delta_E} k_2 M_{\dot{\eta}} - F_{\delta_C} k_6 M_{\delta_E} k_3 + M_{\delta_E} k_2 \tilde{F}_\eta + F_q M_{\delta_E} k_3 + F_q M_{\delta_C} k_7 - F_\alpha \tilde{Z}_\eta + M_{\delta_E} k_2 F_{\delta_C} k_7 + k_6 M_{\delta_C} \tilde{F}_\eta + \tilde{Z}_\alpha M_q - \tilde{Z}_\alpha F_{\delta_C} k_7 - \tilde{Z}_\alpha \tilde{F}_\eta)\varepsilon^{-1} + (-F_{\delta_C} k_5 \tilde{Z}_{\delta_E} k_3 + M_\alpha \tilde{Z}_{\delta_E} k_2 + \tilde{Z}_\alpha M_{\delta_C} k_7 + F_{\delta_C} k_5 \tilde{Z}_\eta - \tilde{Z}_\alpha M_{\delta_E} k_2 + M_{\delta_E} k_1 \tilde{Z}_q)\varepsilon^{-2} + (-\tilde{Z}_{\delta_E} k_1 M_q - \tilde{Z}_{\delta_C} k_5 M_q + \tilde{Z}_{\delta_C} k_5 \tilde{F}_\eta + \tilde{Z}_{\delta_E} k_1 F_{\delta_C} k_7 + M_\alpha \tilde{Z}_{\delta_C} k_6 + F_{\delta_E} k_1 \tilde{Z}_{\dot{\eta}} + F_{\delta_E} k_5 \tilde{Z}_{\delta_C} k_3 - k_2 M_{\delta_C} k_5 \tilde{Z}_{\delta_E} + \tilde{Z}_{\delta_E} k_5 \tilde{F}_{\dot{\eta}})\varepsilon^{-3} + (\tilde{Z}_{\delta_C} k_5 M_{\delta_E} k_2 - F_{\delta_E} k_1 \tilde{Z}_{\delta_C} k_7 + \tilde{Z}_{\delta_E} k_1 M_{\delta_C} k_6)\varepsilon^{-4} + (M_{\delta_E} k_1 \tilde{Z}_{\delta_E} k_6)\varepsilon^{-5} \quad (4.30)$$

If the goal is to obtain insight from the final expressions, there are far to many terms in Equation (4.30). However, note many of the terms are of higher order indicated by the $\varepsilon^{-1}, \varepsilon^{-2}, \varepsilon^{-3}, \varepsilon^{-4}$ and ε^{-5} terms. Retention the ε^1 terms and a partial subset of the ε^0 terms yields

$$\delta_2 \approx \tilde{F}_\eta - M_q (F_{\delta_E} k_3 + F_{\delta_C} k_7) - M_\alpha \tilde{Z}_q \quad (4.31)$$

Note ε has been taken as 1 in Equation (4.31). Equation (4.31) provides a much more tractable relationship.

Following similar steps for all polynomial coefficients in Equation (4.28) yields the simplified expressions listed in Tables 4.6 and 4.7. These relationships correspond to Equation (4.14) in the general framework. In these tables, the closed-loop transfer function polynomial coefficients are displayed as functions of the aircraft parameters and feedback gains. With utilization of Tables 4.4 and 4.2, the gains can be traced back to the cost function design parameters and additional vehicle parameters. Tables 4.8 and 4.9 compare the accuracy from these expressions with exact values. Accuracy is again deemed sufficient for the intent here.

Table 4.6 Symbolic Expressions for δ(s) Coefficients

$$\delta_3 \approx \tilde{F}_\eta - M_q - \tilde{Z}_\alpha + M_{\delta_E} k_2 + F_{\delta_C} k_7 + F_{\delta_E} k_3$$

$$\delta_2 \approx \tilde{F}_\eta - M_q (F_{\delta_E} k_3 + F_{\delta_C} k_7) - M_\alpha \tilde{Z}_q$$

$$\delta_1 \approx -M_q \tilde{F}_\eta - \tilde{Z}_\alpha \tilde{F}_\eta + M_{\delta_E} k_2 \tilde{F}_\eta - F_q M_\eta$$

$$\delta_0 \approx -F_\alpha \tilde{Z}_q M_\eta - M_\alpha \tilde{Z}_q \tilde{F}_\eta - \tilde{Z}_\alpha M_{\delta_E} k_2 \tilde{F}_\eta$$

Table 4.7 Symbolic Expressions for $\eta_{ij}(s)$ Coefficients

$$\eta_{11_3} = M_{\delta_E}$$
$$\eta_{11_2} \approx M_{\delta_E} (F_{\delta_C} k_7 - \tilde{Z}_\alpha)$$
$$\eta_{11_1} \approx F_{\delta_E} M_\eta + M_{\delta_E} \tilde{F}_\eta$$
$$\eta_{11_0} \approx F_{\delta_E} M_\eta \tilde{Z}_\alpha + M_{\delta_E} \tilde{Z}_\eta F_\alpha$$

$$\eta_{12_3} = M_{\delta_C}$$
$$\eta_{12_2} \approx F_{\delta_C} M_\eta + M_{\delta_C} \tilde{F}_\eta - F_{\delta_C} M_{\delta_E} k_3 + M_{\delta_C} F_{\delta_E} k_3$$
$$\eta_{12_1} \approx F_{\delta_C} M_\eta + F_{\delta_C} M_\alpha \tilde{Z}_\eta + M_{\delta_C} \tilde{F}_\eta$$
$$\eta_{12_0} \approx -M_{\delta_C} \tilde{F}_\eta \tilde{Z}_\alpha - F_{\delta_C} M_\eta \tilde{Z}_\alpha + F_{\delta_C} \tilde{Z}_\eta M_\alpha$$

$$\eta_{21_3} = M_{\delta_E} - \phi' F_{\delta_E}$$
$$\eta_{21_2} \approx M_{\delta_E} \tilde{F}_\eta + \phi' F_{\delta_E} M_q$$
$$\eta_{21_1} \approx M_{\delta_E} \tilde{F}_\eta$$
$$\eta_{21_0} \approx F_{\delta_E} M_\eta \tilde{Z}_\alpha + M_{\delta_E} \tilde{Z}_\eta F_\alpha$$

$$\eta_{22_3} = M_{\delta_C} - \phi' F_{\delta_C}$$
$$\eta_{22_2} \approx F_{\delta_C} M_\eta + \phi' F_{\delta_C} M_q + \phi' F_{\delta_C} \tilde{Z}_\alpha - F_{\delta_C} M_{\delta_E} k_3 - M_{\delta_C} \tilde{Z}_\alpha - \phi' F_{\delta_C} M_{\delta_E} k_2 + \tilde{Z}_{\delta_C} M_\alpha$$
$$\eta_{22_1} \approx -(\phi' M_{\delta_C} \tilde{Z}_q F_\alpha + \phi' F_{\delta_C} \tilde{Z}_\alpha M_q + \phi' F_{\delta_C} \tilde{Z}_\alpha M_{\delta_E} k_2 - \phi' F_{\delta_C} M_\alpha \tilde{Z}_q - F_{\delta_C} M_\eta - M_{\delta_C} \tilde{F}_\eta)$$
$$\eta_{22_0} \approx -M_{\delta_C} \tilde{F}_\eta \tilde{Z}_\alpha - F_{\delta_C} M_\eta \tilde{Z}_\alpha + F_{\delta_C} \tilde{Z}_\eta M_\alpha$$

Table 4.8 Accuracy of the Symbolic Expressions for $\delta(s)$ Coefficients

δ_i Coefficient	Exact	Approximate Symbolic
δ_3 s^{-1}	4.9	4.8
δ_2 s^{-2}	44	40
δ_1 s^{-3}	57	58
δ_0 s^{-4}	58	57

Table 4.9 Accuracy of the Symbolic Expressions for $\eta_{ij}(s)$ Coefficients

η_{ij} Coefficient	Exact	Approximate Symbolic
η_{11_1} s^{-2}	-5.1	-5.1
η_{11_2} s^{-3}	-10	-9
η_{11_1} s^{-4}	-110	-120
η_{11_0} s^{-5}	-36	-38
η_{12_1} s^{-2}	0.81	0.81
η_{12_2} s^{-3}	8.2	7.8
η_{12_1} s^{-4}	82	69
η_{12_0} s^{-5}	25	23
η_{21_1} s^{-2}	13	13
η_{21_2} s^{-3}	10	12

η_{21_1} s^{-4}	-150	-180
η_{21_0} s^{-5}	-36	-38
η_{22_2} s^{-2}	14	14
η_{22_2} s^{-3}	35	31
η_{22_1} s^{-4}	150	180
η_{22_0} s^{-5}	25	23

The final step is to analytically factor the numerator and denominator polynomials in Equation (4.28). The polynomial factors are represented as

$$\begin{aligned}
\delta(s) &= (s+\alpha_1 - i\beta_1)(s+\alpha_1 + i\beta_1)(s+\alpha_2 - i\beta_2)(s+\alpha_2 + i\beta_2) \\
\eta_{11}(s) &= k_{11}(s+r_{11})(s+\alpha_{11} - i\beta_{11})(s+\alpha_{11} + i\beta_{11}) \\
\eta_{12}(s) &= k_{12}(s+r_{12})(s+\alpha_{12} - i\beta_{12})(s+\alpha_{12} + i\beta_{12}) \\
\eta_{21}(s) &= k_{21}(s+r_{21_1})(s+r_{21_2})(s+r_{21_3}) \\
\eta_{22}(s) &= k_{22}(s+r_{22})(s+\alpha_{22} - i\beta_{22})(s+\alpha_{22} + i\beta_{22})
\end{aligned} \tag{4.32}$$

Numerical values for these factors can be determined from data in Table 2.5. Expansion of Equation (4.32) and equating like powers of s with Equation (4.28) gives

$$\begin{aligned}
\delta_3 &= 2(\alpha_1 + \alpha_2) \\
\delta_2 &= \alpha_1^2 + 4\alpha_1\alpha_2 + \alpha_2^2 + \beta_1^2 + \beta_2^2 \\
\delta_1 &= 2(\alpha_1^2\alpha_2 + \alpha_2^2\alpha_1 + \alpha_1\beta_2^2 + \alpha_2\beta_1^2) \\
\delta_0 &= \alpha_1^2\alpha_2^2 + \alpha_1^2\beta_2^2 + \alpha_2^2\beta_1^2 + \beta_1^2\beta_2^2
\end{aligned}$$

$$\begin{aligned}
\eta_{11_3} &= k_{11} \\
\eta_{11_2} &= k_{11}(r_{11} + 2\alpha_{11}) \\
\eta_{11_1} &= k_{11}(2r_{11}\alpha_{11} + \alpha_{11}^2 + \beta_{11}^2) \\
\eta_{11_0} &= k_{11}r_{11}(\alpha_{11}^2 + \beta_{11}^2)
\end{aligned}$$

$$
\begin{aligned}
\eta_{12_4} &= k_{12} \\
\eta_{12_3} &= k_{12}(r_{12} + 2\alpha_{12}) \\
\eta_{12_2} &= k_{12}(2r_{12}\alpha_{12} + \alpha_{12}^2 + \beta_{12}^2) \\
\eta_{12_0} &= k_{12}r_{12}(\alpha_{12}^2 + \beta_{12}^2)
\end{aligned}
\tag{4.33}
$$

$$
\begin{aligned}
\eta_{21_4} &= k_{21} \\
\eta_{21_3} &= k_{21}(r_{21_1} + r_{21_2} + r_{21_3}) \\
\eta_{21_2} &= k_{21}(r_{21_1}r_{21_2} + r_{21_1}r_{21_3} + r_{21_2}r_{21_3}) \\
\eta_{21_0} &= k_{21}r_{21_1}r_{21_2}r_{21_3}
\end{aligned}
$$

$$
\begin{aligned}
\eta_{22_4} &= k_{22} \\
\eta_{22_3} &= k_{22}(r_{22} + 2\alpha_{22}) \\
\eta_{22_2} &= k_{22}(2r_{22}\alpha_{22} + \alpha_{22}^2 + \beta_{22}^2) \\
\eta_{22_0} &= k_{22}r_{22}(\alpha_{22}^2 + \beta_{22}^2)
\end{aligned}
$$

Based on the numerical data in Table 2.5, the factors in Equation (4.32) are given ε assignments as

$$
\begin{aligned}
\delta(s) &= (s + \alpha_1\varepsilon^0 - i\beta_1\varepsilon^0)(s + \alpha_1\varepsilon^0 + i\beta_1\varepsilon^0)(s + \alpha_2\varepsilon^0 - i\beta_2\varepsilon^1)(s + \alpha_2\varepsilon^0 + i\beta_2\varepsilon^1) \\
\eta_{11}(s) &= k_{11}(s + r_{11}\varepsilon^{-1})(s + \alpha_{11}\varepsilon^0 - i\beta_{11}\varepsilon^0)(s + \alpha_{11}\varepsilon^0 + i\beta_{11}\varepsilon^0) \\
\eta_{12}(s) &= k_{12}(s + r_{12}\varepsilon^{-1})(s + \alpha_{12}\varepsilon^0 - i\beta_{12}\varepsilon^1)(s + \alpha_{12}\varepsilon^0 + i\beta_{12}\varepsilon^1) \\
\eta_{21}(s) &= k_{21}(s + r_{21_1}\varepsilon^{-1})(s + r_{21_2}\varepsilon^0)(s + r_{21_3}\varepsilon^0) \\
\eta_{22}(s) &= k_{22}(s + r_{22}\varepsilon^{-1})(s + \alpha_{22}\varepsilon^0 - i\beta_{22}\varepsilon^0)(s + \alpha_{22}\varepsilon^0 + i\beta_{22}\varepsilon^0)
\end{aligned}
\tag{4.34}
$$

When the tracking parameter ε is carried over to Equation (4.33), and higher order terms in ε are dropped, the relationships become

$$
\begin{aligned}
\delta_3 &= (2\alpha_2 + 2\alpha_1) \\
\delta_2 &\approx \beta_2^2 \\
\delta_1 &\approx 2\alpha_1\beta_2^2 \\
\delta_0 &\approx \beta_1^2\beta_2^2
\end{aligned}
$$

$$
\begin{aligned}
\eta_{11_3} &= k_{11} \\
\eta_{11_2} &\approx k_{11}(2\alpha_{11}) \\
\eta_{11_1} &\approx k_{11}(\alpha_{11}^2 + \beta_{11}^2) \\
\eta_{11_0} &= k_{11} r_{11}(\alpha_{11}^2 + \beta_{11}^2)
\end{aligned}
\qquad (4.35)
$$

$$
\begin{aligned}
\eta_{12_3} &= k_{12} \\
\eta_{12_2} &\approx k_{12}(2\alpha_{12}) \\
\eta_{12_1} &\approx k_{12}(\alpha_{12}^2 + \beta_{12}^2) \\
\eta_{12_0} &= k_{12} r_{12}(\alpha_{12}^2 + \beta_{12}^2)
\end{aligned}
$$

$$
\begin{aligned}
\eta_{21_3} &= k_{21} \\
\eta_{21_2} &\approx k_{21}(r_{21_2} + r_{21_3}) \\
\eta_{21_1} &\approx k_{21}(r_{21_2} r_{21_3}) \\
\eta_{21_0} &= k_{21} r_{21_1} r_{21_2} r_{21_3}
\end{aligned}
$$

$$
\begin{aligned}
\eta_{22_3} &= k_{22} \\
\eta_{22_2} &\approx k_{22}(2\alpha_{22}) \\
\eta_{22_1} &\approx k_{22}(\alpha_{22}^2 + \beta_{22}^2) \\
\eta_{22_0} &= k_{22} r_{22}(\alpha_{22}^2 + \beta_{22}^2)
\end{aligned}
$$

These relationships correspond to Equation (4.18) in the general framework.

The solution for the factors in terms of the polynomial coefficients from Equation (4.35) is

$$
\begin{aligned}
\alpha_1 &\approx \frac{\delta_1}{2\delta_2} \\
\beta_1 &\approx \sqrt{\frac{\delta_0}{\delta_2}} \\
\alpha_2 &\approx \frac{\delta_3}{2} - \frac{\delta_1}{2\delta_2} \\
\beta_2 &\approx \sqrt{\delta_2}
\end{aligned}
$$

$$k_{11} = \eta_{11_1}$$

$$r_{11} \approx \frac{\eta_{11_0}}{\eta_{11_1}}$$

$$\alpha_{11} \approx \frac{\eta_{11_2}}{2\eta_{11_1}}$$

$$\beta_{11} \approx \frac{1}{2}\sqrt{(4\frac{\eta_{11_1}}{\eta_{11_1}} - \frac{\eta_{11_2}^2}{\eta_{11_1}^2})}$$

$$k_{12} = \eta_{12_1}$$

$$r_{12} \approx \frac{\eta_{12_0}}{\eta_{12_1}}$$

$$\alpha_{12} \approx \frac{\eta_{12_2}}{2\eta_{12_1}}$$

$$\beta_{12} \approx \frac{1}{2}\sqrt{(4\frac{\eta_{12_1}}{\eta_{12_1}} - \frac{\eta_{12_2}^2}{\eta_{12_1}^2})}$$

$$k_{21} = \eta_{21_1}$$

$$r_{21_1} \approx \frac{\eta_{21_0}}{\eta_{21_1}}$$

$$r_{21_2} \approx -\sqrt{\frac{-\eta_{21_1}}{\eta_{21_1}}} \qquad (4.36)$$

$$r_{21_1} \approx \sqrt{\frac{-\eta_{21_1}}{\eta_{21_1}}}$$

$$k_{22} = \eta_{22_1}$$

$$r_{22} \approx \frac{\eta_{22_0}}{\eta_{22_1}}$$

$$\alpha_{22} \approx \frac{\eta_{22_2}}{2\eta_{22_1}}$$

$$\beta_{22} \approx \frac{1}{2}\sqrt{(4\frac{\eta_{22_1}}{\eta_{22_1}} - \frac{\eta_{22_2}^2}{\eta_{22_1}^2})}$$

After substitution from Tables 4.6 and 4.7 for the coefficients, the factors are given in terms of the system parameters and feedback gains. The results are listed in Tables 4.10 through 4.14. These expressions provide the final link in the highly sought after relationships between design parameters and closed-loop factors. Tables 4.15 through 4.19 compare numerical accuracy of these approximations with exact values. Further, Figures 4.1-4.4 show the closed-loop frequency responses computed by "exact" numerical techniques and from the approximate expressions. After such a long process, the accuracy is quite good. Utilization of these expressions is deferred until Chapter VI.

Table 4.10 Symbolic Expressions for δ(s) Factors

$$\alpha_1 \approx \frac{-M_q\tilde{F}_\eta - \tilde{Z}_\alpha\tilde{F}_\eta + M_{\delta_E}k_2\tilde{F}_\eta + F_qM_\eta}{2(\tilde{F}_\eta - M_q(F_{\delta_E}k_3 + F_{\delta_C}k_7) - M_\alpha\tilde{Z}_q)}$$

$$\beta_1 \approx \sqrt{\frac{-F_\alpha\tilde{Z}_qM_\eta - M_\alpha\tilde{Z}_q\tilde{F}_\eta - \tilde{Z}_\alpha M_{\delta_E}k_2\tilde{F}_\eta}{\tilde{F}_\eta - M_q(F_{\delta_E}k_3 + F_{\delta_C}k_7) - M_\alpha\tilde{Z}_q}}$$

$$\alpha_2 \approx \frac{\tilde{F}_\eta - M_q - \tilde{Z}_\alpha + M_{\delta_E}k_2 + F_{\delta_C}k_7 + F_{\delta_E}k_3}{2} - \frac{-M_q\tilde{F}_\eta - \tilde{Z}_\alpha\tilde{F}_\eta + M_{\delta_E}k_2\tilde{F}_\eta + F_qM_\eta}{2(\tilde{F}_\eta - M_q(F_{\delta_E}k_3 + F_{\delta_C}k_7) - M_\alpha\tilde{Z}_q)}$$

$$\beta_2 \approx \sqrt{\tilde{F}_\eta - M_q(F_{\delta_E}k_3 + F_{\delta_C}k_7) - M_\alpha\tilde{Z}_q}$$

Table 4.11 Symbolic Expressions for $\eta_{11}(s)$ Factors

$$k_{11} = M_{\delta_E}$$

$$r_{11} \approx \frac{M_{\delta_E} F_\alpha \tilde{Z}_\eta + F_{\delta_E} \tilde{Z}_\alpha M_\eta}{F_{\delta_E} M_\eta + M_{\delta_E} \tilde{F}_\eta}$$

$$\alpha_{11} \approx \frac{1}{2}(F_{\delta_C} k_7 - \tilde{Z}_\alpha)$$

$$\beta_{11} \approx \frac{1}{2}\sqrt{4(\frac{M_{\delta_E} \tilde{F}_\eta + F_{\delta_E} M_\eta}{M_{\delta_E}}) - (F_{\delta_C} k_7 - \tilde{Z}_\alpha)^2}$$

Table 4.12 Symbolic Expressions for $\eta_{12}(s)$ Factors

$$k_{12} = M_{\delta_C}$$

$$r_{12} \approx -\tilde{Z}_\alpha + \frac{F_{\delta_C} M_\alpha \tilde{Z}_\eta}{F_{\delta_C} M_\eta + M_{\delta_C} \tilde{F}_\eta}$$

$$\alpha_{12} \approx \frac{1}{2}\frac{F_{\delta_C} M_\eta + (M_{\delta_C} F_{\delta_E} - F_{\delta_C} M_{\delta_E}) k_3}{M_{\delta_C}}$$

$$\beta_{12} \approx \frac{1}{2}\sqrt{4(\frac{M_{\delta_C} \tilde{F}_\eta + F_{\delta_C} M_\eta}{M_{\delta_C}}) - \frac{(F_{\delta_C} M_\eta + M_{\delta_C} \tilde{F}_\eta + (M_{\delta_C} F_{\delta_E} - F_{\delta_C} M_{\delta_E}) k_3)^2}{M_{\delta_C}^2}}$$

Table 4.13 Symbolic Expressions for $\eta_{21}(s)$ Factors

$$k_{21} = M_{\delta_E} - \phi' F_{\delta_E}$$

$$r_{21_1} \approx \frac{M_{\delta_E} F_\alpha \tilde{Z}_\eta + F_{\delta_E} \tilde{Z}_\alpha M_\eta}{M_{\delta_E} \tilde{F}_\eta}$$

$$r_{21_2} \approx -\sqrt{\frac{M_{\delta_E} \tilde{F}_\eta}{\phi' F_{\delta_E} - M_{\delta_E}}}$$

$$r_{21_3} \approx \sqrt{\frac{M_{\delta_E} \tilde{F}_\eta}{\phi' F_{\delta_E} - M_{\delta_E}}}$$

Table 4.14 Symbolic Expressions for $\eta_{22}(s)$ Factors

$$k_{22} = M_{\delta_C} - \phi' F_{\delta_C}$$

$$r_{22} \approx \frac{-M_{\delta_C} \tilde{Z}_\alpha \tilde{F}_\eta + F_{\delta_C}(M_\alpha \tilde{Z}_\eta - \tilde{Z}_\alpha M_\eta)}{\phi' \tilde{Z}_q(-M_{\delta_C} F_\alpha + F_{\delta_C} M_\alpha) + F_{\delta_C} M_\eta + M_{\delta_C} \tilde{F}_\eta}$$

$$\alpha_{22} \approx \frac{1}{2}(M_{\delta_E} k_2 - M_q - \tilde{Z}_\alpha - \frac{M_\eta - M_{\delta_E} k_3}{\phi'})$$

$$\beta_{22} \approx \frac{1}{2}\sqrt{4(\frac{\phi' \tilde{Z}_q(+M_{\delta_C} F_\alpha - F_{\delta_C} M_\alpha) - F_{\delta_C} M_\eta - M_{\delta_C} \tilde{F}_\eta}{\phi' F_{\delta_C}}) - \frac{\Delta^2}{\phi'^2}}$$

where $\Delta = (M_\eta - M_{\delta_E} k_3) + \phi'(-M_{\delta_E} k_2 + \tilde{Z}_\alpha + M_q)$

Table 4.15 Accuracy of the Symbolic Expressions for δ(s) Factors

δ (s) Factors	Exact	Approximate Symbolic
α_1	0.70	0.66
β_1	1.0	1.2
α_2	1.8	1.8
β_2	5.8	6.6

Table 4.16 Accuracy of the Symbolic Expressions for $\eta_{11}(s)$ Factors

$\eta_{11}(s)$ Factors	Exact	Approximate Symbolic
k_{11}	-5.1	-5.1
α_{11}	0.86	0.88
β_{11}	4.5	4.8
r_{11}	0.33	0.30

Table 4.17 Accuracy of the Symbolic Expressions for $\eta_{12}(s)$ Factors

$\eta_{12}(s)$ Factors	Exact	Approximate Symbolic
k_{12}	0.81	0.81
α_{12}	4.9	4.5
β_{12}	8.6	7.9
r_{12}	0.32	0.34

Table 4.18 Accuracy of the Symbolic Expressions for $\eta_{21}(s)$ Factors

$\eta_{21}(s)$ Factors	Exact	Approximate Symbolic
k_{21}	13	13
r_{21_1}	0.24	0.20
r_{21_2}	-3.2	-3.7
r_{21_3}	3.7	3.7

Table 4.19 Accuracy of the Symbolic Expressions for $\eta_{22}(s)$ Factors

$\eta_{22}(s)$ Factors	Exact	Approximate Symbolic
k_{22}	14	14
α_{22}	1.2	1.2
β_{22}	3.0	2.9
r_{22}	0.17	0.17

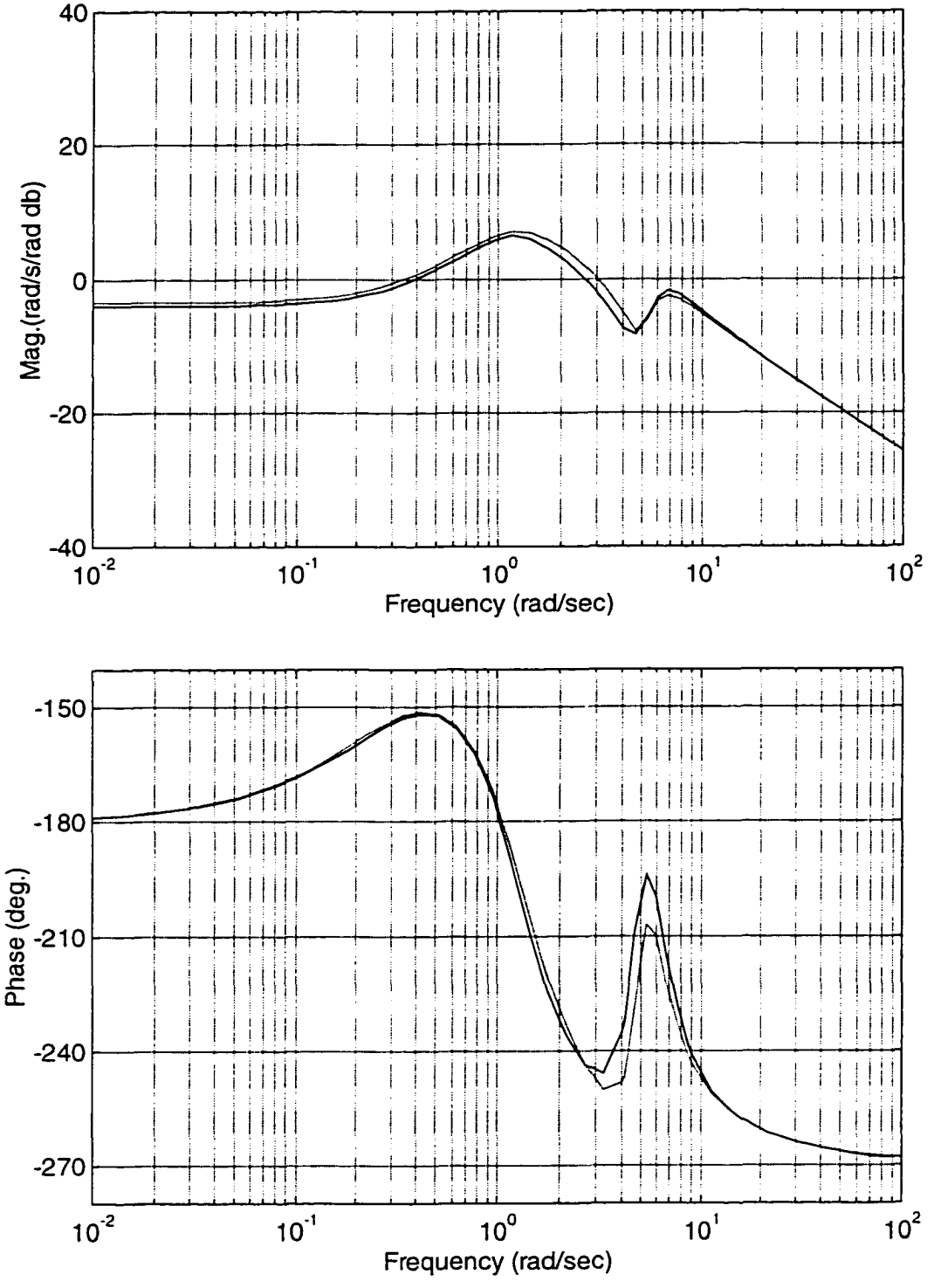

Figure 4.1 Comparison of q/δ_E Closed-Loop Frequency Responses Using the Approximate Symbolic Calculations

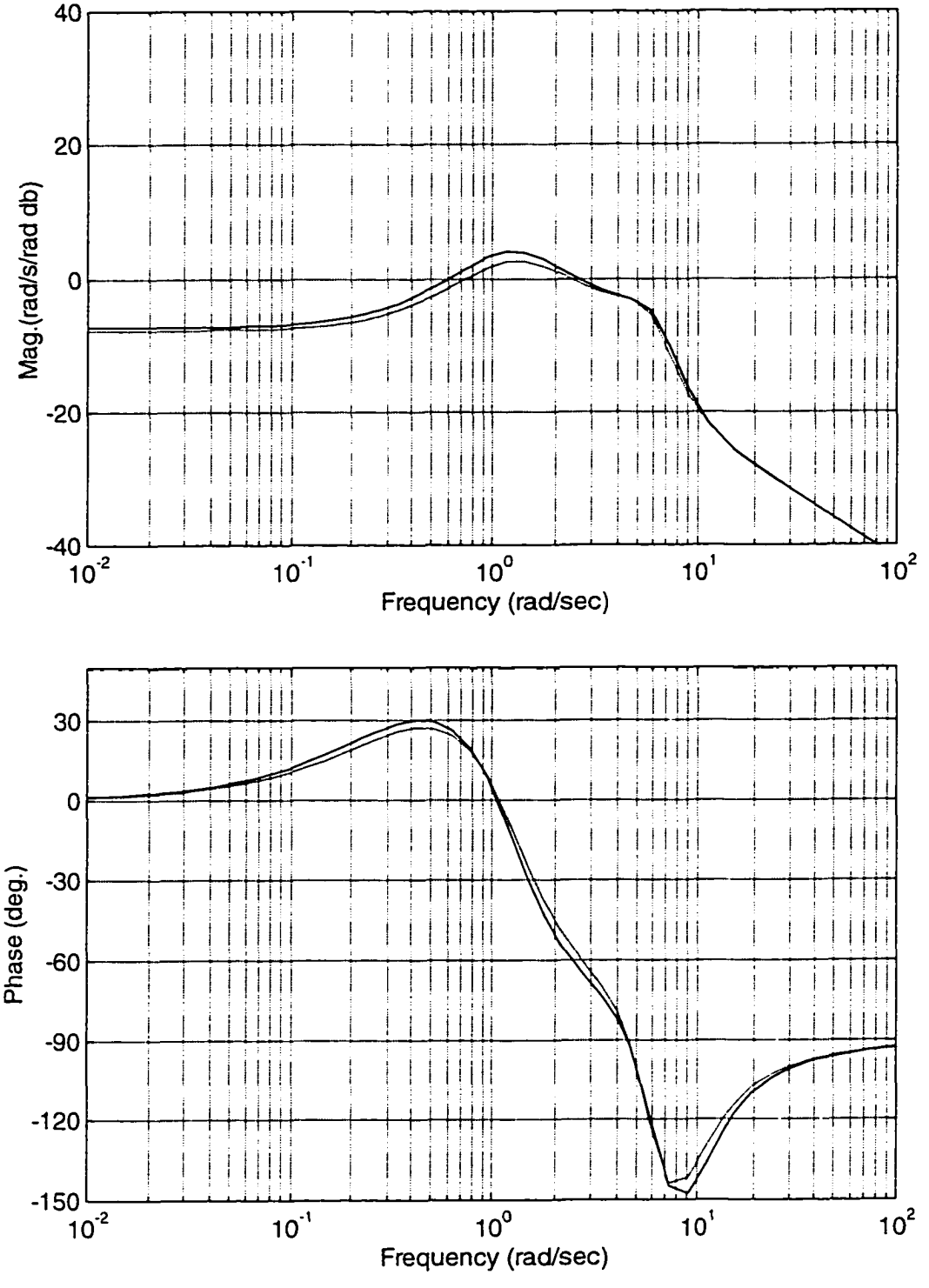

Figure 4.2 Comparison of q/δ_C Closed-Loop Frequency Responses Using the Approximate Symbolic Calculations

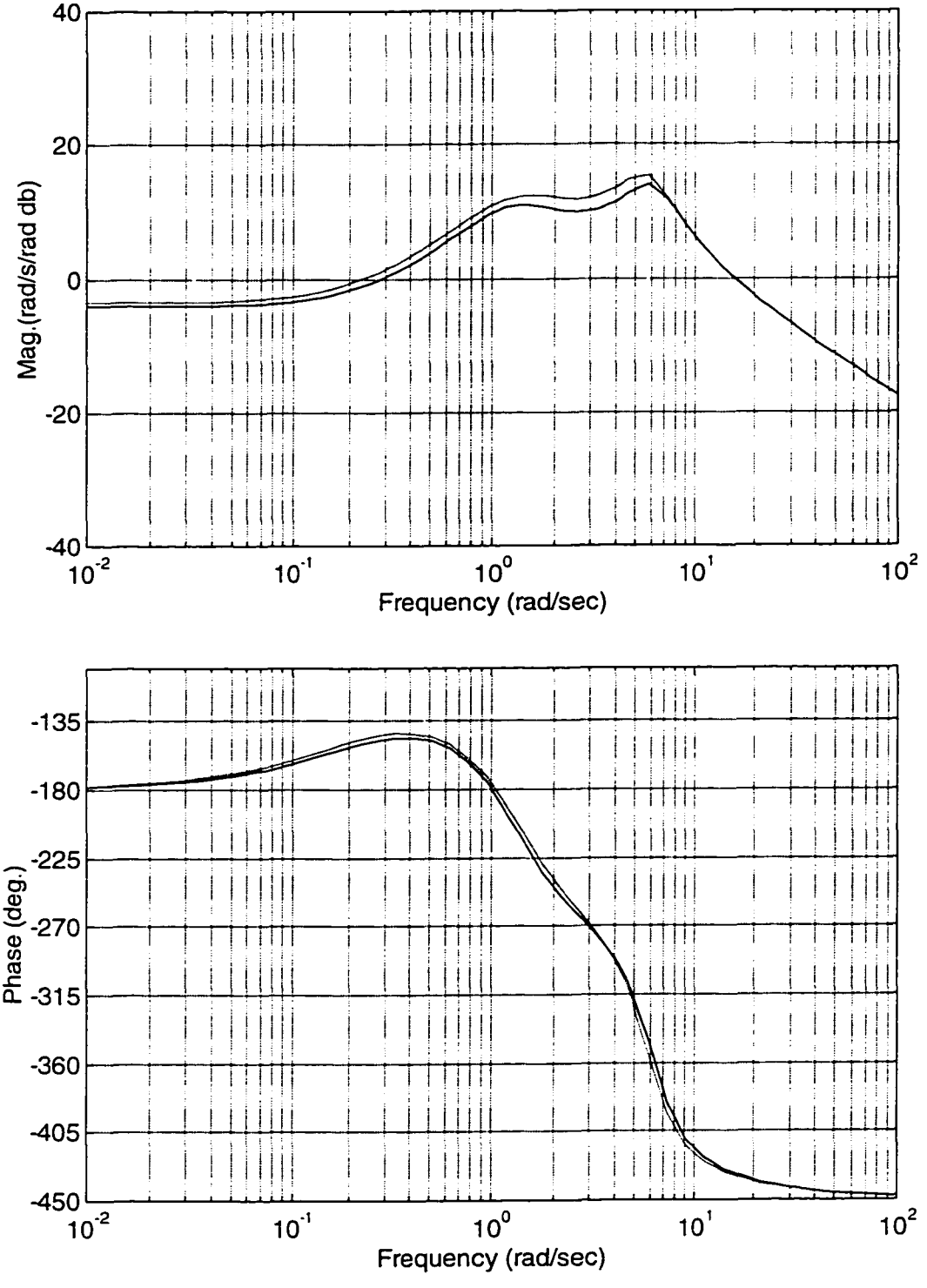

Figure 4.3 Comparison of q'/δ_E Closed-Loop Frequency Responses Using the Approximate Symbolic Calculations

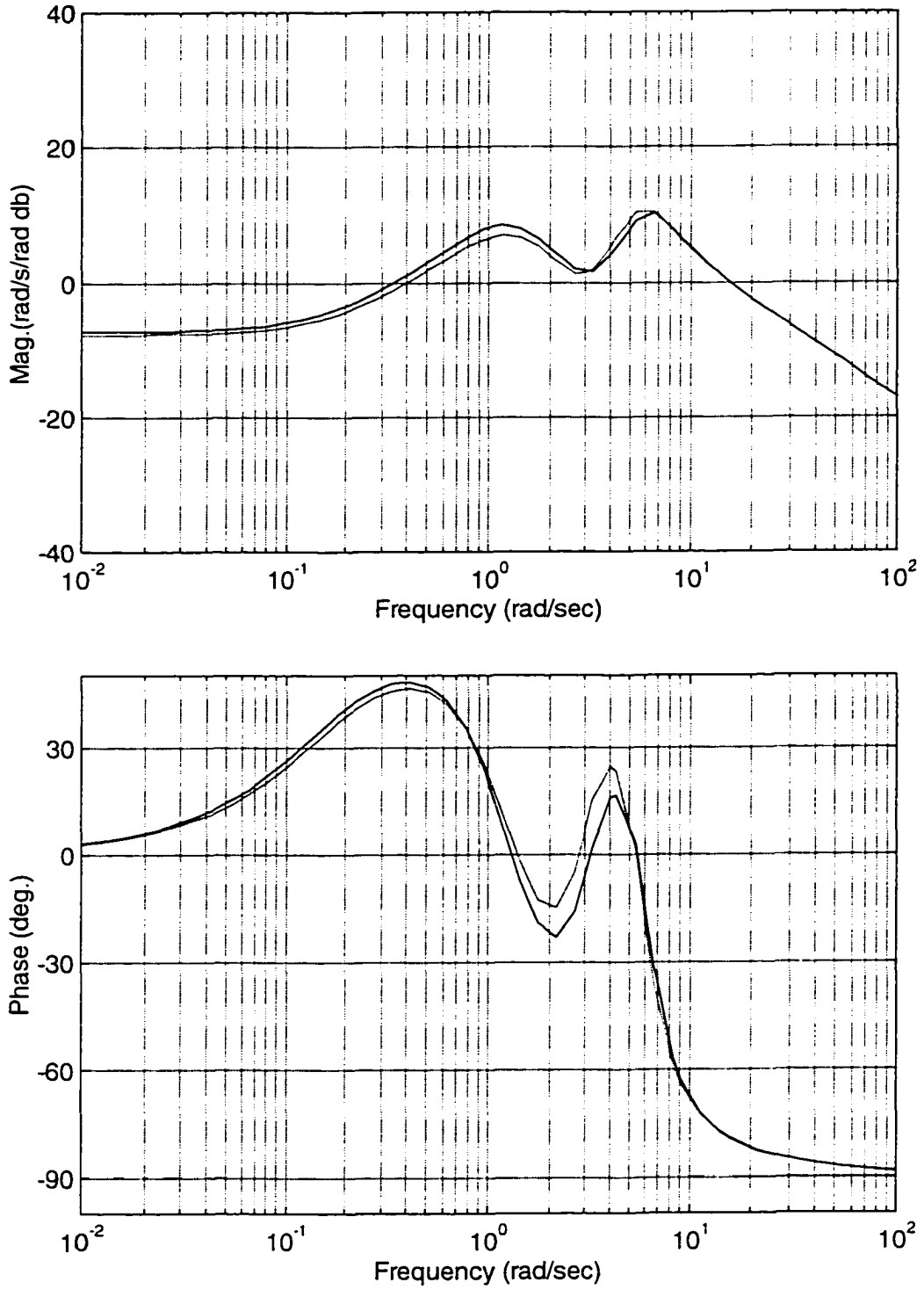

Figure 4.4 Comparison of q'/δ_C Closed-Loop Frequency Responses Using the Approximate Symbolic Calculations

CHAPTER V

COST FUNCTION IMBEDDING TECHNIQUE

5.1 Overview

In this chapter, a new method called the Cost Function Imbedding Technique is introduced as a means to develop analytical expressions for the closed-loop factors associated with the LQ design strategy. The cost function is the initial point where the vehicle dynamics and design weights interface, and the technique exploits this feature. By imbedding the closed-loop response inside the cost function through the input and output terms, the cost function can be explicitly written as a function of the vehicle parameters, design weights, and feedback gains. With the feedback gains representing the independent parameters, first order variations of the cost with respect to these gains yields the necessary conditions for the optimum gains. The resulting expressions provide a link between the feedback gains and system parameters without having to address the Riccati equation. However, the resulting nonlinear algebraic expressions may be difficult to solve and some form of approximation may be necessary. After analytical expressions for the gains are computed, techniques such as described in Chapters III and IV of this dissertation and Reference 44 could be used to analytically factor the closed-loop polynomials. This technique makes use of existing linear systems theory and applies it in a novel manner. Simplified examples are used to demonstrate the technique.

5.2 Cost Function Manipulation

Reconsider the closed-loop state space system in Equation (2.18), which corresponds to the LQ state feedback design technique described in Chapter II. Since this system is linear, state transition matrix concepts, such as those described in References 2 and 82-83, can be applied to Equation (2.18). The general initial condition response for the state vector can be written as

$$x(t) = e^{(A-BK_R)(t-t_i)}x(t_i) \tag{5.1}$$

where t_i denotes the initial time, t denotes the current time, and $x(t_i)$ represents the initial conditions for the states. Recall that $e^{(A-BK_R)(t-t_i)}$ is the state transition matrix and converts the initial condition into the current state value. Note the command signal u_c in Equation (2.18) has been zeroed out in the analysis here.

Now consider the input and output signals from Equations (2.17)-(2.18) when expressed in terms of the state vector. Substitution of the state vector from Equation (5.1) leads to

$$\begin{aligned} y(t) &= Ce^{(A-BK_R)(t-t_i)}x(t_i) \\ u(t) &= -K_R e^{(A-BK_R)(t-t_i)}x(t_i) \end{aligned} \tag{5.2}$$

The signals y(t) and u(t) are now in an appropriate form for imbedding into the cost function J in Equation (2.7). With an infinite horizon ($t_f=\infty$) and an initial temporal reference of zero ($t_i=0$), this process yields

$$\begin{aligned} J &= \frac{1}{2}x^T(0)\mathcal{J}\,x(0) \\ \mathcal{J} &= \int_0^\infty e^{(A-BK_R)^T\tau}\{C^TQC + K_R^TRK_R\}e^{(A-BK_R)\tau}d\tau \end{aligned} \tag{5.3}$$

The cost function is now explicitly dependent upon the vehicle state-space matrices, the design weight matrices, and feedback gain matrix. In Equation (5.3) note that although J is a scalar variable, the inner variable $\mathcal{J}$ is a symmetric matrix with dimension equivalent to that for the matrix A.

Although an analytical expression for the matrix $\mathcal{J}$ could be computed directly from Equation (5.3), in theory, it would involve considerable effort. Fortunately, additional theory can be focused on this issue to provide alternative means for computing $\mathcal{J}$. Consider a generalized linear differential equation for matrix Z(t).

$$\dot{Z}(t) = A_1 Z(t) + Z(t)A_2^T + F \tag{5.4}$$

In Equation (5.4), matrices A_1, A_2 and F are constant and square. Additionally, F is symmetric. The solution to this differential equation for Z(t) is

$$Z(t) = e^{A_1(t-t_0)}Z(t_0)e^{A_2^T(t-t_0)} + \int_{t_0}^{t} e^{A_1(t-\tau)}Fe^{A_2^T(t-\tau)}d\tau \tag{5.5}$$

and can be confirmed by substitution back into Equation (5.4). In the above equation, $Z(t_0)$ denotes the initial condition. Of most interest here is the steady state solution as $t \to \infty$. In the limit as time approaches infinity with the initial time set to zero, and after some manipulation, Equation (5.5) becomes

$$Z(\infty) = \int_0^{\infty} e^{A_1\tau}Fe^{A_2^T\tau}d\tau \tag{5.6}$$

Additionally, from Equation (5.4), the steady state solution for Z(t) satisfies

$$A_1 Z(\infty) + Z(\infty)A_2^T + F = 0 \tag{5.7}$$

Equation (5.7) is the well-known matrix Liapunov equation and provides an alternative means for computing the integral expression in Equation (5.6) or (5.3). References 82-83 provide a concise explanation of these results.

Observe the similarity of Equations (5.3) and (5.6). The matrix $\mathcal{J}$ corresponds to $Z(\infty)$, $A\text{-}BK_R$ corresponds to $A_1=A_2$, and F represents $C^TQC+K_R^TRK_R$. With this association, the matrix $\mathcal{J}$ in Equation (5.3) can be computed from

$$\mathcal{J}(A-BK_R)+(A-BK_R)^T\mathcal{J}+C^TQC+K_R^TRK_R=0 \tag{5.8}$$

Equation (5.8) provides an attractive alternative to the integral expression in Equation (5.3). However, the symbolic computational effort will still be a challenge for higher dimensional dynamic systems. Computation of $\mathcal{J}$ is not the ultimate goal here, but rather the variation of $\mathcal{J}$ with respect to K_R, and the equalities that result thereof.

5.3 Cost Function Variation

Since the input u(t) no longer appears in Equation (5.3), the independent parameter has become the feedback gain matrix K_R. Therefore, necessary conditions for minimal cost are

$$\frac{\partial J}{\partial K_{R_{ij}}}=0 \quad \text{for } 1\le i\le n_u, 1\le j\le n \tag{5.9}$$

where n and n_u denote the number of states and inputs. Note Equation (5.9) involves the variation of the scalar cost with respect to each gain matrix element. Thus, Equation (5.9) provides n x n_u necessary equalities for the determination of K_R. Note from Equation (5.3) that these necessary conditions will be quadratic functions of the initial state values.

In this time invariant problem, the optimal feedback gains are independent of the initial conditions. Thus, necessary conditions for the minimal cost, which are independent from the initial conditions, are

$$\frac{\partial \mathcal{J}}{\partial K_{R_{ij}}} = 0 \quad \text{for } 1 \le i \le n_u, 1 \le j \le n \tag{5.10}$$

Equation (5.10) considers the variation of the matrix cost kernel relative to each gain matrix element. Equation (5.10) represents more scalar equalities than Equation (5.9). However, due to the symmetry of $\mathcal{J}$, there will be only n x n_u independent equalities.

Several options are available for generating the necessary conditions of Equation (5.10). Since a closed-form integral expression for $\mathcal{J}$ is available, one approach would consider taking partial derivatives of Equation (5.3) directly. The advantage of this would be avoidance of analytical calculations for the matrix $\mathcal{J}$ itself. Explicit expressions for $\mathcal{J}_{ij}$ would be unnecessary in this approach. The disadvantage appears to be the computational tractability. Computing partial derivatives of the matrix exponential terms would pose considerable difficulty. Note the partial derivatives are with respect to the individual elements of K_R, not the overall-multiplying variable τ. Such partial derivatives would require expansion of the matrix exponential series. Solvability of this approach is low, at best. Another approach would be to apply the partial derivatives to the expressions for $\mathcal{J}$ that originate from the solution of Equation (5.8). Disadvantages would appear to be the need to explicitly compute $\mathcal{J}$ as well as symbolic manipulation effort needed to carry out the partial derivatives to a useful form by eliminating dependent equations. On the other hand, the computations are straightforward and tractable.

The preferred option is a mixture of these two extremes. The approach is to apply partial derivatives to Equation (5.8), followed by enforcement of the necessary condition in Equation (5.10). The advantages are that partial derivative computations applied to the analytic expressions representing $\mathcal{J}$ are avoided. First order variations are only applied to the symbol $\mathcal{J}$ and then are eliminated with Equation (5.10). The structure also facilitates isolating a reduced set of independent equalities. The main drawback to this approach is the requirement for analytical expressions for the elements of $\mathcal{J}$, as the resulting equalities will still be functions of $\mathcal{J}$. The mechanics of this procedure are discussed next.

First consider the computation for $\mathcal{J}$. Suppose Equation (5.8) is rewritten as

$$\mathcal{J} A_{cl} + A_{cl}^T \mathcal{J} + W = 0 \tag{5.11}$$

where

$$\begin{aligned} A_{cl} &= A - BK_R \\ W &= C^T Q C + K_R^T R K_R \end{aligned} \tag{5.12}$$

If the individual elements of $\mathcal{J}$, A_{cl}, and W are denoted as $\mathcal{J}_{ij}$, $A_{cl_{ij}}$, and W_{ij}, and with symmetry $\mathcal{J}_{ij} = \mathcal{J}_{ji}$, $W_{ij} = W_{ji}$, then the independent equalities in Equation (5.11) can be represented in scalar forms as

$$\sum_{k=1}^{n} \mathcal{J}_{ik} A_{cl_{kj}} + \sum_{k=1}^{i-1} \mathcal{J}_{ki} A_{cl_{ki}} + \sum_{k=1}^{j} A_{cl_{ki}} \mathcal{J}_{kj} + \sum_{k=j+1}^{n} A_{cl_{ki}} \mathcal{J}_{jk} + W_{ij} = 0 \quad \text{for} \begin{bmatrix} i = 1, 2, \ldots\ldots n \\ j = i, i+1, \ldots.n \end{bmatrix} \tag{5.13}$$

Solving Equation (5.13) will yield the required expressions for $\mathcal{J}$ in terms of the vehicle parameters, cost weight parameters and feedback gains. This result is represented as

$$\mathcal{J}_{ij} = f_{ij}(A, B, C, Q, R, K_R) \qquad \text{for} \begin{bmatrix} i = 1, 2, \ldots\ldots n \\ j = i, i+1, \ldots.n \end{bmatrix} \tag{5.14}$$

Now consider taking first order variations of Equation (5.8) with respect to the feedback gain parameters, or

$$\frac{\partial \mathcal{J}}{\partial K_{R_{ij}}}(A - BK_R) - \mathcal{J}\, B\frac{\partial K_R}{\partial K_{R_{ij}}} - \frac{\partial K_R^T}{\partial K_{R_{ij}}} B^T \mathcal{J}$$

$$+ (A - BK_R)^T \frac{\partial \mathcal{J}}{\partial K_{R_{ij}}} + \frac{\partial K_R^T}{\partial K_{R_{ij}}} RK_R + K_R^T R \frac{\partial K_R}{\partial K_{R_{ij}}} = 0 \tag{5.15}$$

With the enforcement of the necessary condition (Equation (5.10)), Equation (5.15) reduces to

$$-\mathcal{J}\, B\frac{\partial K_R}{\partial K_{R_{ij}}} - \frac{\partial K_R^T}{\partial K_{R_{ij}}} B^T \mathcal{J} + \frac{\partial K_R^T}{\partial K_{R_{ij}}} RK_R + K_R^T R \frac{\partial K_R}{\partial K_{R_{ij}}} = 0 \tag{5.16}$$

Equation (5.16) represents a set of independent equalities. Solution of Equation (5.16) for the optimal gains is represented as

$$K_{R_{ij}} = g_{ij}(A, B, C, Q, R) \tag{5.17}$$

The procedural steps for this technique now become clear. Analytical expressions for the elements of $\mathcal{J}$ are initially computed from Equation (5.13), leading to Equation (5.14). These expressions are substituted into the necessary conditions in Equation (5.16). The result is a set of coupled nonlinear algebraic expressions involving the vehicle parameters, the cost function design weights, and the feedback gains. The feedback gains are to be solved for in terms of system parameters from these equalities leading to Equation (5.17). From these expressions, the closed-loop transfer function polynomials can be written in terms of the parameters by utilizing Equation (2.18) and Equation (4.13), or by rewriting the closed-loop system in terms of a polynomial matrix form, such as in Equation (2.1). Factoring techniques such as in Chapters III and IV and Reference

44, can then be utilized as the final step. Of course, adherence to " exact " computations may need relaxing to achieve useful, tractable expressions from Equations (5.14) and (5.17). When considering the intended application for these expressions, simplifications are justified as long as sufficient accuracy is maintained. To demonstrate this technique, several simplified examples are considered next.

5.4 Simplified Example 1

Consider a one state/one input/one output example where

$$\begin{aligned} \dot{x} &= Ax + Bu \\ y &= Cx \qquad\qquad x, y, u \in R^{1\times 1} \end{aligned} \tag{5.18}$$

The cost function is given by

$$\begin{aligned} J &= \frac{1}{2} x_0^T \left[\int_0^\infty e^{(A-BK_R)^T\tau}\{C^TQC + K_R^TRK_R\}e^{(A-BK_R)\tau}d\tau\right]x_0 \\ &= \frac{1}{2} x_0^2\{QC^2 + RK_R^2\}\int_0^\infty e^{2(A-BK_R)\tau}d\tau \\ &= \frac{1}{2} x_0^2\{QC^2 + RK_R^2\}\frac{1}{2(A-BK_R)} e^{2(A-BK_R)\tau}\Big|_0^\infty \\ &= \frac{1}{2} x_0^2\{QC^2 + RK_R^2\}\frac{1}{2(A-BK_R)}\{\underbrace{e^{2(A-BK_R)\infty}}_{0} - \underbrace{e^{2(A-BK_R)0}}_{1}\} \\ \therefore J &= \frac{-x_0^2}{4(A-BK_R)}\{QC^2 + RK_R^2\} \end{aligned} \tag{5.19}$$

Differentiating with respect to K_R and equating with zero

$$\begin{aligned} \frac{\partial J}{\partial K_R} &= \frac{-x_0^2}{4(A-BK_R)}\{2RK_R\} - \frac{x_0^2}{4(A-BK_R)^2}\{QC^2 + RK_R^2\}B \\ &= \frac{-x_0^2\{2RK_R(A-BK_R) + \{QC^2 + RK_R^2\}B}{4(A-BK_R)^2} = 0 \end{aligned}$$

$$\therefore 2RK_R(A - BK_R) + \{QC^2 + RK_R^2\}B = 0$$

$$-RBK_R^2 + 2RAK_R + QBC^2 = 0 \tag{5.20}$$

Utilizing the final result in Equation (5.20), the gain K_R is given by

$$K_R = \frac{A \pm \sqrt{(A^2 + \frac{Q}{R}B^2C^2)}}{B} \tag{5.21}$$

The result in Equation (5.21) can be verified by using the Riccati equation directly to obtain K_R. This approach is summarized in Table 5.1.

Table 5.1 Analytical Calculation of K_R Using Riccati Equation Directly

$$PA + A^TP - PBR^{-1}B^TP + C^TQC = 0$$

$$2AP - \frac{B^2}{R}P^2 + QC^2 = 0$$

$$-\frac{B^2}{R}P^2 + 2AP + QC^2 = 0$$

$$\therefore P = \frac{R\{A \pm \sqrt{(A^2 + \frac{Q}{R}B^2C^2)}\}}{B^2}$$

$$K_R = R^{-1}B^TP$$

$$\therefore K_R = \frac{A \pm \sqrt{(A^2 + \frac{Q}{R}B^2C^2)}}{B}$$

5.5 Simplified Example 2

Consider a two state/one input/one output example where

$$\begin{bmatrix}\dot{x}_1\\ \dot{x}_2\end{bmatrix}=\begin{bmatrix}A_{11} & A_{12}\\ A_{21} & A_{22}\end{bmatrix}\begin{bmatrix}x_1\\ x_2\end{bmatrix}+\begin{bmatrix}B_1\\ B_2\end{bmatrix}u$$

$$y=\begin{bmatrix}C_1 & C_2\end{bmatrix}\begin{bmatrix}x_1\\ x_2\end{bmatrix} \qquad y,u\in R^{1\times 1}, x\in R^{2\times 1} \tag{5.22}$$

$$K_R=\begin{bmatrix}K_{R1} & K_{R2}\end{bmatrix}$$

Some preliminary calculations are necessary to prepare for substitution into Equation (5.8) or (5.13). These preliminary calculations are given in Table 5.2.

Table 5.2 Preliminary Computations for Equation (5.8)

$$C^TQC=Q\begin{bmatrix}C_1^2 & C_1C_2\\ C_2C_1 & C_2^2\end{bmatrix}$$

$$K_R^TRK_R=\begin{bmatrix}K_{R1}\\ K_{R2}\end{bmatrix}R\begin{bmatrix}K_{R1} & K_{R2}\end{bmatrix}=R\begin{bmatrix}K_{R1}^2 & K_{R1}K_{R2}\\ K_{R2}K_{R1} & K_{R2}^2\end{bmatrix}$$

$$F=C^TQC+K_R^TRK_R=\begin{bmatrix}QC_1^2+RK_{R1}^2 & QC_1C_2+RK_{R1}K_{R2}\\ QC_2C_1+RK_{R2}K_{R1} & QC_2^2+RK_{R2}^2\end{bmatrix}=\begin{bmatrix}F_{11} & F_{12}\\ F_{12} & F_{22}\end{bmatrix}$$

$$A-BK_R=\begin{bmatrix}A_{11} & A_{12}\\ A_{21} & A_{22}\end{bmatrix}-\begin{bmatrix}B_1\\ B_2\end{bmatrix}\begin{bmatrix}K_{R1} & K_{R2}\end{bmatrix}=\begin{bmatrix}A_{11}-B_1K_{R1} & A_{12}-B_1K_{R2}\\ A_{21}-B_2K_{R1} & A_{22}-B_2K_{R2}\end{bmatrix}$$

$$A_{cl}=A-BK_R=\begin{bmatrix}A_{cl11} & A_{cl12}\\ A_{cl21} & A_{cl22}\end{bmatrix}$$

$$\mathcal{J}=\begin{bmatrix}\mathcal{J}_{11} & \mathcal{J}_{12}\\ \mathcal{J}_{12} & \mathcal{J}_{22}\end{bmatrix}$$

$$\mathcal{J}A_{cl}=\begin{bmatrix}\mathcal{J}_{11} & \mathcal{J}_{12}\\ \mathcal{J}_{12} & \mathcal{J}_{22}\end{bmatrix}\begin{bmatrix}A_{cl11} & A_{cl12}\\ A_{cl21} & A_{cl22}\end{bmatrix}=\begin{bmatrix}\mathcal{J}_{11}A_{cl11}+\mathcal{J}_{12}A_{cl21} & \mathcal{J}_{11}A_{cl12}+\mathcal{J}_{12}A_{cl22}\\ \mathcal{J}_{12}A_{cl11}+\mathcal{J}_{22}A_{cl21} & \mathcal{J}_{12}A_{cl12}+\mathcal{J}_{22}A_{cl22}\end{bmatrix}$$

$$A_{cl}^T\mathcal{J}=(\mathcal{J}A_{cl})^T$$

Utilizing the information in Table 5.2, and after some manipulation, Equations (5.8)-(5.13) can be written as

$$\begin{bmatrix}2A_{cl11} & 2A_{cl21} & 0\\ A_{cl12} & A_{cl11}+A_{cl22} & A_{cl21}\\ 0 & 2A_{cl12} & 2A_{cl22}\end{bmatrix}\begin{bmatrix}\mathcal{J}_{11}\\ \mathcal{J}_{12}\\ \mathcal{J}_{22}\end{bmatrix}=\begin{bmatrix}-F_{11}\\ -F_{12}\\ -F_{22}\end{bmatrix} \tag{5.23}$$

Equation (5.23) is a simple set of simultaneous linear equations. The solution for $\mathcal{J}_{ij}$ is

$$\mathcal{J}_{11} = \frac{-2\{A_{cl22}(A_{cl11}+A_{cl22})-A_{cl12}A_{cl21}\}F_{11}+4A_{cl21}A_{cl22}F_{12}-2A_{cl21}^2F_{22}}{4(A_{cl11}+A_{cl22})(A_{cl11}A_{cl22}-A_{cl12}A_{cl21})}$$

$$\mathcal{J}_{12} = \frac{2A_{cl12}A_{cl22}F_{11}-4A_{cl11}A_{cl22}F_{12}+2A_{cl11}A_{cl21}F_{22}}{4(A_{cl11}+A_{cl22})(A_{cl11}A_{cl22}-A_{cl12}A_{cl21})} \tag{5.24}$$

$$\mathcal{J}_{22} = \frac{-2A_{cl12}^2F_{11}+4A_{cl11}A_{cl12}F_{12}-2\{A_{cl11}(A_{cl11}+A_{cl22})-A_{cl12}A_{cl21}\}F_{22}}{4(A_{cl11}+A_{cl22})(A_{cl11}A_{cl22}-A_{cl12}A_{cl21})}$$

Note Equation (5.24) represents Equation (5.14) in the general case.

Now consider the necessary conditions for the optimal gains in Equation (5.16). Preparatory calculations before substitution into Equation (5.16) are given in Table 5.3.

Table 5.3 Preliminary Computations for Equation (5.16)

$$\mathcal{J}B = \begin{bmatrix} \mathcal{J}_{11}B_1 + \mathcal{J}_{12}B_2 \\ \mathcal{J}_{12}B_1 + \mathcal{J}_{22}B_2 \end{bmatrix}$$

$$\frac{\partial K_R}{\partial K_{R1}} = [1 \quad 0]$$

$$\mathcal{J}B\frac{\partial K_R}{\partial K_{R1}} = \begin{bmatrix} \mathcal{J}_{11}B_1 + \mathcal{J}_{12}B_2 & 0 \\ \mathcal{J}_{12}B_1 + \mathcal{J}_{22}B_2 & 0 \end{bmatrix}$$

$$K_R^T R\frac{\partial K_R}{\partial K_{R1}} = \begin{bmatrix} K_{R1} \\ K_{R2} \end{bmatrix} R[1 \quad 0] = \begin{bmatrix} RK_{R1} & 0 \\ RK_{R2} & 0 \end{bmatrix}$$

$$\frac{\partial K_R}{\partial K_{R2}} = [0 \quad 1]$$

$$\mathcal{J}B\frac{\partial K_R}{\partial K_{R2}} = \begin{bmatrix} 0 & \mathcal{J}_{11}B_1 + \mathcal{J}_{12}B_2 \\ 0 & \mathcal{J}_{12}B_1 + \mathcal{J}_{22}B_2 \end{bmatrix}$$

$$K_R^T R\frac{\partial K_R}{\partial K_{R2}} = \begin{bmatrix} K_{R1} \\ K_{R2} \end{bmatrix} R[0 \quad 1] = \begin{bmatrix} 0 & RK_{R1} \\ 0 & RK_{R2} \end{bmatrix}$$

Substitution of the data from Table 5.3 into Equation (5.16) gives two independent equations, or

$$\begin{aligned} -(\mathcal{J}_{11}B_1 + \mathcal{J}_{12}B_2) + RK_{R1} &= 0 \\ -(\mathcal{J}_{12}B_1 + \mathcal{J}_{22}B_2) + RK_{R2} &= 0 \end{aligned} \tag{5.25}$$

These equations look deceivingly simple for the solution of K_{R1} and K_{R2}. Recall, however, that terms $\mathcal{J}_{ij}$ from Equation (5.24) are highly nonlinear functions of K_R through the matrix A_{cl}. Therefore, some form of approximation, such as described in Chapters III and IV, will most likely be required in the solution for K_R. Nevertheless, these equations have significant potential for the dissertation goal since they provide a direct link between the feedback gains and basic system and design parameters without addressing the Riccati solution P.

Substitution of Equation (5.24) into Equation (5.25) and clearing the denominator leads to

$$\begin{aligned} &-\{-2\{A_{cl22}(A_{cl11}+A_{cl22})-A_{cl12}A_{cl21}\}F_{11}+4A_{cl21}A_{cl22}F_{12}-2A_{cl21}^2F_{22}\}B_1 \\ &-\{2A_{cl12}A_{cl22}F_{11}-4A_{cl11}A_{cl22}F_{12}+2A_{cl11}A_{cl21}F_{22}\}B_2 \\ &+4(A_{cl11}+A_{cl22})(A_{cl11}A_{cl22}-A_{cl12}A_{cl21})RK_{R_1}=0 \\ \\ &-\{2A_{cl12}A_{cl22}F_{11}-4A_{cl11}A_{cl22}F_{12}+2A_{cl11}A_{cl21}F_{22}\}B_1 \\ &-\{-2A_{cl12}^2F_{11}+4A_{cl11}A_{cl12}F_{12}-2\{A_{cl11}(A_{cl11}+A_{cl22})-A_{cl12}A_{cl21}\}F_{22}\}B_2 \\ &+4(A_{cl11}+A_{cl22})(A_{cl11}A_{cl22}-A_{cl12}A_{cl21})RK_{R_2}=0 \end{aligned} \tag{5.26}$$

Expanding the A_{clij} terms with Table 5.2 and further manipulation yields

$$R\{B_1^2A_{22} - B_1B_2A_{12}\}K_{R_1}^3 + R\{-B_1^2A_{21} + B_1B_2A_{11} - B_2^2A_{12} + B_1B_2A_{22}\}K_{R_1}^2K_{R_2}$$
$$+ R\{B_2^2A_{11} - B_1B_2A_{21}\}K_{R_1}K_{R_2}^2 + R\{B_1(-3A_{11}A_{22} + A_{21}A_{12} - A_{22}^2) + B_2(2A_{11}A_{12}$$
$$+ A_{12}A_{22})\}K_{R_1}^2 + R\{B_1A_{21}^2 - B_2A_{21}A_{11}\}K_{R_2}^2 + 2R\{B_2(-A_{11}A_{22} + A_{21}A_{12} - A_{11}^2)$$
$$+ B_1A_{21}A_{11}\}K_{R_1}K_{R_2} + \{2R(A_{11}^2A_{22} - A_{12}A_{21}(A_{11} + A_{22}) + A_{11}A_{22}^2) + Q(C_1^2(B_1B_2A_{12}$$
$$- B_1^2A_{22}) + C_2^2(B_2^2A_{11} - B_1B_2A_{21})\}K_{R_1} + Q\{C_1^2(B_1^2A_{21} - B_1B_2(A_{11} + A_{22}) + B_2^2A_{12})$$
$$+ 2C_1C_2(B_1B_2A_{21} - B_2^2A_{11})\}K_{R_2} + Q\{C_1^2(B_1(A_{11}A_{22} - A_{12}A_{21} + A_{22}^2) - B_2(A_{12}A_{22})$$
$$+ 2C_1C_2(B_2A_{11} - B_1A_{21})A_{22} + C_2^2(B_1A_{21}^2 - B_2A_{21}A_{11})\} = 0$$

(5.27)

$$R\{B_2^2A_{11} - B_1B_2A_{21}\}K_{R_2}^3 - R\{B_1^2A_{21} - B_1B_2(A_{11} + A_{22}) + B_2^2A_{12}\}K_{R_2}^2K_{R_1}$$
$$+ R\{B_1^2A_{22} - B_1B_2A_{12}\}K_{R_2}K_{R_1}^2 + R\{B_2(-3A_{11}A_{22} + A_{21}A_{12} - A_{11}^2) + B_1(2A_{21}A_{22}$$
$$+ A_{21}A_{11})\}K_{R_2}^2 + R\{B_2A_{12}^2 - B_1A_{12}A_{22}\}K_{R_1}^2 + 2R\{B_1(-A_{11}A_{22} + A_{21}A_{12} - A_{22}^2)$$
$$+ B_2A_{12}A_{22}\}K_{R_1}K_{R_2} + \{2R(A_{11}^2A_{22} - A_{12}A_{21}(A_{11} + A_{22}) + A_{11}A_{22}^2) + Q(C_2^2(B_1B_2A_{21}$$
$$- B_2^2A_{11}) + C_1^2(B_1^2A_{22} - B_1B_2A_{12})\}K_{R_2} + Q\{C_2^2(B_1^2A_{21} - B_1B_2(A_{11} + A_{22}) + B_2^2A_{12})$$
$$+ 2C_1C_2(B_1B_2A_{12} - B_1^2A_{22})\}K_{R_1} + Q\{C_2^2(B_2(A_{11}A_{22} - A_{12}A_{21} + A_{11}^2) - B_1(A_{21}A_{11})$$
$$+ 2C_1C_2(B_1A_{22} - B_2A_{12})A_{11} + C_1^2(B_2A_{12}^2 - B_1A_{12}A_{22})\} = 0$$

The nonlinearities in these general equations for K_{R_i} are now explicit. The equations are coupled polynomials in terms of the gain matrix elements. For specific applications, these equations could be possibly simplified based on relative numerical magnitudes for the parameters and gains, allowing approximate closed-form solutions. Such calculations are left mostly for future work, but one special case which allows an exact closed-form solution is considered.

5.6 Inverted Pendulum Example

Assume the system dynamics of the previous example in Section 5.5 represents an inverted pendulum (see Reference 83). The system description is given as

$$\dot{x} = Ax + Bu \quad \text{where } A = \begin{bmatrix} 0 & 1 \\ \omega^2 & 0 \end{bmatrix}, \; B = \begin{bmatrix} 0 \\ 1 \end{bmatrix}, \; x = \begin{bmatrix} \theta & \dot{\theta} \end{bmatrix}^T$$
$$y = Cx \qquad C = [1 \quad 0], \qquad K_R = [K_{R_1} \quad K_{R_2}] \tag{5.28}$$

where θ is the angular position and ω is the natural frequency of the open-loop system.

A control law is sought which minimizes the angular position and the control activity. The cost function is selected as

$$J = \int_0^\infty (\theta^2 + \frac{u^2}{c^2}) d\tau \tag{5.29}$$

From Equation (5.29) the weighting functions are given by

$$Q = 1 \quad , R = \frac{1}{c^2} \tag{5.30}$$

After substitution into Equation (5.24) the $\mathcal{J}_{ij}$ elements are given by

$$\begin{aligned} \mathcal{J}_{11} &= \frac{1}{2} \frac{-K_{R_2}^2\omega^4 + \omega^2 c^2 - K_{R1}c^2 + K_{R1}^2\omega^2 - K_{R1}^3 - K_{R_2}^2 c^2}{(\omega^2 - K_{R1})K_{R_2}c^2} \\ \mathcal{J}_{12} &= -\frac{1}{2} \frac{c^2 + K_{R1}^2}{(\omega^2 - K_{R1})K_{R_2}c^2} \\ \mathcal{J}_{22} &= -\frac{1}{2} \frac{c^2 + K_{R1}^2 - K_{R_2}^2\omega^2 + K_{R_2}^2 K_{R1}}{(\omega^2 - K_{R1})K_{R_2}c^2} \end{aligned} \tag{5.31}$$

Using Equation (5.31), substitution into Equation (5.25) yields the following two independent equations.

$$\begin{aligned} -\frac{1}{2} \frac{c^2 + K_{R1}^2}{(\omega^2 - K_{R1})K_{R_2}c^2} + \frac{K_{R1}}{c^2} &= 0 \\ -\frac{c^2 + K_{R1}^2 - K_{R_2}^2\omega^2 + K_{R_2}^2 K_{R1}}{2(\omega^2 - K_{R1})K_{R_2}c^2} + \frac{K_{R_2}}{c^2} &= 0 \end{aligned} \tag{5.32}$$

After some manipulations, Equation (5.32) reduces to

$$\begin{aligned} c^2 - K_{R1}^2 + 2\omega^2 K_{R1} &= 0 \\ c^2 + K_{R1}^2 + \omega^2 K_{R2}^2 - K_{R2}^2 K_{R1} &= 0 \end{aligned} \tag{5.33}$$

For this special case, the general relations in Equation (5.27) simplify to Equation (5.33).

Closed-form solutions for K_{R1} and K_{R2} are

$$\begin{aligned} K_{R1} &= \omega^2 + \sqrt{(c^2 + \omega^4)} \\ K_{R2} &= \sqrt{2(\omega^2 + \sqrt{(c^2 + \omega^4)})} \end{aligned} \tag{5.34}$$

This result matches the result found by solving the Riccati equation directly.[83]

CHAPTER VI

UTILIZATION OF ANALYTICAL EXPRESSIONS

6.1 Overview

In this chapter, utilization of the approximate analytical expressions for the closed-loop factors computed in Chapters III and IV is considered. Recall these expressions relate the closed-loop factors to the basic aircraft and control design parameters such as stability and control derivatives and cost function weight matrices. As shown previously, these expressions possess sufficient numerical accuracy for engineering purposes, thus allowing the ultimate goal of the dissertation to be addressed. This objective is to explore the underlying relationships these expressions represent, and thereby gain insightful knowledge pertaining to how a contemporary LQ control law augments flight vehicle dynamics. The analytical expressions are used to address topics such as damping, nonminimum phase behavior, stability, and performance, with robustness considerations and design modification guidelines. Emphasis is given to uncovering the source of key dynamic features of the closed-loop system and possible modifications to further improve these characteristics. The additional knowledge afforded by the analytical expressions would be difficult to attain by other means such as pure numerically based techniques.

6.2 Damping Analysis

Aeroelastic mode damping, through feedback, has been increased approximately three fold when the open-loop value from Table 2.2 and the closed-loop value from Table 2.5 are compared (1.0 vs. 3.5). Consider the expression for $(2\zeta\omega)_2$ in Table 3.1. The first line represents the open-loop contribution and was discussed in Chapter II, whereas the second line indicates the effect from feedback. One contribution from feedback is represented by the $q_{22}r_{11}$ term. Recall q_{22} penalizes a poor response at the cockpit (q'), and r_{11} penalizes activity of the elevator (δ_E). In other words, large values for q_{22} and r_{11} imply increased utilization of cockpit pitch rate (q') as a "feedback" signal and increased canard deflection (δ_C) as a control input. The $q_{22}r_{11}$ term indicates the cockpit pitch rate to canard feedback path ($q' \rightarrow q_{22}r_{11} \rightarrow \delta_C$) is a key player in the damping increase. Rigorously speaking, q' is not a feedback signal, but its effect through state feedback is.

The associated combination of vehicle parameters $F_{\delta c}$ ϕ' appearing with $q_{22}r_{11}$ reveals the physical mechanism for this damping increase. Suppose a disturbance is present in the generalized structural deflection rate $\dot{\eta}$. Through the mode slope ϕ', this disturbance excites the cockpit response q'. Because of feedback represented by $q_{22}r_{11}$, the canard δ_C is activated. Finally through the control derivative F_{δ_c}, the initial disturbance in the generalized structural deflection rate $\dot{\eta}$ is countered. This feedback damping mechanism ($\dot{\eta} \rightarrow \phi' \rightarrow q' \rightarrow q_{22}r_{11} \rightarrow \delta_C \rightarrow F_{\delta_c} \rightarrow \dot{\eta}$) can be emphasized further by increases in r_{11} or q_{22}.

The approximate expression for $(2\zeta\omega)_2$ from Table 3.1 also indicates the cockpit pitch rate to elevator feedback path ($q' \rightarrow q_{22}r_{22} \rightarrow \delta_E$) is an important player in the

damping augmentation. A simple calculation from Table 3.1 indicates that the cockpit pitch rate to canard feedback path contributes +67 percent to damping augmentation, whereas the cockpit pitch rate to elevator feedback path contributes +33 percent. This +33 percent contribution is further decomposed into a stabilizing contribution from $F_{\delta_E}\phi'$ and a destabilizing contribution from M_{δ_E} (i.e., damping loss). The generalized force from the elevator deflection damps structural vibrations, but the associated pitch moment destabilizes the "out of phase" rigid pitch motion.

Now consider the augmented short period mode damping. Tables 2.2 and 2.5 indicate this damping value has been increased by a factor of 1.6 through the control system (0.88 vs. 1.44). Table 3.1 contains the approximate expression for this term denoted as $(2\zeta\omega)_1$. The first line again represents the open-loop contribution. Within this subset of terms, note $-\frac{Z_\alpha}{V_T} - M_q$ is the classic short period damping effect and the remaining terms are due to coupling from the aeroelastic mode. Based on the numerical values, these coupling terms are all destabilizing.

The second and third lines in the expressions for $(2\zeta\omega)_1$ indicate the feedback effects. Two terms represented by $q_{22}r_{11}$ and $q_{22}r_{22}$ are again present. Substitution of numerical values communicates to the designer that the cockpit pitch rate to elevator signal path contributes +55% to damping augmentation, whereas the cockpit pitch rate to canard path contributes +45%. If $\tilde{\omega}_2^2$ is considered to be approximately $\omega^2 - F_\eta$ (see Equation (3.37)), then the control derivative M_{δ_E} associated with the $q_{22}r_{22}$ term indicates the feedback damping mechanism represented by this term. An initial disturbance in rigid pitch rate is opposed by the following dynamic effect: $q \rightarrow 1 \rightarrow q' \rightarrow$ $q_{22}r_{22}$

$\rightarrow \delta_E \rightarrow M_{\delta_E} \rightarrow q$. Note the rigid pitch rate signal driving the elevator deflection is not originating directly from the first output signal q in Equation (2.2). Instead, the signal q is indirectly driving the elevator deflection through the second output signal q' (see Equation (2.2)). A pitch stability augmentation system based on such logic is nonstandard.

Now consider the $q_{22}r_{11}$ term. The three contributions to this term can be decomposed in a relative sense as +36% from $M_\eta F_{\delta_C}$, +25% from $M_{\delta_C}(\omega^2 - F_\eta)$, and +39% from $(1+\frac{Z_q}{V_T})M_\alpha F_{\delta_C}\phi'$. If $\tilde{\omega}_2^2$ is again taken as $\omega^2 - F_\eta \approx \omega_{ae}^2$, the control derivative term M_{δ_C} indicates the short period mode is partially damped in the following way $q \rightarrow 1 \rightarrow q' \rightarrow q_{22}r_{11} \rightarrow \delta_C \rightarrow M_{\delta_C} \rightarrow q$. Next consider the term $(1+\frac{Z_q}{V_T})M_\alpha F_{\delta_C}\phi'$. Recall that the classic short period approximation yields, $(1+\frac{Z_q}{V_T})M_\alpha \approx -\omega_{sp}^2$ (see Table 2.3). Thus, the $F_{\delta_C}\phi'$ term and the M_{δ_C} term have similar mathematical structures $-\omega_{sp}^2 F_{\delta_C}$ vs. $\omega_{ae}^2 M_{\delta_C}$, and hence similar physical effects. The damping mechanism for the $F_{\delta_C}\phi'$ term is illustrated as $q \rightarrow Z_q \rightarrow \alpha \rightarrow M_\alpha \rightarrow q$ coupled with $\dot{\eta} \rightarrow \phi' \rightarrow q' \rightarrow q_{22}r_{11} \rightarrow \delta_C \rightarrow F_{\delta_C} \rightarrow \dot{\eta}$. The final term is $M_\eta F_{\delta_C}$. The damping mechanism represented by this term is $\eta \rightarrow M_\eta \rightarrow q \rightarrow 1 \rightarrow q' \rightarrow q_{22}r_{11} \rightarrow \delta_C \rightarrow F_{\delta_C} \rightarrow \eta$. These effects are all highly nonstandard means of eliciting pitch-damping augmentation, yet for this control system they provide nearly half of the overall feedback effect.

In summary, the cost weights for this design were biased towards the aeroelastic suppression role, relative to the pitch augmentation role, in a 2-to-1 ratio (see Equation (2.28)). This selection was based on the severity of the structural vibrations seen in the open-loop dynamics. The insight provided here correlates with this weighting selection. Even though the control architecture is fully coupled, the collocated cockpit pitch rate to canard path provides two-thirds of the augmentation for the aeroelastic damping. This mechanism is the expected dominant effect. However, one-third of the augmentation originates from the noncollocated cockpit pitch rate to elevator path. Only one-half of the short period damping augmentation can be loosely traced to conventional stability augmentation logic utilizing rigid pitch rate and elevator. In this effect, it was noted that rigid pitch rate determined the elevator deflection indirectly through the cockpit pitch rate. The other half of the closed-loop short period damping effect was traced to nonstandard effects. Even though the control architecture provides high levels of stability and performance, it is not clear that such control logic should be applied to the flight vehicle.

6.3 Nonminimum Phase Analysis

As noted in Chapter II, the bare airframe characteristics exhibit nonminimum phase behavior. The cockpit pitch rate time response due to an elevator step (see Figure 2.7) shows an initial reversal in the response direction. This characteristic was traced to the right-half plane factor $(s-3.4)$ appearing in the $n_{21}(s)$ transfer function polynomial (see Table 2.2). Further analysis, using approximate analytical factors for the open-loop system, showed this root location was due to the relative control power entering the

aeroelastic mode and rigid pitch mode. Fundamentally, the nonminimum phase behavior is due to the separated aft tail control and forward response with compliant structure in-between.

Even though the LQ-based flight control system provided high levels of damping as discussed in Section 6.2, the nonminimum phase characteristic still appears to be present in the closed-loop system. Figure 2.20 shows the closed-loop cockpit pitch rate time response still has an initial tendency of response reversal. The behavior would be objectionable to a pilot attempting to close a manual feedback loop around this system. Therefore, some type of control design modification is necessary. The closed-loop analytical expressions are used next to explore how the numerical factor is altered by the LQ control system and what modification could be considered to improve the system characteristics pertaining to this issue.

Table 4.13 contains the analytical expressions for the cockpit pitch rate to elevator command numerator factors appearing in the closed-loop $\eta_{21}(s)$ transfer function polynomial. The root of interest is r_{21_2} . The most important observation from this expression is the absence of any feedback gain elements from matrix K_R. Table 4.13 indicates the LQ flight control system ignores the right-half plane zero and basically leaves the open-loop characteristic intact (compare r_{21_2} from Table 4.13 with $_{ae}(\frac{1}{\tau})_q^{\delta_E}$ in Equations (2.4)-(2.5)). In a rigorous sense, r_{21_2} does depend on the feedback gains. Note the root location changes from +3.4 1/s to +3.2 1/s due to feedback (see Tables 2.2 and 2.5). However, this change is small and for engineering purposes, the root location is unaffected. The expression in Table 4.13 communicates similar information.

The implications from this knowledge are significant. Even though the LQ design technique can provide highly damped regulator-type systems, this design technique does not appear to be well suited for flight control applications where tailoring of both numerator and denominator characteristics is important. No amount of tuning (within a local region surrounding the nominal design) will significantly impact the response reversal problem. The key root location is simply not affected by the feedback strategy. Other feedback strategies can effectively address such characteristics.[84] Ultimately, the analytical expressions suggest the need for alternative design strategies.

6.4 Two-State vs. Full-State Feedback

From the analytical expressions found in Chapter IV, only the gains k_2, k_3, and k_7 are effective in the closed-loop system. This information tells the designer that only two states, q and $\dot{\eta}$, are needed to effectively implement this control system. The insight that closed-loop objectives can be achieved with a reduced set of feedback signals and gains is very useful for the design engineer for many reasons. First, it will reduce the number of sensors needed to measure the other states. Only two state measurements are needed rather than four. The other sensors could be used to provide redundancy and fail-safe precautions needed for such flight controllers. Secondly, it will reduce the real-time control law computations. Only three gain multiplications are necessary. Finally, in cases where an estimator is utilized, estimation of only two states will speed up calculations, and reduces calculation error.

Consider replacing the gain matrix in Equation (4.25) and Table 4.5 by

$$K_R = \begin{bmatrix} 0 & k_2 & k_3 & 0 \\ 0 & 0 & k_7 & 0 \end{bmatrix} \tag{6.1}$$

Table 6.1 shows the closed-loop frequencies and dampings for both the original full state system and the partial state feedback system.

Table 6.1 Two-State vs. Full-State Feedback Frequencies and Dampings

Closed-Loop Factors	Two-State Feedback	Full-State Feedback
ω_1 1/s	1.3	1.3
ζ_1	0.48	0.56
ω_2 1/s	6.0	6.1
ζ_2	0.30	0.29

Overall, Table 6.1 shows that closed-loop factors are not significantly altered by the simplified gain matrix in Equation (6.1). The most significant change is associated with the short period damping ζ_1. This damping value has been compromised somewhat (0.56 vs. 0.48), but could be recovered by increasing the magnitude of k_2 (more negative) as noted from the expressions for α_1 and δ_1 in Tables 4.6 and 4.10. Further, with Tables 4.2 and 4.4, adjustments to Q and R could be formulated to produce such an effect. Other values in Table 6.1 are not compromised by elimination of the state feedback signals α and η. Figures 6.1-6.4 compare the two-state feedback design with the full-state feedback design. The match is quite good.

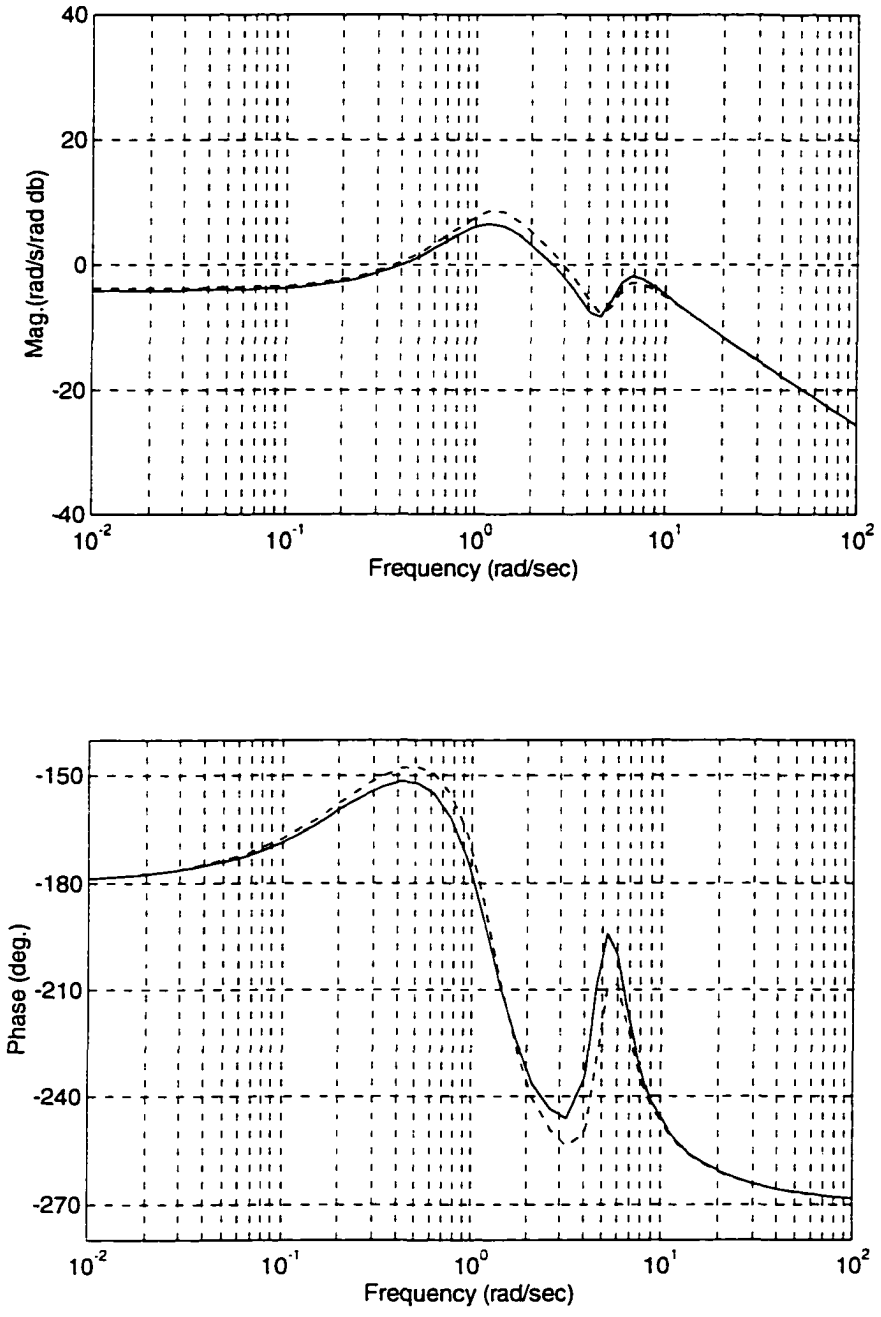

Figure 6.1 Comparison of q/δ_E Frequency Responses Using Full-State and Two-State Feedback

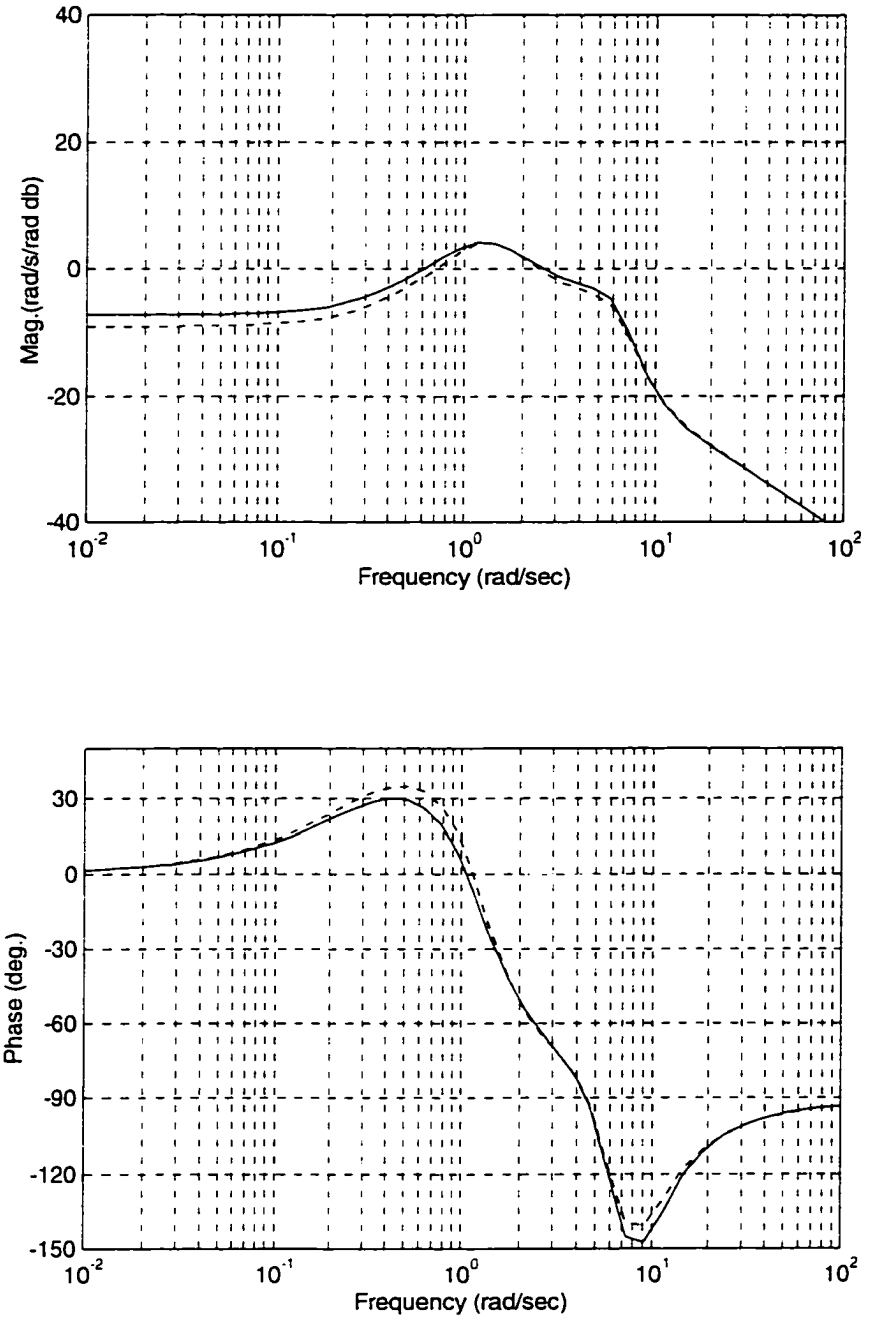

Figure 6.2 Comparison of q/δ_C Frequency Responses Using Full-State and Two-State Feedback

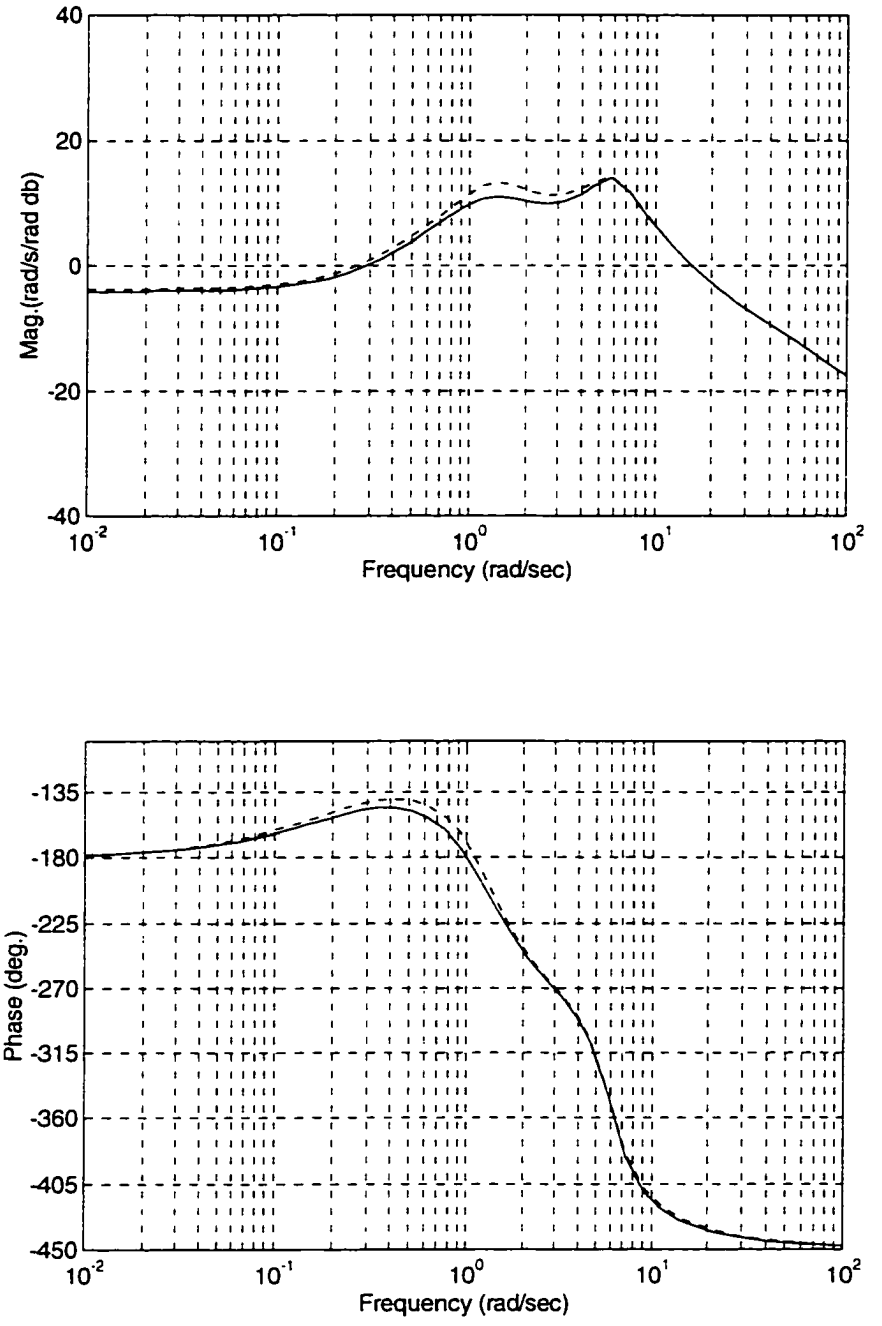

_____ Full-State Feedback

-------- Two-State Feedback

Figure 6.3 Comparison of q'/δ_E Frequency Responses Using Full-State and Two-State Feedback

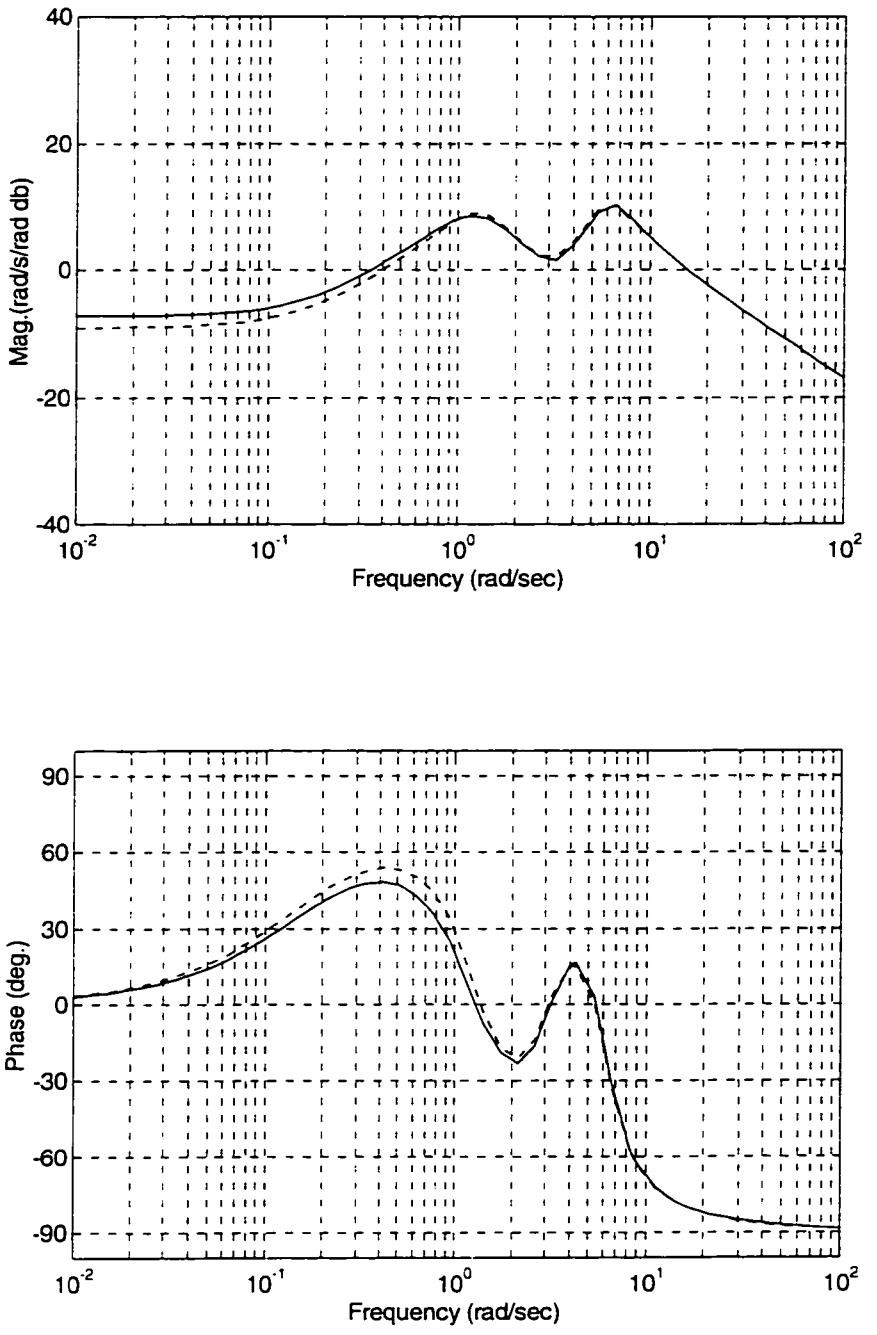

Figure 6.4 Comparison of $q^{\cdot}/\delta_C$ Frequency Responses Using Full-State and Two-State Feedback

6.5 Performance Improvement

The closed-loop analytical relations are explored further to learn more about how to improve the system performance. The closed-loop denominator factors in Table 4.10 are used as an example of how to apply these analytical relations to design problems. The expressions from Table 4.10 are rewritten here for convenience.

$$\alpha_2 \approx \frac{1}{2}(\tilde{F}_\eta - M_q - \tilde{Z}_\alpha + M_{\delta_E} k_2 + F_{\delta_C} k_7 + F_{\delta_E} k_3) - \frac{-M_q \tilde{F}_\eta - \tilde{Z}_\alpha \tilde{F}_\eta + M_{\delta_E} k_2 \tilde{F}_\eta - F_q M_\eta}{2(\tilde{F}_\eta - M_q(F_{\delta_E} k_3 + F_{\delta_C} k_7) - M_\alpha \tilde{Z}_q)} \tag{6.2a}$$

$$\beta_2 \approx \sqrt{\tilde{F}_\eta - M_q(F_{\delta_E} k_3 + F_{\delta_C} k_7) - M_\alpha \tilde{Z}_q} \tag{6.2b}$$

$$\alpha_1 \approx \frac{-M_q \tilde{F}_\eta - \tilde{Z}_\alpha \tilde{F}_\eta + M_{\delta_E} k_2 \tilde{F}_\eta - F_q M_\eta}{2(\tilde{F}_\eta - M_q(F_{\delta_E} k_3 + F_{\delta_C} k_7) - M_\alpha \tilde{Z}_q)} \tag{6.2c}$$

$$\beta_1 \approx \sqrt{\frac{-F_\alpha \tilde{Z}_q M_\eta - M_\alpha \tilde{Z}_q \tilde{F}_\eta - \tilde{Z}_\alpha M_{\delta_E} k_2 \tilde{F}_\eta}{\tilde{F}_\eta - M_q(F_{\delta_E} k_3 + F_{\delta_C} k_7) - M_\alpha \tilde{Z}_q}} \tag{6.2d}$$

To improve the system performance, the response must be quickened and more damping must be added. To speed the system response, the value of α_1 and α_2 must be increased, and to add damping the ratios α_1/β_1 and α_2/β_2 must increase. Figures 6.5-6.7 show several design graphs based on the analytical relations given in Equation (6.2), which illustrate how α_1, α_2, α_1/β_1 and α_2/β_2 vary with the gains k_2, k_3, and k_7. In Figures

6.6 and 6.7 some of the performance parameters increase with the gain increments (more negative) and some hold a constant value. For example as k_3 is made larger in magnitude, the quickness of the aeroelastic response α_2 is enhanced, but the short period damping α_1/β_1 is essentially constant. These features make the selection process of the gains k_3 and k_7 lacking in the sense that some important closed-loop features are not strongly affected. In Figure 6.5 it can be seen that nearly all performance parameters in Equations (6.2a)-(6.2d) are increasing with larger magnitudes for k_2. This feature makes k_2 the best candidate for adjusting the system closed-loop poles, as most performance parameters are moving in the desired direction.

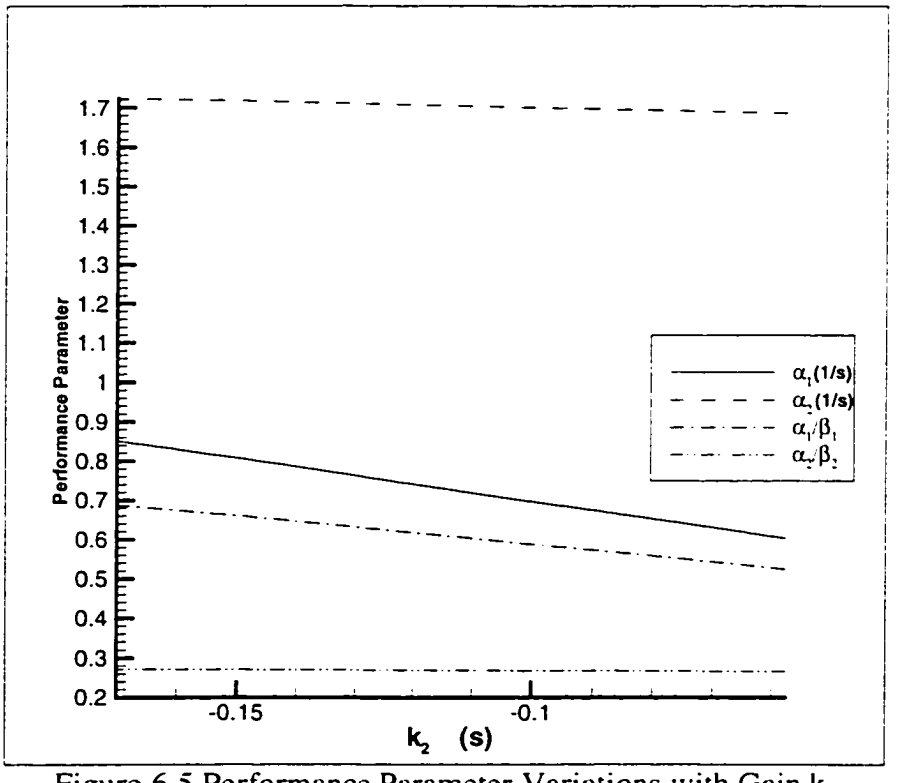

Figure 6.5 Performance Parameter Variations with Gain k_2

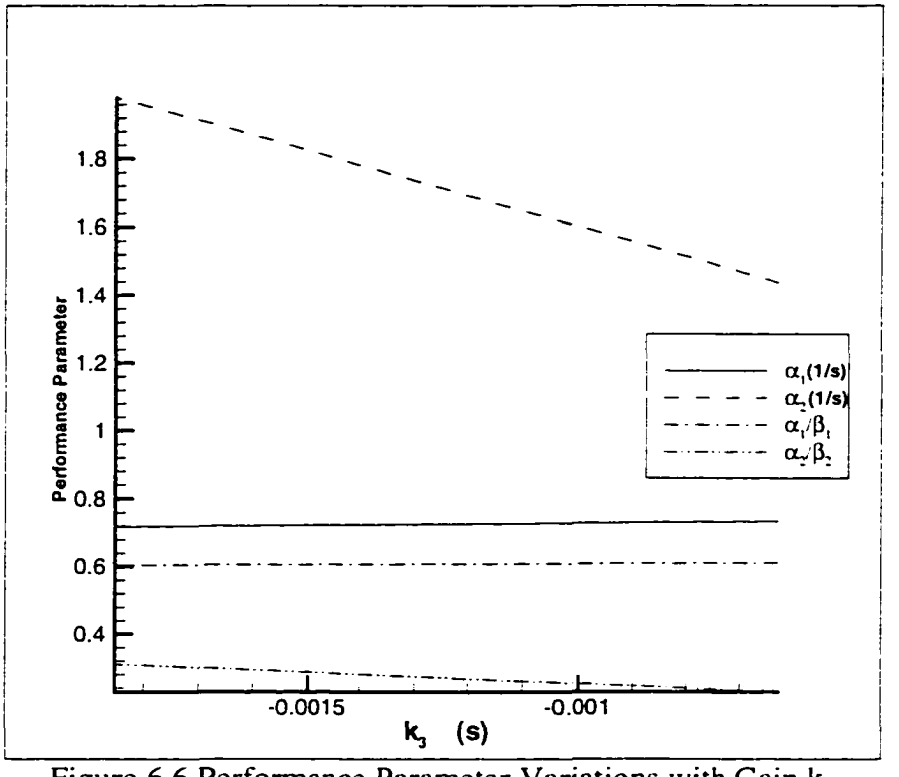

Figure 6.6 Performance Parameter Variations with Gain k_3

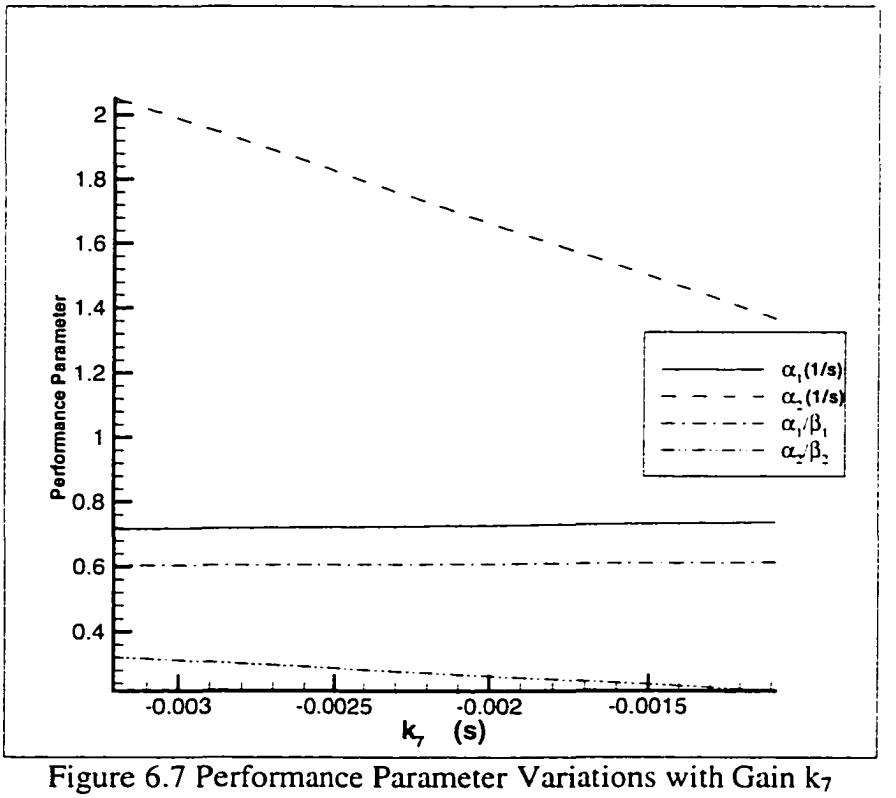

Figure 6.7 Performance Parameter Variations with Gain k_7

As an example, if the feedback gain k_2 is doubled in magnitude, the new closed-loop poles are as indicated in Table 6.2. The damping of the short period poles increase by 25 percent, while the aeroelastic poles increase damping by 7 percent. If k_2 is doubled again, the damping increases are 75 percent and 17 percent, respectively. Figure 6.8 shows the rigid pitch rate time response to an elevator command step of 0.01 rad for the different k_2 values, and Figure 6.9 shows similar information for the cockpit pitch rate time response. The improvements in the speed of response and in damping of the overshoot can be seen in these figures.

Table 6.2 Effect of k_2 on System Closed-Loop Poles

Closed-Loop Factors	k_2	2 k_2	4 k_2
α_1 1/s	0.7	0.87	1.3
β_1 1/s	1.0	0.97	0.67
α_2 1/s	1.8	1.9	2.1
β_2 1/s	5.8	5.7	5.5

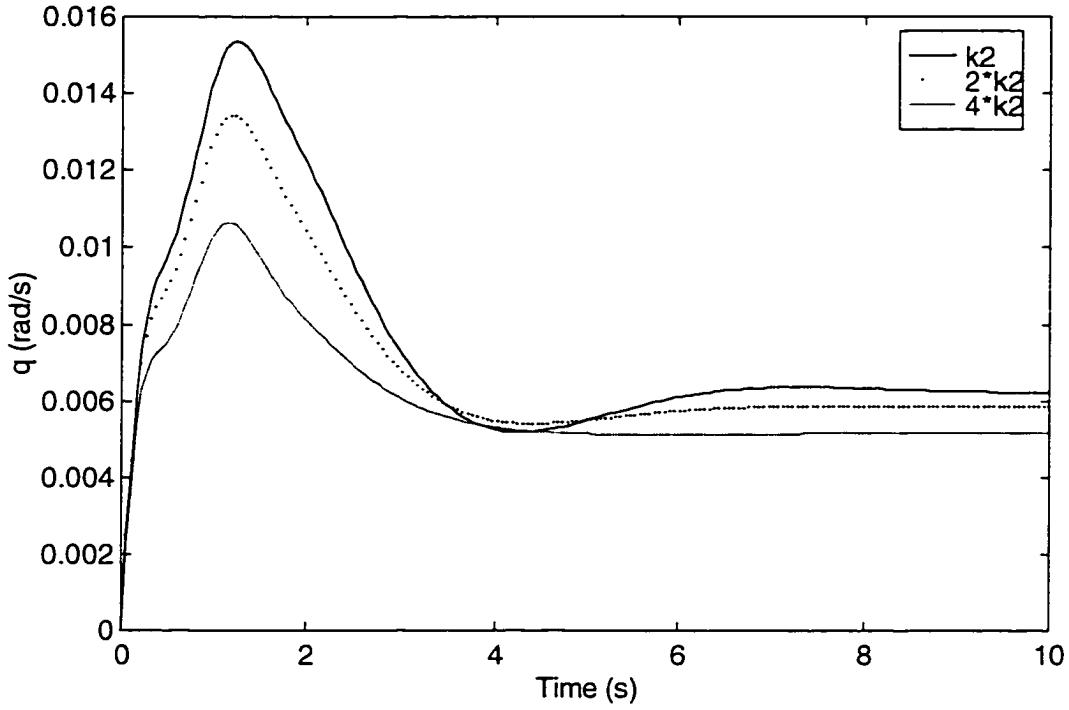

Figure 6.8 Rigid Pitch Rate Time Response to Elevator Command Step

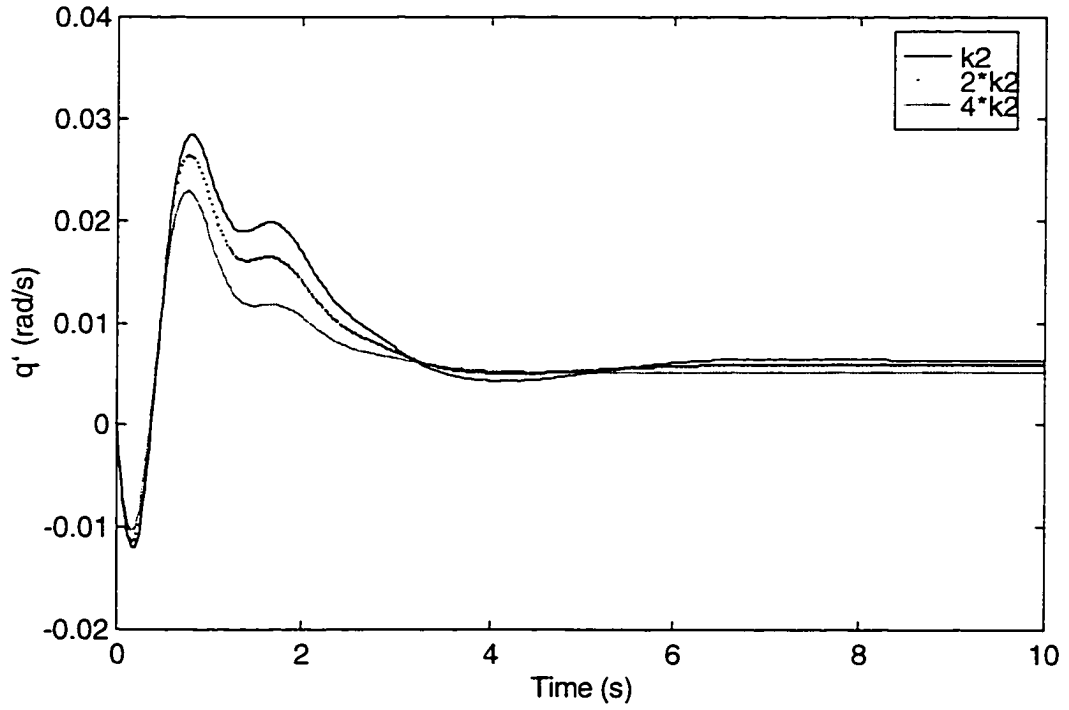

Figure 6.9 Cockpit Pitch Rate Time Response to Elevator Command Step

As another example, consider fixing the ratio between the gains k_2, k_3, and k_7 and introduce an overall scaling factor k. The gain matrix becomes

$$K_R = k\begin{bmatrix} 0 & k_2 & k_3 & 0 \\ 0 & 0 & k_7 & 0 \end{bmatrix} \tag{6.3}$$

Figure 6.10 show the variation of the system closed-loop parameters with the scaling factor k. It can be seen that increasing the scaling factor k will improve the system performance. This information is quite valuable to the design engineers since they could not easily obtain such information using numerical techniques unless considerable efforts were devoted to simulation and sensitivity analysis.

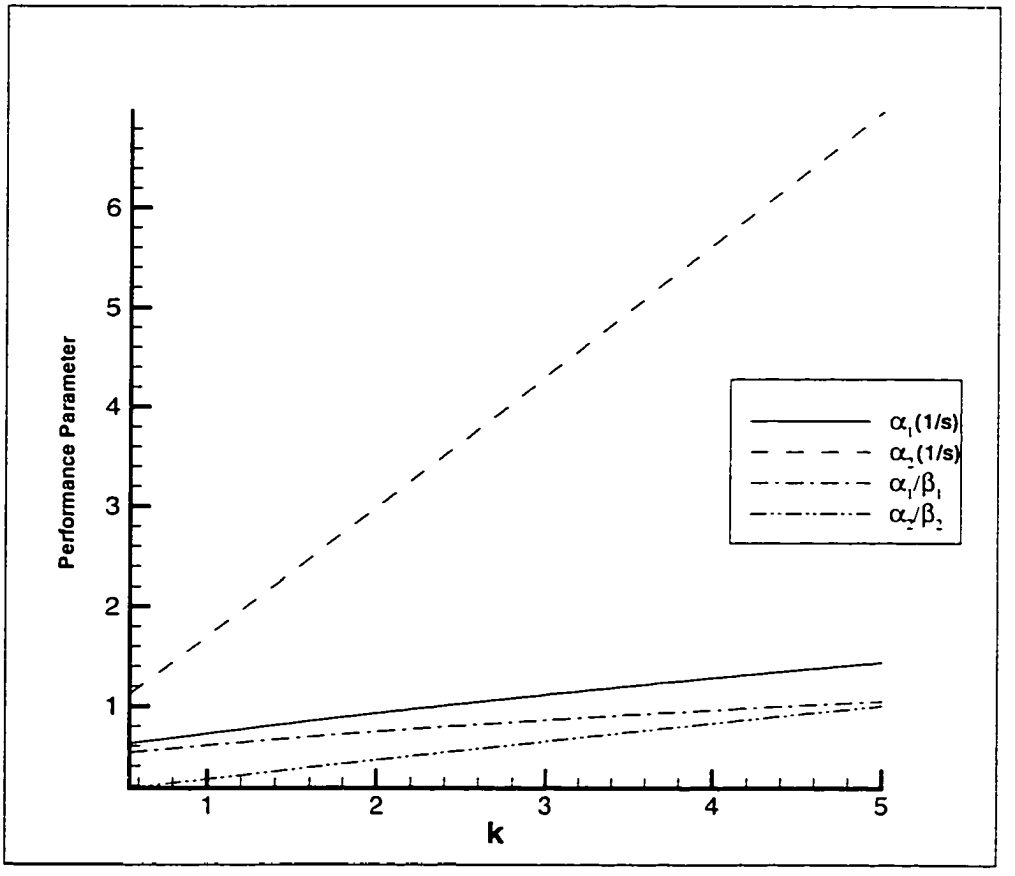

Figure 6.10 Variation of the Closed-Loop Parameters with Scaling Factor k

6.6 Robustness Improvement

System robustness is a very important issue in the design of flight control systems. Its importance comes from the fact that the dynamics of the flying vehicles are sensitive to variations in velocity and altitude. The goal is to have a control system which can accommodate these changes and keep the overall flight system stable. Having the approximate analytical relations can make the robustness analysis much easier. All that is needed is to find the gains which will hold the real parts of the closed-loop poles ($-\alpha_1$ and $-\alpha_2$) negative. To that end, consider the following procedure.

The first step is to define the range of variation for every parameter in α_1 and α_2 (i.e., the minimum and maximum values). Such data could be obtained from wind tunnel tests or computational aerodynamic runs. Table 6.3 shows the parameter range.

Table 6.3 Variation Range for System Parameters for Robustness Study

$$\tilde{F}_\eta\big|_{min} < \tilde{F}_\eta < \tilde{F}_\eta\big|_{max}$$
$$M_q\big|_{min} < M_q < M_q\big|_{max}$$
$$\tilde{Z}_\alpha\big|_{min} < \tilde{Z}_\alpha < \tilde{Z}_\alpha\big|_{max}$$
$$M_{\delta_E}\big|_{min} < M_{\delta_E} < M_{\delta_E}\big|_{max}$$
$$F_{\delta_C}\big|_{min} < F_{\delta_C} < F_{\delta_C}\big|_{max}$$
$$F_{\delta_E}\big|_{min} < F_{\delta_E} < F_{\delta_E}\big|_{max}$$
$$\tilde{F}_\eta\big|_{min} < \tilde{F}_\eta < \tilde{F}_\eta\big|_{max}$$
$$M_\alpha\big|_{min} < M_\alpha < M_\alpha\big|_{max}$$
$$\tilde{Z}_q\big|_{min} < \tilde{Z}_q < \tilde{Z}_q\big|_{max}$$
$$M_\eta\big|_{min} < M_\eta < M_\eta\big|_{max}$$

The next step is to determine the worst case parameter variation direction. Worst case directions are obtained from the analytical expressions for α_1 and α_2 by considering how the parameter affects the sign of α_1 and α_2. For example, assume a parameter X has a positive value, and is further added to the total collective in the α_1 equation. Assuming the nominal closed-loop system is stable ($-\alpha_1 < 0$), the worst case direction for parameter X is towards Xl_{min}. This direction will destabilize the system. This procedure is conducted for all the parameters. Applying all these variations simultaneously gives the worst case equation, which could be solved for the gains necessary to maintain stability.

Applying this procedure to the α_1 or α_2 expressions introduces several difficulties. The equations for α_1 and α_2 consist of both a numerator and denominator. Further, the mathematical structure involves products of several parameters. These difficulties require extra care while calculating the worst case direction. To explain this process, assume a product of two parameters (+XY) is added to the numerator terms of the α_1 equation. There are four possibilities for the worst case direction: Xl_{min} Yl_{min}, Xl_{min} Yl_{max}, Xl_{max} Yl_{min}, Xl_{max} Yl_{max}. Assuming X is positive and Y is negative, the worst case direction would be Xl_{max} Yl_{min} (assuming the nominal closed-loop system is again stable, $-\alpha_1 < 0$). All possibilities should be checked for the worst case. Applying the procedure to the α_1 equation gives

$$\alpha_1\big|_{cr} \approx \frac{-M_q\big|_{min}\tilde{F}_\eta\big|_{min} - \tilde{Z}_\alpha\big|_{min}\tilde{F}_\eta\big|_{min} + M_{\delta_E}\big|_{min}k_2\tilde{F}_\eta\big|_{min} + F_q\big|_{min}M_\eta\big|_{min}}{2(\tilde{F}_\eta\big|_{max} - M_q\big|_{max}(F_{\delta_E}\big|_{max}k_3 + F_{\delta_C}\big|_{max}k_7) - M_\alpha\big|_{max}\tilde{Z}_q\big|_{max})} \tag{6.4}$$

where $\alpha_1\big|_{cr} = 0$ is the critical value between stability and instability. By fixing k_3 and k_7 and solving for k_2, the critical gain $k_2\big|_{cr}$ is given by

$$k_2\big|_{cr} > \frac{M_q\big|_{min}\tilde{F}_\eta\big|_{min} + \tilde{Z}_\alpha\big|_{min}\tilde{F}_\eta\big|_{min} - F_q\big|_{min}M_\eta\big|_{min}}{M_{\delta_E}\big|_{min}\tilde{F}_\eta\big|_{min}} \tag{6.5}$$

The value $k_2\big|_{cr}$ is the gain that guarantees stability under different flying conditions.

One important issue must not be overlooked. The analytical expressions are only valid in some local region around the nominal design. The size of this region is currently unknown. It is unlikely that the expressions are global in nature due to approximations. However within this region, the expressions can be relied upon to give satisfactory accuracy as shown in Chapter III and IV.

CHAPTER VII

CONCLUSIONS AND RECOMMENDATIONS

7.1 Conclusions

The objectives of this dissertation are 1) formulation of techniques capable of producing analytical expressions to allow useful insight into the design relationships, 2) generation of candidate expressions for contemporary flight control applications, and 3) utilization of the expressions to better understand the mechanisms by which a contemporary flight control law augments flight vehicle dynamics. Considerable efforts were focused on meeting these objectives and good success was achieved in all areas. Three new methods where developed for generating the analytical expressions. These methods include the Direct Eigen-Based Technique, the Order of Magnitude Technique, and the Cost Function Imbedding Technique. The first two methods were applied to an aeroelastic flight control system designed with the LQ state feedback technique. Accurate and simple analytical expressions for the closed-loop eigenvalues and zeros in terms of basic parameters, such as stability and control derivatives, structural vibration damping and natural frequency, and cost function weights were generated. The expressions were used to obtain valuable insight and understanding that is not readily available by other means. Overall, the dissertation has made significant and unique contributions to the flight dynamics and control profession.

The Direct Eigen-Based Technique bypasses the algebraic Riccati equation to directly calculate the closed-loop poles. Its applicability is limited to the study of stability and robustness of the closed-loop poles. The Order of Magnitude Technique is applicable

for the calculation of both zeros and poles but it depends on the ability to simplify the Riccati equation to a set of analytically solvable equations. Performance, stability, and robustness can easily be studied by this method. Although closed-loop poles can be calculated using this method (Riccati matrix P $\rightarrow$ gain matrix $K_R \rightarrow$ closed-loop poles $\det[sI - A + BK_R]$), it is advisable to use the Direct Eigen-Based Technique to reduce the accumulation errors. The Cost Function Imbedding Technique bypasses the Riccati equation and provides a direct calculation of the gain matrix. Calculation of polynomial roots is needed to get the closed-loop poles and zeros. The general limitation for the three methods is the order of the system as there is no exact analytical solution for polynomials of order greater than four. However, clever approximations can be utilized to circumvent this limitation.

The methods discussed in this dissertation give more understanding into the LQ control law. Even though the LQ-based flight control system provided high levels of damping as discussed in Section 6.2, the nonminimum phase characteristic still appears to be present in the closed-loop system. The most important observation from the analytical expression for the nonminimum phase zero is the absence of any feedback gain elements from the gain matrix K_R. Table 4.13 shows that the LQ flight control system does not affect the right-half plane zero and leaves the open-loop characteristic almost intact. The implications of this knowledge are significant. Even though the LQ design technique can provide highly damped regulator-type systems, this design technique does not appear to be well suited for flight control applications where adjusting of both numerator and denominator characteristics is important. No amount of tuning (within a local region surrounding the nominal design) will significantly affect the response reversal

characteristics. The right-half plane root location is simply not affected by the feedback strategy. Other feedback strategies can effectively address such characteristics.[84] Ultimately, the analytical expressions suggest the need for alternative design strategies.

7.2 Recommendations

Several logical extensions to this dissertation and its contents are recommended as future activities. Considerable work in this dissertation involves the ARE. Many control and dynamics problems rely heavily on the solution of ARE. Some examples include optimal filtering and estimation, Kalman-Bucy filter design, etc. The work in this dissertation could be tailored to address one or all of these problems. Studying the robustness of the expressions to other similar airplanes and the extensions to time varying LQ problems are advisable for future work and will increase the range of applicability of these methods. With the fast improvements in symbolic manipulation software and computer systems, larger problems could also been pursued. The Cost Function Imbedding Technique introduced in Chapter V should be applied to the flight control system described in this report.

REFERENCES

1. Bryson, A. E., "New Concepts in Control Theory, 1959-1984," *Journal of Guidance, Control, and Dynamics*, Vol. 8, No. 4, July-August 1985, pp. 417-425.

2. Kwakernaak, H. and Sivan, R., *Linear Optimal Control Systems*, John Wiley & Sons, New York, New York, 1972.

3. Maciejowski, J. M., *Multivariable Feedback Design*, Addison-Wesley, New York, New York, 1989.

4. Doyle, J. C., Francis, B., Tannenbaum, A., and Francis, B. A., *Feedback Control Theory*, Macmillan, USA, 1992.

5. Saberi, A., Chen, B. M., and Sannuti, P., *Loop Transfer Recovery: Analysis and Design*, Springer-Verlag, New York, New York, 1993.

6. Adams, R. J., Buffington, J. M., Sparks, A. G., and Banda, S. S., *Robust Multivariable Flight Control, Advances in Industrial Control*, Springer-Verlag, New York, New York, 1994.

7. Frank L. Lewis, Vassilis L. Syrmos, *Optimal Control*, John Wiley & Sons, 1995.

8. Hyde, R. A., H_∞ *Aerospace Control Design, Advances in Industrial Control*, Springer-Verlag, New York, New York, 1995.

9. McRuer, D., Ashkenas, I., and Graham, D., *Aircraft Dynamics and Automatic Control*, Princeton University Press, Princeton, New Jersey, 1973.

10. Blakelock, J. H., *Automatic Control of Aircraft and Missiles*, John Wiley & Sons, New York, New York, 1991.

11. Stevens, B. L. and Lewis, F. L., *Aircraft Control and Simulation*, John Wiley & Sons, New York, New York, 1992.

12. MacFarlane, A. G. J., "An Eigenvector Solution of the Optimal Linear Regulator Problem," *Journal of Electronic Contributions* , Vol. 14, 1963, pp. 643-654.

13. Potter, J. E., "Matrix Quadratic Solutions," *Journal of SIAM Applied Mathematics*, Vol. 14, No. 3, May 1966, pp. 496-501.

14. Anderson, B. D. O., "Solution of Quadratic Matrix Equations," *Electronic Letters*, Vol. 2, No. 10, October 1966, pp. 371-372.

15. Jamshidi, M., "An Overview on the Solutions of the Algebraic Matrix Riccati Equation and Related Problems," *Large Scale Systems: Theory and Applications*, Vol. 1, No. 3, August 1980, pp. 167-192.

16. Benner, P., Byers, R., "Step Size Control for Newton's Method Applied to Algebraic Riccati Equation," *Proceedings of the Fifth SIAM Conference on Applied Linear Algebra*, Philadelphia, Pennsylvania 1994, pp. 177-181.

17. Thoma, M., Wyner, A., *The Autonomous Linear Quadratic Control Problem (Theory and Numerical Solution)*, Springer-Verlag 1991.

18. Angelika, B. G., Byers, R., and Mehrmann, V., "Numerical Methods for the Algebraic Riccati Equations," *Workshop on the Riccati Equation in Control Systems and Signals*, Como Italy, June 1989, pp. 107-115.

19. Shubert, H. A., "An Analytical Solution for an Algebraic Matrix Riccati Equation," *Transactions on Automatic Control*, Vol. AC-19, No. 3, June 1974, pp. 255-256.

20. Jones, E. L., "A Reformulation of the Algebraic Riccati Equation Problem," *Transactions on Automatic Control*, Vol. AC-21, No. 1, February 1976, pp. 113-114.

21. Repperger, D. W., "A Square Root of a Matrix Approach to Obtain the Solution to a Steady-State Matrix Riccati Equation," *Transactions on Automatic Control*, Vol. AC-21, No. 5, October 1976, pp. 786-787.

22. Incertis Carro, F. and Martinez Torres, J. M., "An Extension on a Reformulation of the Algebraic Riccati Equation Problem," *Transactions on Automatic Control*, Vol. AC-22, No. 1, February 1977, pp. 128-129.

23. Incertis, F. C., "A New Formulation of the Algebraic Riccati Equation Problem," *Transactions on Automatic Control*, Vol. AC-26, No. 3, June 1981, pp. 768-770.

24. Incertis, F., "An Extension on a New Formulation of the Algebraic Riccati Equation Problem," *Transactions on Automatic Control*, Vol. AC-28, No. 2, February 1983, pp. 235-238.

25. Incertis, F., "On Closed Form Solutions for the Differential Matrix Riccati Equation Problem," *Transactions on Automatic Control*, Vol. AC-28, No. 8, August 1983, pp. 845-848.

26. Ish-Shalom, J., "On Symbolic Solution of the Matrix Algebraic and Differential Riccati Equations," *Proceedings of the American Control Conference*, Boston, Massachusetts, June 1985, pp. 1663-1671.

27. Beachy, J. A. and Blair, W. D., *Abstract Algebra With a Concrete Introduction*, Prentice Hall, 1990.

28. Branin, F. H., "Poles and Zeros, Eigenvalues of Matrices, and Roots of Polynomials by the Method of Signatures," *Proceedings of the IEEE International Symposium on Circuits and Systems*, Phoenix, Arizona, April 1975, pp. 89-94.

29. Graham, D., "Special Cubic Solution Function," *Journal of Guidance and Control*, Vol. 4, No. 1, January-February 1981, pp. 90-92.

30. Graham, D., "Factors for Cubics and Quartics," *Journal of Guidance, Control, and Dynamics*, Vol. 5, No. 6, November-December 1982, pp. 564-572.

31. Ashkenas, I. L. and McRuer, D. T., "Approximate Airframe Transfer Functions and Application to Single Sensor Control Systems," WADC-TR-58-82, Aeronautical Systems Division, Wright-Patterson AFB, Ohio, June 1958.

32. Pearce, B. F., Johnson, W. A., and Siskind, R. K., "Analytical Study of Approximate Longitudinal Transfer Functions for a Flexible Airframe," ASD-TDR-62-279, Aeronautical Systems Division, Wright-Patterson AFB, Ohio, June 1962.

33. Pearce, B. F. and Siskind, R. K., "The Application of Flexible Airframe Transfer Function Approximations and the Sensitivity of Airframe Transfer Functions to Elastic Mode Shapes," Topics on Flexible Airplane Dynamics, Part II, ASD-TDR-63-334, Aeronautical Systems Division, Wright-Patterson AFB, Ohio, July 1963.

34. Schmidt, D. K. and Newman, B. A., "Modeling, Model Simplification and Stability Robustness with Aeroelastic Vehicles," *Proceedings of the AIAA Guidance, Navigation, and Control Conference*, Minneapolis, Minnesota, August 1988, pp. 210-221.

35. Newman, B. A. and Schmidt, D. K., "Numerical and Literal Aeroelastic-Vehicle-Model Reduction for Feedback Control Synthesis," *Journal of Guidance, Control, and Dynamics*, Vol. 14, No. 5, September-October 1991, pp. 943-953.

36. Newman, B. A., "Aerospace Vehicle Model Simplification for Feedback Control," Ph.D. Dissertation, School of Aeronautics and Astronautics, Purdue University, West Lafayette, Indiana, August 1992.

37. Livneh, R. and Schmidt, D. K., "New Literal Approximations for the Longitudinal Dynamic Characteristics of Flexible Flight Vehicles," *Proceedings of the AIAA Guidance, Navigation, and Control Conference*, Hilton Head, South Carolina, August 1992, pp. 536-545.

38. Livneh, R., "Improved Literal Approximations for the Lateral-Directional Dynamics of Rigid Aircraft," *Proceedings of the AIAA Guidance, Navigation, and Control Conference*, Baltimore, Maryland, August 1995, pp. 1197-1207.

39. Kwakernaak, H., "Asymptotic Root Loci of Multivariable Linear Optimal Regulators," *Transactions on Automatic Control*, Vol. AC-21, No. 3, June 1976, pp. 378-382.

40. Shaked, U., "The Asymptotic Behavior of the Root-Loci of Multivariable Optimal Regulators," *Transactions on Automatic Control*, Vol. AC-23, No. 3, June 1978, pp. 425-430.

41. Stein, G., "Generalized Quadratic Weights for Asymptotic Regulator Properties," *Transactions on Automatic Control*, Vol. AC-24, No. 4, August 1979, pp. 559-566.

42. Thompson, P. T., Stein, G., and Laub, A. J., "Angles of Multivariable Root Loci," *Transactions on Automatic Control*, Vol. AC-27, No. 6, December 1982, pp. 1241-1243.

43. Yagle, A. E. and Levy, B. C., "Equations for the Angles of Arrival and Departure for Multivariable Root Loci Using Frequency-Domain Methods," *Transactions on Automatic Control*, Vol. AC-28, No. 1, January 1983, pp. 118-121.

44. Newman, B. A. and Kassem, A. H., "Analytical Expressions For Linear Quadratic Aeroelastic Flight Control Eigenvalues," *AIAA Nonlinear Dynamical Systems Symposium*, January 1997, Reno, Nevada, AIAA-97-0457.

45. Newman, B. A. and Kassem, A. H., "Analytical Relationships for Optimal Aeroelastic Flight Control Eigenvalues," *AIAA Guidance, Navigation, and Control Conference*, August 1997, New Orleans, Lousiana, AIAA-97-3621.

46. Newman, B. A. and Kassem, A. H., "Analytical Relationships for Linear Quadratic Aeroelastic Flight Control Eigenvalues," *Journal of Guidance, Control and Dynamics*, Vol. 20, No. 6, November-December 1997.

47. Wolfram, S., *Mathematica, A System for Doing Mathematics by Computer*, Addison-Wesley, 1993.

48. Bonadio, A., *Theorist, Reference Manual*, Prescience Corporation 1990.

49. Boeing Commercial Airplane Group, "High-Speed Civil Transport Study," NASA-CR-4233, 1989.

50. McDonnell Douglas Aircraft Company, "Study of High-Speed Civil Transports," NASA-CR-4235, 1989.

51. Newman, B. A. and Buttrill, C., "Conventional Flight Control for an Aeroelastic, Relaxed Static Stability High-Speed Transport," *Proceedings of the AIAA Guidance, Navigation and Control Conference*, Baltimore, Maryland, August 1995, pp. 717-726.

52. Bisplinghoff, R. L. and Ashley, H., *Principles of Aeroelasticity*, Dover, New York, New York, 1962.

53. Boeing Commercial Airplane Group, "An Analysis of Methods for Predicting the Stability Characteristics of an Elastic Airplane," NASA-CR-73277, 1968.

54. Noll, T. and Blair, M., "A Procedure for Aeroelastic Analyses Involving Aircraft with Analog or Digital Control Systems," AFWAL-TR-86-3040 vol. I, January 1987.

55. Waszak, M.R. and Schmidt, D.K., "Flight Dynamics of Aeroelastic Vehicles," *Journal of Aircraft*, Vol. 25, No. 6, June 1988, pp. 563-571.

56. Arbuckle, P. D. and Buttrill, C. S., "Simulation Model-Building Procedure for Dynamic Systems Integration," *Journal of Guidance, Control and Dynamics*, Vol. 12, No. 6, November-December 1989, pp. 894-900.

57. Adams W. M., Jr. and Hoadley, S. T., "ISAC: A Tool for Aeroeservoelastic Modeling and Analysis," NASA Technical Memorandum 109031, 1993.

58. Kokotovic, P. V., "Singular Perturbations And Order Reduction in Control Theory-An Overview," *Automatica*, Vol. 12, No. 2, March 1976, pp. 123-132.

59. Anderson, B. D. O. and Liu, Y., "Controller Reduction: Concepts and Approaches," *IEEE Transactions on Automatic Control*, Vol. AC-34, No. 8, August 1989, pp. 802-812.

60. Wilson, D. A., "Model Reduction For Multivariable Systems," *International Journal of Control*, Vol. 20, No. 1, July 1974, pp. 57-64.

61. Enns, D., "Model Reduction For Control System Design," Ph.D. Dissertation, Department of Aeronautics and Astronautics, Stanford University, Palo Alto, California, June 1984.

62. Enns, D. F., "Model Reduction With Balanced Realizations: An Error Bound And A Frequency-Weighted Generalization," *Proceedings of the 23rd IEEE Conference on Decision and Control*, Las Vegas, Nevada, December 1984.

63. Lui, Y. and Anderson, B. D. O., "Singular Perturbation Approximation of Balanced Systems," *International Journal of Control*, Vol. 50, No. 4, October 1989, pp. 1379-1405.

64. Bacon, B. J., " Order Reduction For Closed-Loop Systems," Ph.D. Dissertation, School Of Aeronautics And Astronautics, Purdue University, West Lafayette, Indiana, December 1991.

65. Bacon, B. J. and Schmidt, D. K., "Multivariable Frequency-Weighted Order Reduction," *Journal of Guidance, Control and Dynamics*, Vol. 12, No. 1, January-February 1989, pp. 97-107.

66. Newman, B. A. and Schmidt, D. K., "Truncation and Residualiztion with Weighted Balanced Coordinates," *Journal of Guidance, Control and Dynamics*, Vol. 17, No. 6, November-December 1994, pp. 1299-1307.

67. Waszak, M.R., Davidson, J. B. and Schmidt, D. K., "A Simulation Study of the Flight Dynamics of Elastic Aircraft, Volume One-Experiment, Results and Analysis," NASA Contractor Report 4102, 1987.

68. Waszak, M.R., Davidson, J. B. and Schmidt, D. K., "A Simulation Study Of the Flight Dynamics of Elastic Aircraft, Volume Two-Data," NASA Contractor Report 4102, 1987.

69. U.S. Dept. of Defense, "Military Standard: Flying Qualities of Piloted Aircraft," MIL-STD-1797A, January 1990.

70. Crother, C. A., Gabelman, B., and Langton, D., "Structural Mode Effects on Flying Qualities in Turbulence," AFFDL-TR-73-88, Air Force Flight Dynamics Laboratory, Wright-Patterson AFB, Ohio, August 1973.

71. Yen, W. Y., "Effects of Dynamic Aeroelasticity on Handling Qualities and Pilot Rating," Ph.D. Dissertation, School of Aeronautics and Astronautics, Purdue University, West Lafayette, Indiana, December 1977.

72. Swaim, R. L. and Yen, W. Y., "Effects of Dynamic Aeroelasticity on Handling Qualities," *Journal of Aircraft*, Vol. 16, No. 9, September 1979, pp. 635-637.

73. Poopaka, S., "Handling Qualities of Large Flexible Aircraft," Ph.D. Dissertation, School of Mechanical and Aerospace Engineering, Oklahoma State University, Stillwater, Oklahoma, December 1980.

74. Swaim, R. L. and Poopaka, S., "An Analytical Pilot Rating Method for Highly Elastic Aircraft," *Journal of Guidance and Control*, Vol. 5, No. 6, November-December 1982, pp. 578-582.

75. Schmidt, D. K., "Pilot Modeling and Closed-Loop Analysis of Flexible Aircraft in the Pitch Tracking Task," *Journal of Guidance, Control and Dynamics*, Vol. 8, No. 1, January-February 1985, pp. 56-61.

76. Schmidt, D. K., "Modal Analysis of Flexible Aircraft Dynamics with Handling Qualities Implications," *Journal of Guidance and Control*, Vol. 8, No. 2, March-April 1985, pp. 194-200.

77. Noble, B. and Daniel, J. W., *Applied Linear Algebra*, Prentice-Hall, Englewood Cliffs, New Jersey, 1977.

78. Bryson, A.E. and Ho, Y.C., *Applied Optimal Control: Optimization, Estimation, and Control*, Hemisphere Publishing, New York, New York, 1975.

79. Doyle J. C. and Stien, G. "Multivariable Feedback Deign: Concepts for a Classical/ Modern Synthesis," *Transactions on Automatic Control*, Vol. AC-26, No.1, February, 1981, pp. 4-16.

80. Hess, R.A., "Unified Theory for Aircraft Handling Qualities and Adverse Aircraft-Pilot Coupling," *Journal of Guidance, Control and Dynamics*, Vol. 20, No. 6, November-December 1997, pp. 1141-1148.

81. Aviation Safety And Pilot Control-Understanding and Preventing Unfavorable Pilot-Vehicle Interaction, Report of the NRC Committee on the Effects of Aircraft-Pilot Coupling on Flight Safety, National Academy Press, Washington, D.C., 1997.

82. Sjkelton, R.E., *Dynamic Systems Control*, John Wiley & Sons, New York, New York, 1988.

83. Benard F., *Control System Design, An Introduction to State-Space Methods*, McGraw Hill, 1986.

84. Newman, B. A. and Schmidt, D. K., "Aeroelastic Vehicle Multivariable Control Synthesis with Analytical Robustness Evaluation," *Journal of Guidance, Control and Dynamics*, Vol. 17, No. 6, November-December 1994, pp. 1145-1153.

VITA

Ayman Hamdy Kassem was born on July 16th 1968 in Cairo, Egypt. He graduated with a B.Sc. degree from the Aerospace Engineering Department at Cairo University, Cairo, Egypt, August 1990. He got his M.Sc. in Aerospace Engineering from Cairo University, Cairo, Egypt, June 1993 and his Ph.D. from the Aerospace Engineering Department, Old Dominion University, Norfolk, Virginia, August 1998.

RECENT PUBLICATIONS:

"Analytical Expressions For Linear Quadratic Aeroelastic Flight Control Eigenvalues," Newman B. A. and Kassem A. H., *AIAA Nonlinear Dynamical Systems Symposium*, January 6-9, 1997, Reno, Nevada, AIAA-97-0457.

"Analytical Relationships for Optimal Aeroelastic Flight Control Eigenvalues," Newman B. A. and Kassem A. H., *AIAA Guidance, Navigation, and Control Conference* August 11-13, 1997, New Orleans, Louisiana, AIAA-97-3621

"Analytical Relationships For Linear Quadratic Aeroelastic Flight Control Eigenvalues," Newman B. A. and Kassem A. H., *Journal of Guidance, Control and Dynamics*, Vol. 20, No. 6, November-December 1997.

IMAGE EVALUATION
TEST TARGET (QA-3)

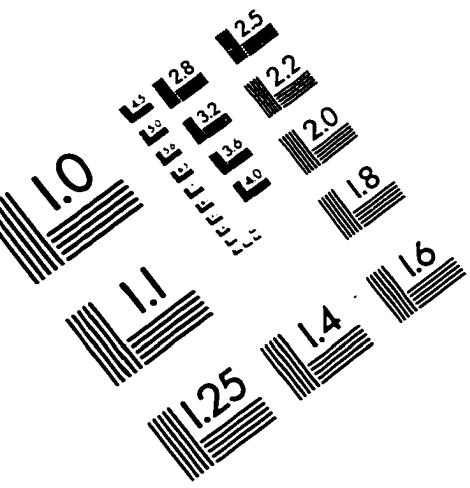

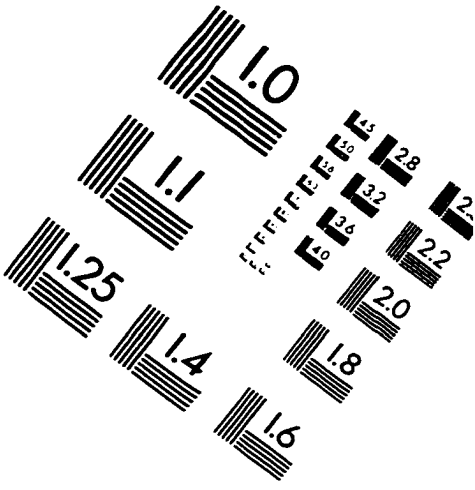

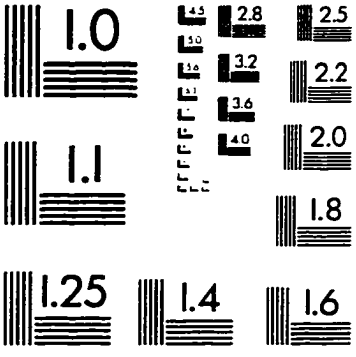

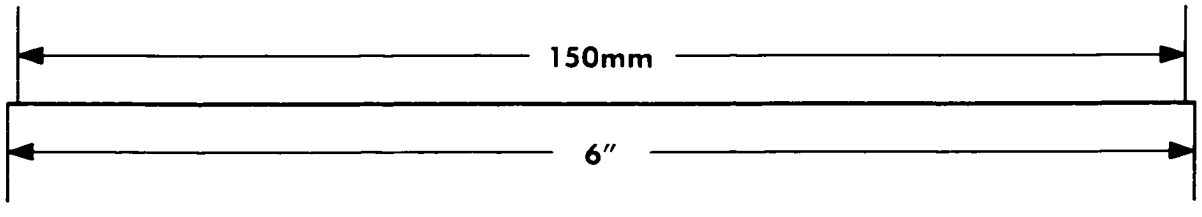

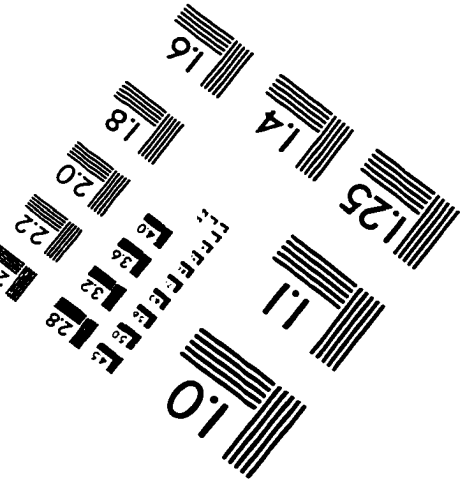

APPLIED IMAGE, Inc
1653 East Main Street
Rochester, NY 14609 USA
Phone: 716/482-0300
Fax: 716/288-5989